

Overview of the Mesoscale Eddies Surveyed during NAAMES

Peter Gaube
Alice Della Penna

Contents

1	About this document	4
2	A Subregional Classification Scheme for the North Atlantic	5
3	Overview of Coherent Mesoscale Structures in the NAAMES Region	5
4	Lagrangian re-analyses of altimetry	6
4.0.1	Finite Size Lyapunov Exponents – an index of frontal activity [units = d^{-1}] . . .	7
4.0.2	Eddy retention parameter – how eddies trap or leak [units = d]	8
4.0.3	Origin of water parcels – where do tracers come from? [units = °]	8
5	Summary of eddy features sampled during the NAAMES program	9
6	NAAMES 2015	11
6.1	S1 NAAMES-1	11
6.2	S2 NAAMES-1	14
6.3	S3 NAAMES-1	16
6.4	S4 NAAMES-1	18
6.5	S5 NAAMES-1	20
6.6	S5b NAAMES-1	22
6.7	S6 NAAMES-1	24
6.8	S7 NAAMES-1	26
7	NAAMES 2016	28
7.1	S0 NAAMES-2	28
7.2	S1 NAAMES-2	30
7.3	S2 NAAMES-2	32
7.4	S3 NAAMES-2	34
7.5	S4 NAAMES-2	36
7.6	S5 NAAMES-2	38
8	NAAMES 2017	40
8.1	S1a NAAMES-3	40
8.2	S1 NAAMES-3	42
8.3	S1.5 NAAMES-3	44
8.4	S2 NAAMES-3	46
8.5	S3 NAAMES-3	48
8.6	S3.5 NAAMES-3	50
8.7	S4 NAAMES-3	52
8.8	S4.5 NAAMES-3	54
8.9	S5 NAAMES-3	56
8.10	S5.5 NAAMES-3	58
8.11	S6 NAAMES-3	60
9	NAAMES 4	62
9.1	S1 NAAMES-4	62
9.2	S2 NAAMES-4	64

9.3	S2.5 NAAMES-4	66
9.4	S3 NAAMES-4	68
9.5	S4 NAAMES-4	70
9.6	SE4 NAAMES-4	72
9.7	S2RD NAAMES-4	74
9.8	S2RF NAAMES-4	76
10	Planned Additions and Updates	78

1 About this document

The North Atlantic Aerosol and Marine Ecosystem Study aims to characterize the rates of biological processes in the surface ocean and how changes in ocean biology affect aerosols in the marine boundary layer. The northwestern Atlantic, the region of focus for NAAMES, is characterized by a rousingly energetic mesoscale eddy field and therefore the selection of study sites was informed by satellite observations of the mesoscale field.

Areas within the study region that are expected to be influenced by mesoscale eddies and meanders can be estimated by quantifying the portion of time a given location is inside a mesoscale eddy or current meander (defined collectively as coherent mesoscale structures, or CMS). This measure of eddy coverage varies nearly an order of magnitude over the greater NAAMES regions (Fig. 1), with nearly 80% coverage in the proximity of the Gulf Stream to less than 10% in the location of the northernmost NAAMES stations. In light of the spatial variability in the coverage of eddies, and hence the importance of eddies, here I provide a brief analysis of the mesoscale eddy field at each NAAMES stations. Each of the following subsections is organized by expedition and station number.

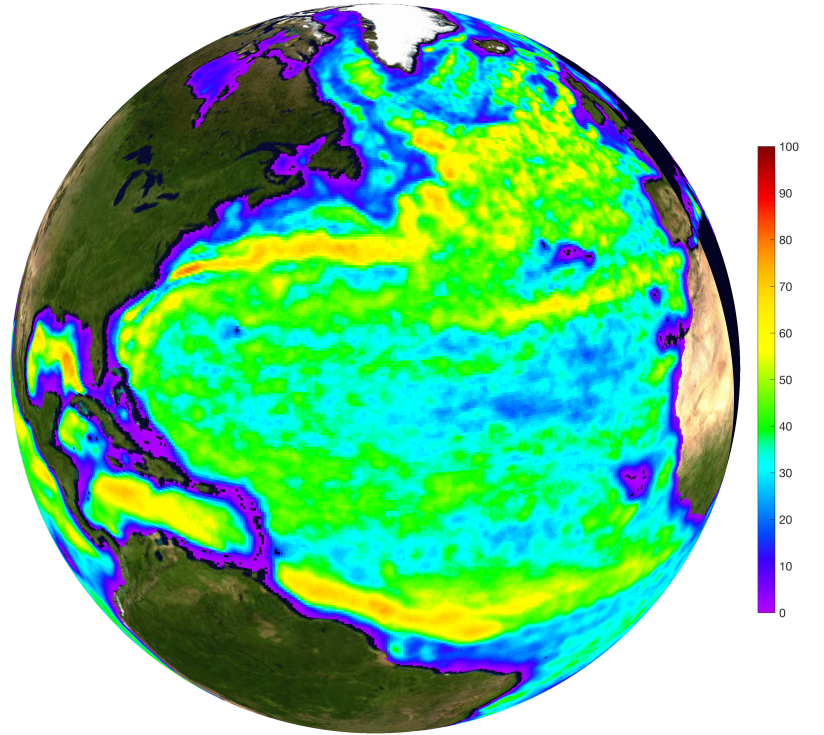


Figure 1: Map of the percent of time that an individual $1/4^\circ$ pixel is located within the interior of mesoscale eddies or meanders, as defined by the outermost closed contour of SLA defining a coherent mesoscale structure.

The accompanying figure for each section displays the sea level anomaly (SLA) as estimated by high-pass filtering of the satellite altimetry-derived sea surface height fields. Overlaid are the trajectory of the *R/V Atlantis*, location of Argo float profiles, and the paths of drifters within 15 days of out arrival at the station.

Besides instantaneous images of the SLA field, this document contains images of several Lagrangian diagnostics calculated from the altimetry-derived velocity field: the Finite Size Lyapunov Exponents (FSLE) – an indicator of frontal activity, the eddy Retention Parameter (RP) – a measure of for how long water parcels are trapped within the eddy core, and the origin of water parcels – i.e. the location of water parcels 15 days before the observations.

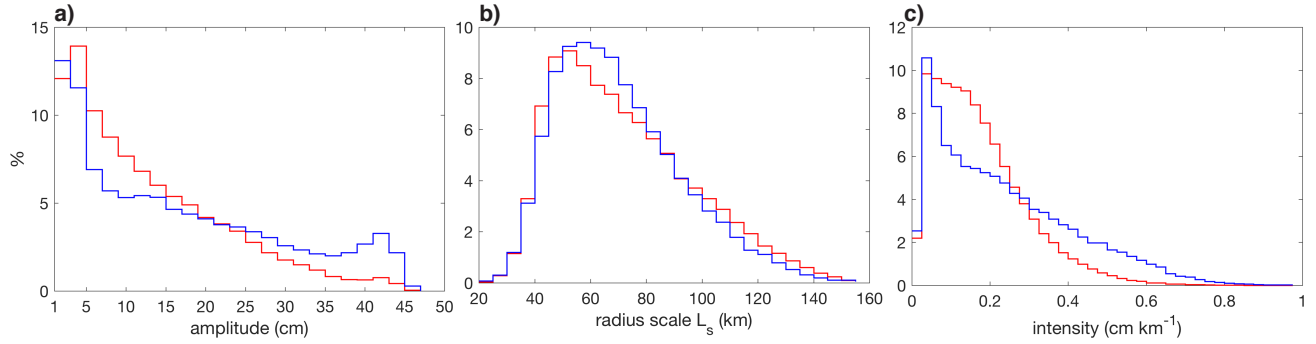


Figure 2: Histograms of (a) CMS amplitude, (b) speed-based radius scale L_s , and (c) intensity, defined as A/L_s where A is CMS amplitude. These are constructed from all eddies in the NAAMES region over the 20-year satellite altimetry era. Anticyclones are shown in red and cyclones in blue. In the Northern Hemisphere, anticyclones rotate clockwise and cyclones counterclockwise. Generally, cyclones are characterized by up-welled isopycnals, cold water, and shallower mixed layers, and anticyclones by down-welled isopycnals, warm water, and deeper mixed layers.

2 A Subregional Classification Scheme for the North Atlantic

The NAAMES expeditions covered a larger region of the North Atlantic with significance in spatial variability in physical and biological properties. To first order, much of this variability scales with latitude, however, a simple geographic binning of the NAAMES observations would not correctly capture the spatial variability in the mesoscale eddy field (Fig. 1). We propose a subregional classification scheme that is based on the mean dynamic topography (MDT), defined as the 20-year average of sea surface height measured by a consolidation of satellite altimeters. We have chosen 4 subregions: (1) The subarctic, defined as regions with $MDT \leq -51$ cm; (2) temperate, defined as the area with MDT in the range -51 cm $< MDT \leq -10$ cm; (3) subtropical, defined as the region with MDT in the range -10 cm $< MDT \leq 30$ cm; (4) and the Sargasso Sea and Gulf Stream ($MDT > 30$ cm).

3 Overview of Coherent Mesoscale Structures in the NAAMES Region

The northwestern Atlantic is a region of large amplitude CMSs, with the largest features falling in the upper 95th percentile of amplitude globally. The largest amplitude CMSs are found in the Gulf Stream region where average amplitude can exceed 40 cm (Fig. 4). This results from mesoscale meanders of the Gulf Stream becoming unstable and pinching off to become eddies. In the region of focus for NAAMES (see black rectangle in Fig. 4), there is a general southward gradient in increasing CMS amplitude, with a region of moderate amplitude CMS (≈ 20 cm) entering from the east near the middle of the domain. Eddies in the northern portion of the NAAMES region likely form in the open ocean as a result of baroclinic instabilities.

The distribution of CMS amplitudes in the NAAMES region is not symmetric with respect to polarity; a larger proportion of large amplitude CMSs are cyclones, when compared to anticyclones (Fig. 2a). Conversely, a greater number of large radius eddies are anticyclones (Fig. 2b). This combines to result in higher intensity CMS, defined here as the ratio of amplitude to radius, that are preferentially cyclonic. (Fig. 2c).

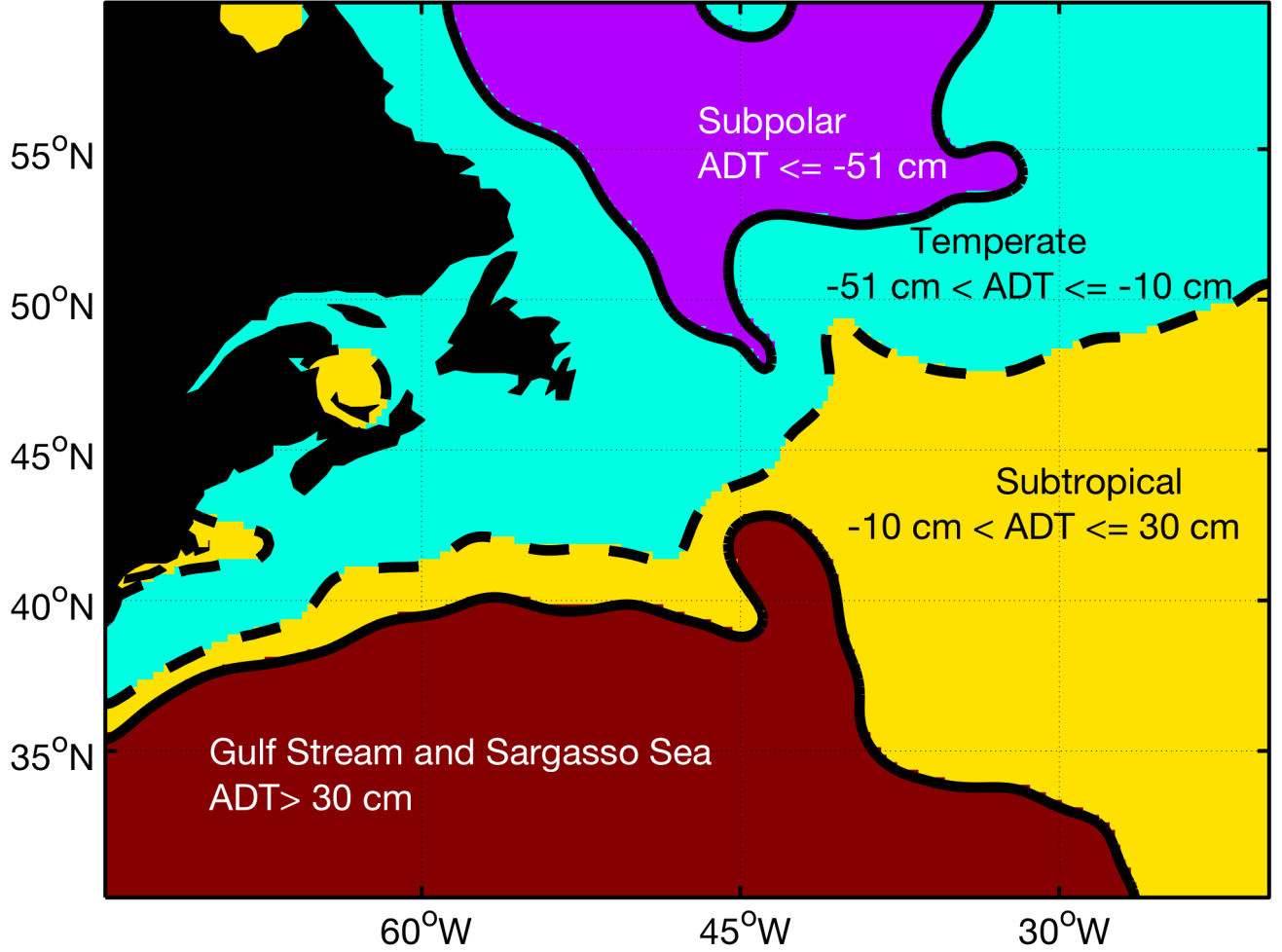


Figure 3: North Atlantic sub regions based on mean dynamic topography.

4 Lagrangian re-analyses of altimetry

Lagrangian diagnostics are generally defined as quantities calculated in the frame of reference of a water parcel that is followed through time. To calculate any Lagrangian diagnostic, an estimate of the velocity field is needed: in the analyses presented in this document (as in a good amount of literature) the velocity field is estimated using altimetry (i.e. measures of Sea Surface Height). Since estimating horizontal velocities from altimetry requires making the assumption of geostrophic equilibrium, the velocity field -and the derived Lagrangian diagnostics- are expected to describe the ocean geostrophic layer, that typically overlaps with the mixed layer, with the exception of the top surface layer (Ekman layer) where wind driven circulation is dominant. Nevertheless Lagrangian diagnostics have been successfully used, among others, to estimate biogeochemical rates [d'Ovidio et al. (2015); Sanial et al. (2014)], defining phytoplankton biogeographical boundaries [Lehahn et al. (2007); d'Ovidio et al. (2010)], identify hotspots of biodiversity [De Monte et al. (2013)], locate key regions of large animals foraging activity [Kai et al. (2009); De Monte et al. (2012); Cotté et al. (2015); Della Penna et al. (2015)], detect favorable fishery conditions [Prants et al. (2014)], and suggest boundaries of open ocean marine protected areas [Della Penna et al. (2017)].

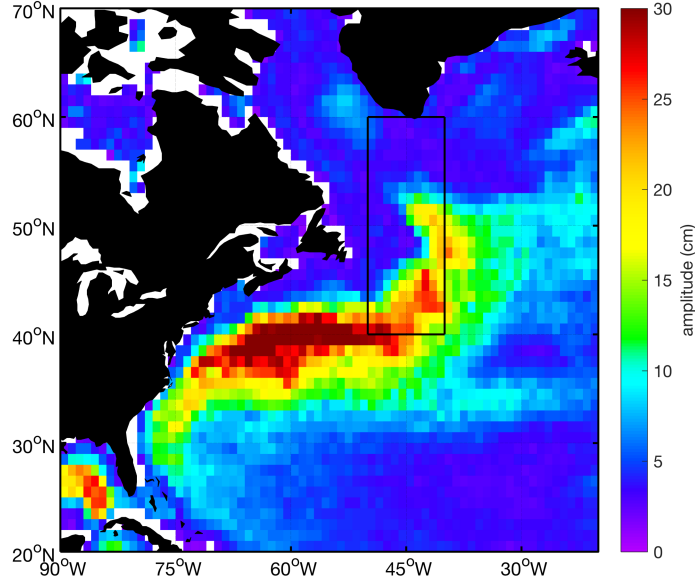


Figure 4: Map of 10-19.7ms amplitude per 1° square. The regions over which statistics and the histograms shown in Fig. 2 are computed is indicated by the black rectangle.

Caveats

1. Altimetry-derived diagnostics do not perform well in the presence of very strong vertical velocities (e.g. in upwelling regions) or regions with very shallow bathymetry (because altimetry tends to under-estimate horizontal velocities).
2. It is generally a good idea to look at the map of a Lagrangian diagnostic before using the extracted value for a specific location. Using an extracted value only it is easy to miss a structure that was indeed encountered but was misplaced of a few km by altimetry (the error can be up to 30 km!).
3. Even if the resolution of the diagnostics can be as small as we like, the velocity field's resolution is limited to the detection of mesoscale features and mesoscale-induced submesoscale ones (I.e. we miss most of submesoscale features).
4. All the Lagrangian diagnostics presented in this study are calculated from horizontal velocities. This means that if a tracer has been transported to the surface by any kind of vertical movement, the diagnostics are not correctly identifying its origin.

4.0.1 Finite Size Lyapunov Exponents – an index of frontal activity (units = d^{-1})

Finite Size Lyapunov Exponents (FSLE) are defined as the rate of convergence of water parcels initially far apart (how much far apart is one of the parameter of the calculation). High values of FSLE refer to regions where water parcels that were initially far have converged quickly. In the calculations for this document, FSLE were computed using the formula:

$$FSLE(lon, lat, t, \delta_0, \delta) = \frac{1}{\tau} \log\left(\frac{\delta}{\delta_0}\right) \quad (1)$$

where τ is the time taken for water parcels at an initial distance of δ (in this study = 0.3 deg) to reach a final separation of δ_0 (in this study = 0.01 deg). (lon,lat) refer to the location in time and space of the region where the FSLE is computed. In this analysis τ can reach a maximum value of 60 days. A good study of the robustness of FSLE can be found in (?).

4.0.2 Eddy retention parameter – how eddies trap or leak (units = d)

The eddy retention parameter (RP) quantifies for how long a water parcel has been recirculating within the core of an eddy [d'Ovidio et al. (2013)]. The eddy core is defined as a region of negative values of the Okubo-Weiss parameter OW [Okubo (1970); Weiss (1991)] [units = d^{-2}]. The OW is defined as:

$$OW(t, lon, lat) = s(t, lon, lat)^2 - \omega(t, lon, lat)^2; \quad (2)$$

$$s^2 = \left(\frac{\partial v_x}{\partial x} - \frac{\partial v_y}{\partial y} \right)^2 + \left(\frac{\partial v_y}{\partial x} + \frac{\partial v_x}{\partial y} \right)^2; \quad (3)$$

$$\omega^2 = \left(\frac{\partial v_y}{\partial x} - \frac{\partial v_x}{\partial y} \right)^2 \quad (4)$$

where x and y refer to longitude and latitude and v_x and v_y are the zonal and meridional components of the velocity field. The OW basically represents the difference between the vorticity of the velocity field and the strain. It is expected to be negative in regions where the rotational component of the velocity field dominates over the strain (e.g. within eddy cores) and positive in regions where strain dominates over vorticity (e.g. at the peripheries of eddies 5).

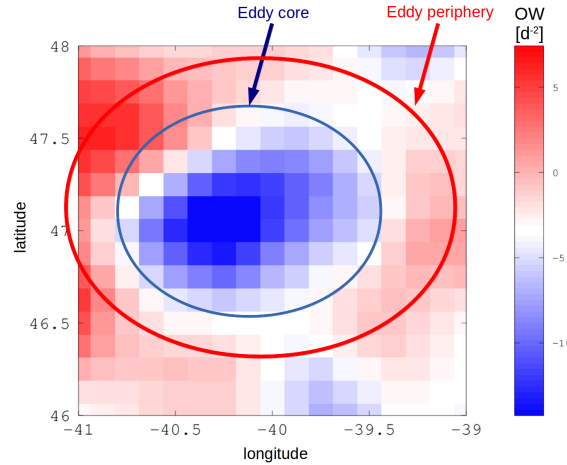


Figure 5: An example of the typical core vs periphery structure of the OW parameter for the eddy at Station 3 during NAMES-3. The retention parameter calculates for how long a water parcel has remained within the negative region (blue in this plot).

In the study the maximum time used for the backward advection of water parcels is 30 days.

4.0.3 Origin of water parcels – where do tracers come from? (units = °)

These diagnostics are a measure of the latitude and longitude of water parcels 15 days before the “sampling date”. The same analysis can be done for other times if it is interesting, but the accuracy of advection decreases with the increase of time.

5 Summary of eddy features sampled during the NAAMES program

Figure 6 and table 1 summarize the stations sampled during the four NAAMES cruises and their properties in respect to the mesoscale eddy field. Out of the total of 32 stations sampled in the course of the four cruises, one was located within a mode-water eddy, 7 within anticyclonic features and 7 within cyclones.

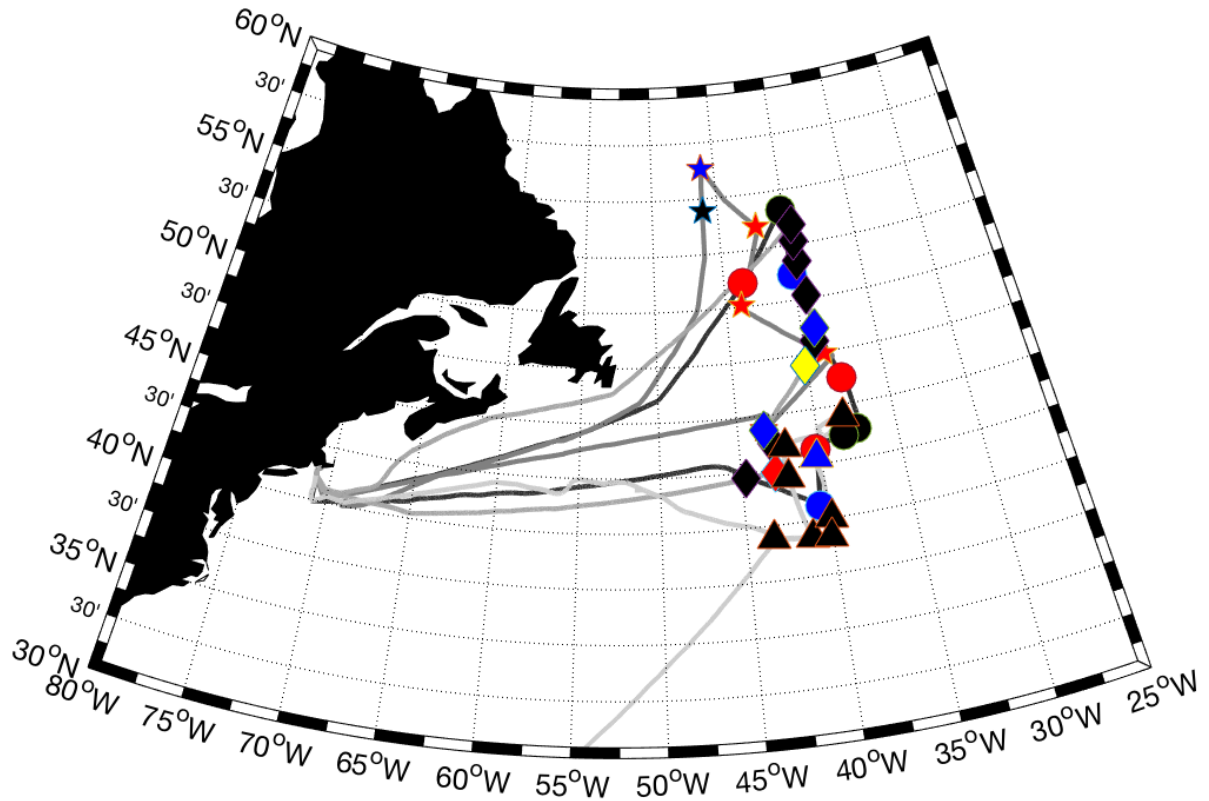


Figure 6: Eddy features sampled during the four cruises of the NAAMES program. Circles refer to NAAMES1, starts to NAAMES2, diamonds to NAAMES3 and triangles to NAAMES4. Cyclonic features are color coded in blue, anticyclones in red and the mode-water eddy sampled during NAAMES3 is marked in yellow. Stations that were not located within an eddy are marked in black.

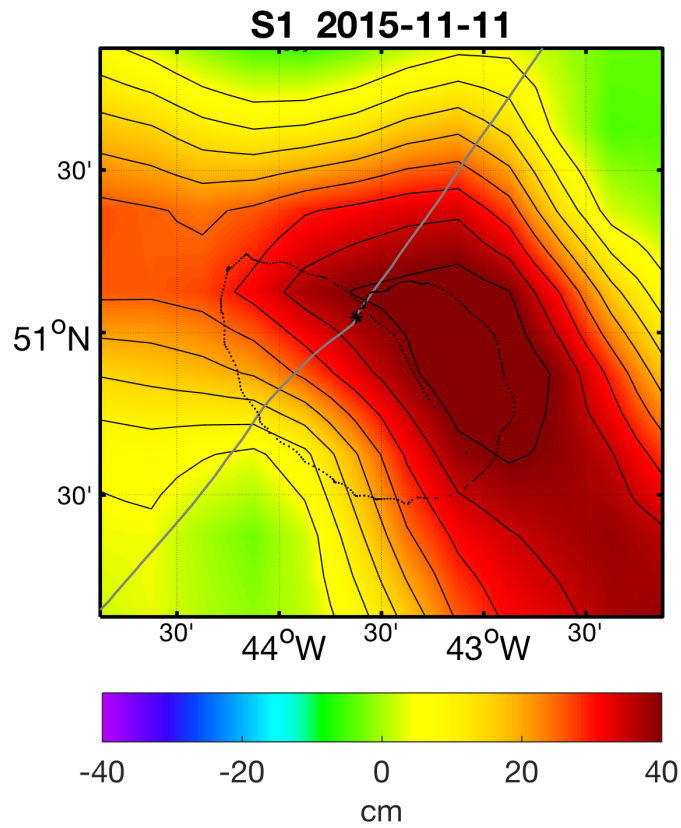
Table 1: Summary of eddy properties for the station sampled during the NAAMES program. Red lines refer to anticyclonic eddies, blue lines to cyclonic eddies and the yellow line refers to the mode-water eddy sampled during NAAMES3. Solid red and blue refer to eddy cores and light red and blue refer to eddy peripheries.

Cruise	Station	Eddy?	Core/periphery	Polarity	Retention	Subregion
N1	1	Y	periphery	anticyclone	weak	Temperate
	2	N	N/A	N/A	N/A	Subpolar
	3	Y	periphery	cyclone	strong	Temperate
	4	Y	periphery	anticyclone	weak	Subtropical
	5	N	N/A	N/A	N/A	Subtropical
	6	Y	periphery	anticyclone	strong (?)	Subtropical
	7	Y	core	cyclone	strong	Subtropical
N2	0	N	N/A	N/A	N/A	Subpolar
	1	Y	core?	cyclone	weak	Subpolar
	2	Y	periphery	anticyclone	weak	Subpolar
	3	Y	periphery	anticyclone	strong	Temperate
	4	Y	core	anticyclone	moderate	Subtropical
N3	5	Y	periphery	cyclone	weak	Subtropical
	1a	N	N/A	N/A	N/A	Gulf Stream and Sargasso Sea
	1b	Y	core	anticyclone	strong	Gulf Stream and Sargasso Sea
	1.5	N	N/A	N/A	N/A	Subtropical
	2	Y	core	cyclone	strong	Subtropical
	3	Y	core	mode-water	strong	Subtropical
	3.5	N	N/A	N/A	N/A	Subtropical
	4	Y	periphery	cyclone	strong	Subtropical
	4.5	N	N/A	N/A	N/A	Temperate
	5	N	N/A	N/A	N/A	Temperate
N4	5.5	N	N/A	N/A	N/A	Subpolar
	6	N	N/A	N/A	N/A	Subpolar
	1	N	N/A	N/A	N/A	Gulf Stream and Sargasso Sea
	2	N	N/A	N/A	N/A	Gulf Stream and Sargasso Sea
	2.5	N	N/A	N/A	N/A	Gulf Stream and Sargasso Sea
	3	N	N/A	N/A	N/A	Subtropical
	4	N	N/A	N/A	N/A	Subtropical
	E4	Y	periphery	cyclone	weak	Subtropical
	2RD	N	N/A	N/A	N/A	Subtropical
	2RF	N	N/A	N/A	N/A	Subtropical

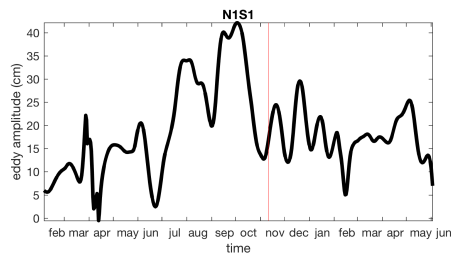
6 NAAMES 2015

6.1 S1 NAAMES-1

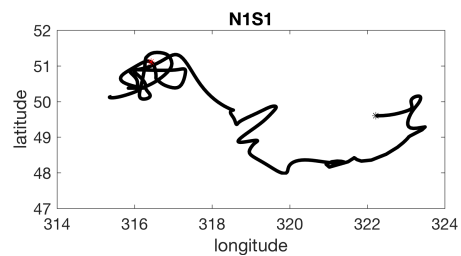
This station was chosen as a “dry run” and was placed on the path to the northernmost station and was position where we crossed into a non-retentive (8) anticyclonic eddy. As luck would have it, this particular anticyclone was sampled again on NAAMES-2 at S3. The drifter deployed in this particular eddy during NAAMES-1 made a full loop around the anticyclone and returned to within 1 km of its deployment location, before moving eastward and into the Gulf Stream.



(a) Sea Level Anomaly



(b) Amplitude



(c) Eddy Trajectory

Figure 7: (a) Mapped sea level anomaly at Station 1. Solid (broken) black contours indicate SLA at an interval of 5 cm. Grey line is the track of the R/V Atlantis. Small black points indicate hourly drifter location for all drifters within the region starting on the first day of occupation of the station and continuing for 15 days. Black * indicates the location of CTD cast with cast number indicated to the northwest of the cast location. (b) Amplitude time series of eddy at Station 1, red line indicates time of occupation. (c) Trajectory of eddy. * indicates eddy location at time of occupation and * location of origination.

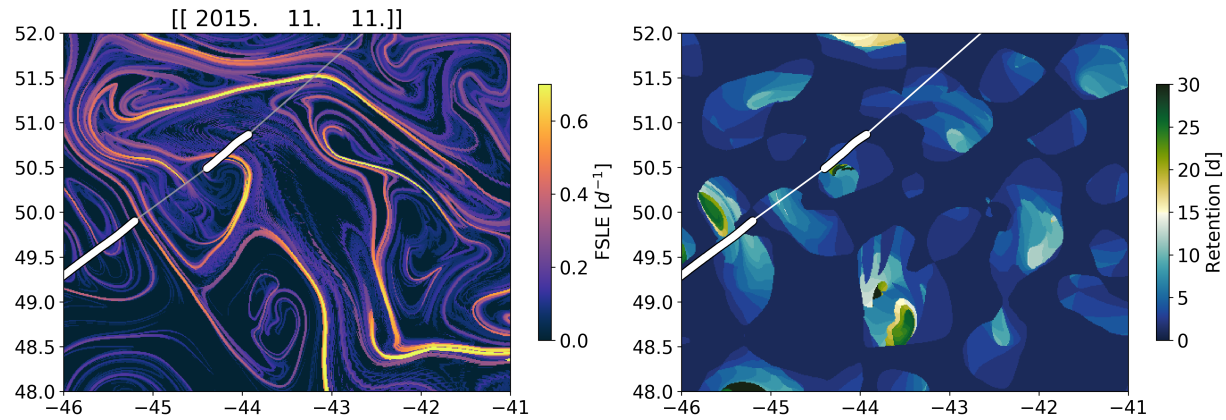


Figure 8: FSLE and RP calculated for Station 1 and surrounding waters. While the region is not particularly retentive, FSLE and water origin (Fig. 9) suggest the presence of strong gradients that could be interesting to compare with observations from the in-line system.)

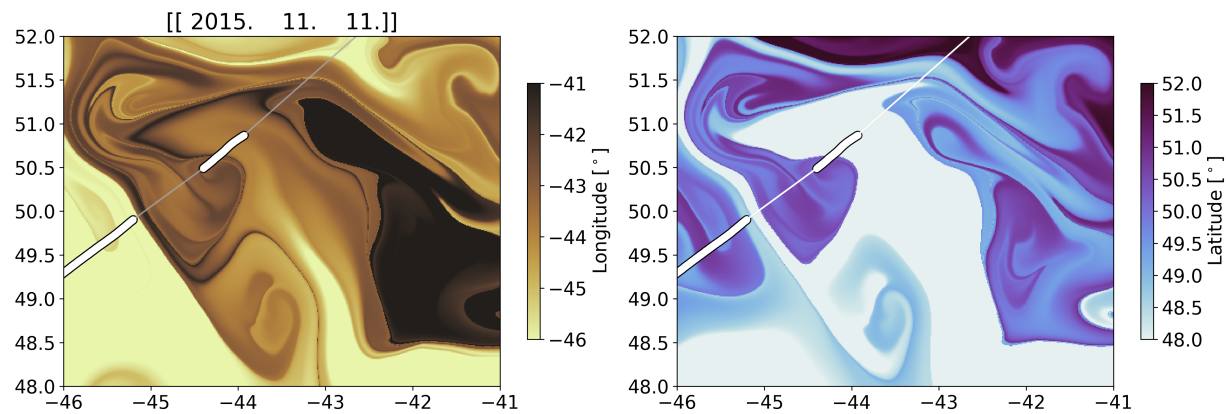


Figure 9: Water origin (longitude and latitude) for Station 1 and surrounding waters.

6.2 S2 NAAMES-1

Station 2 was our northern-most station on NAAMES-1. In addition, this station was located in a region that could be called an “eddy desert.” The trajectories of the drifters indicate that there was very little surface current and most of the motion is limited to small inertial loops.

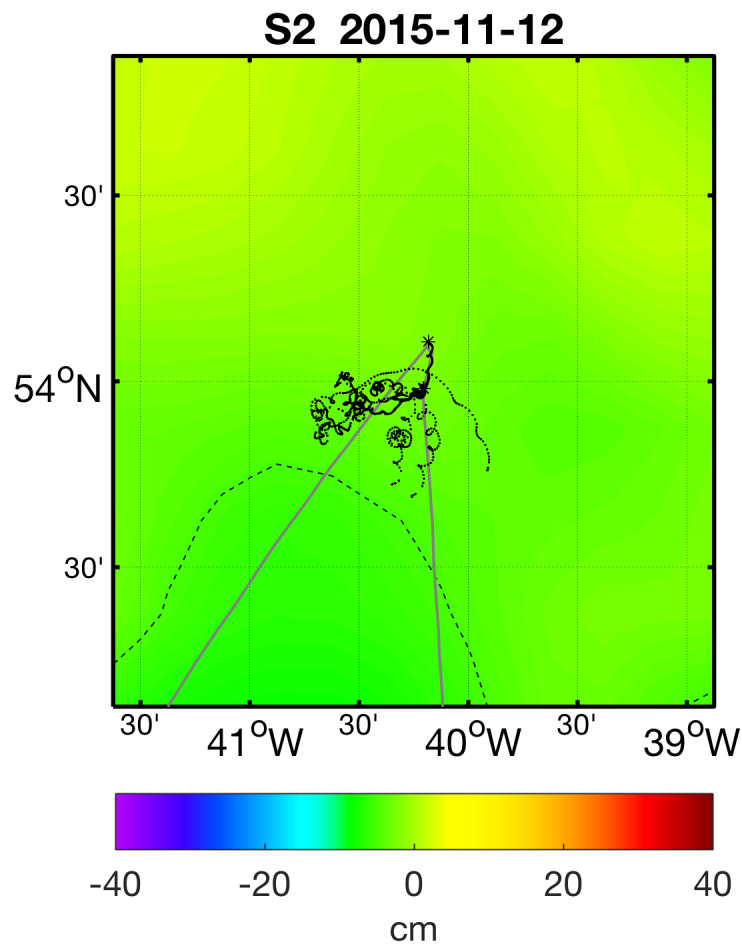


Figure 10: (Mapped sea level anomaly at Station 2. Solid (broken) black contours indicate SLA at an interval of 5 cm. Grey line is the track of the R/V Atlantis. Small black points indicate hourly drifter location for all drifters within the region starting on the first day of occupation of the station and continuing for 15 days. Black * indicates the location of CTD casts.

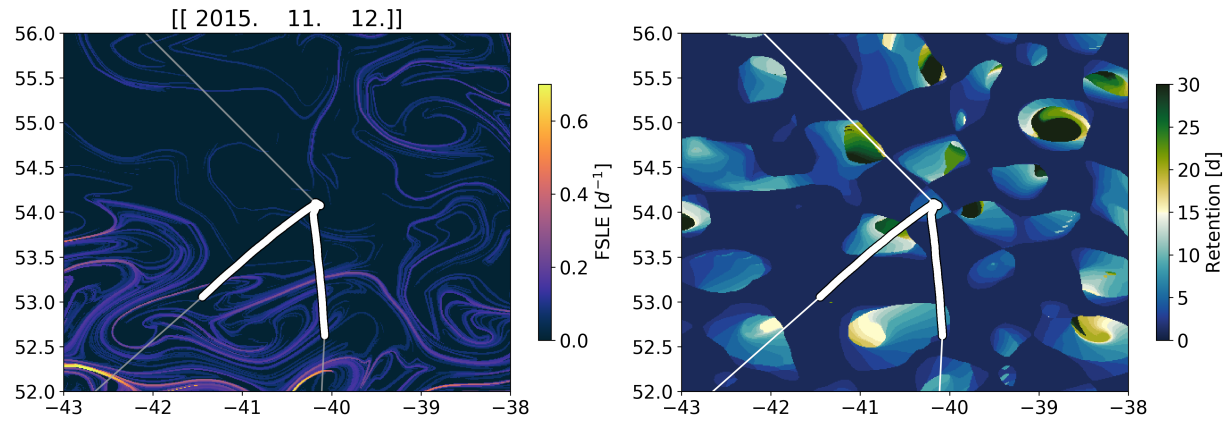


Figure 11: FSLE and RP calculated for Station 2 and surrounding waters.

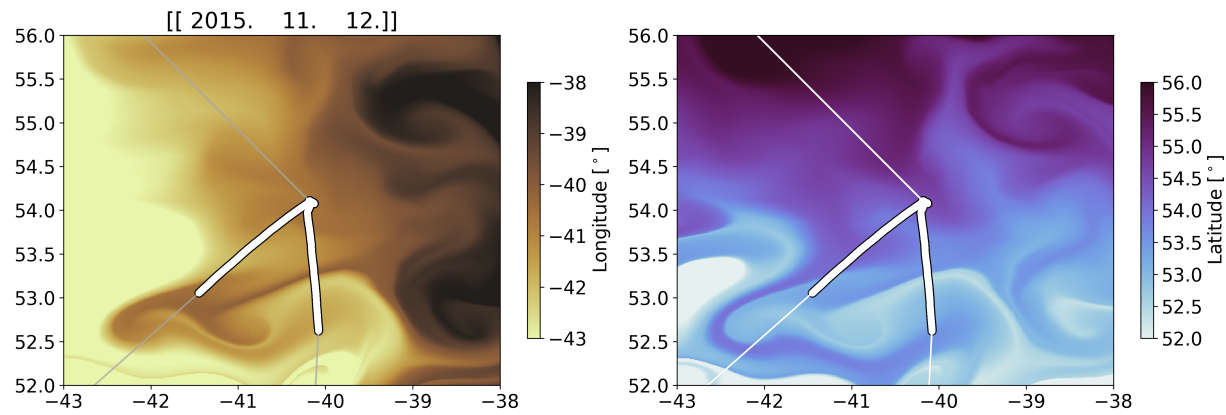


Figure 12: Water origin (longitude and latitude) for Station 2 and surrounding waters.

6.3 S3 NAAMES-1

Station 3 was initially chosen because it looked to be the location of a small and compact cyclonic eddy. Following the expedition, investigation of the SLA fields revealed that this feature was very short lived and therefore was either never truly an eddy, or was quickly absorbed by another CMS. The amplitude of this cyclone was very small, on the order of 8 cm, yet Lagrangian re-analyses suggest that it may have been retentive (Figure 14).

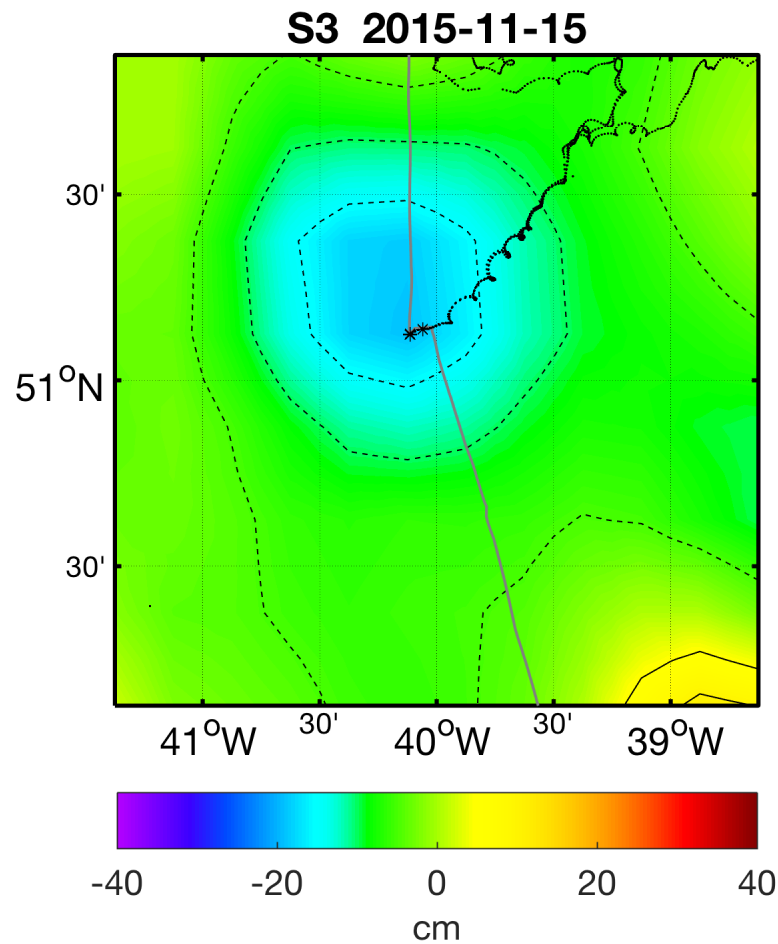


Figure 13: Same as Fig. 10

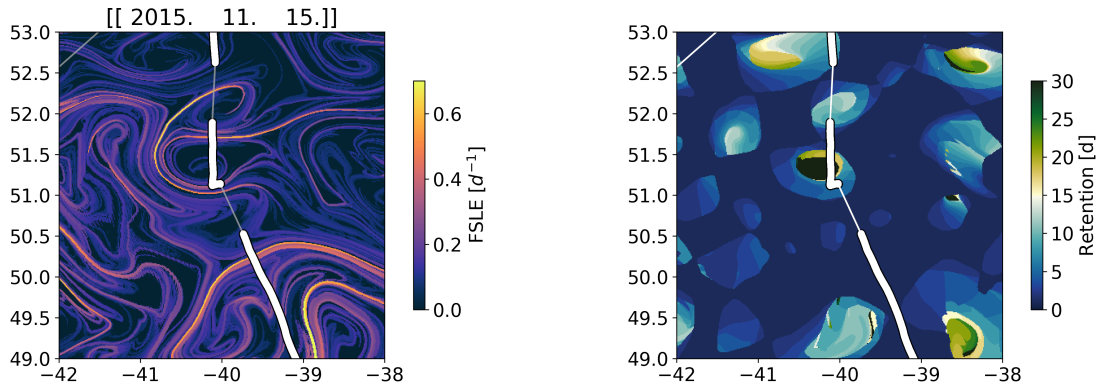


Figure 14: FSLE and RP calculated for Station 3.

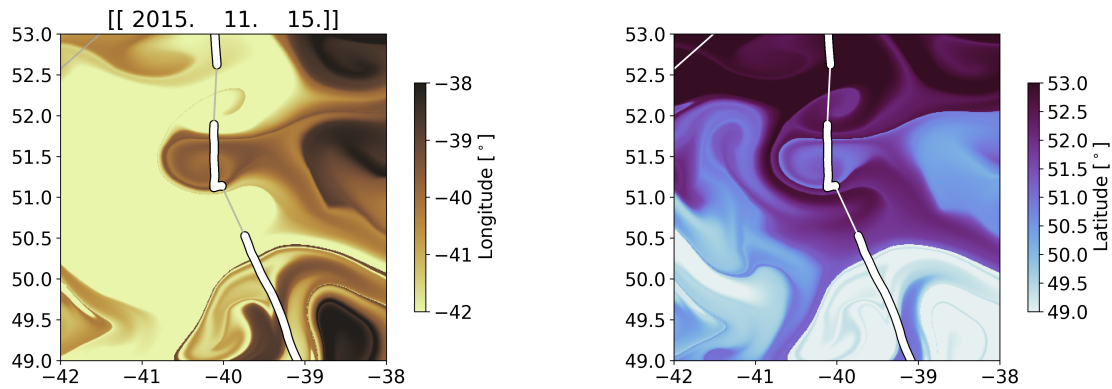


Figure 15: Water origin (longitude and latitude) for Station 3.

6.4 S4 NAAMES-1

This location represent the environment along the periphery of an anticyclonic eddy. This anticyclone was of moderate amplitude when we sampled it (17 cm) and towards the end of its life (Fig. 82b). The drifters released at this location propagated northeastward around the anticyclone and remained within(?) the eddy for at least 15 days following occupation. Lagrangian re-analyses indicate that this eddy was weakly retentive (Figure 17), but its retentiveness may have increased during its life cycle.

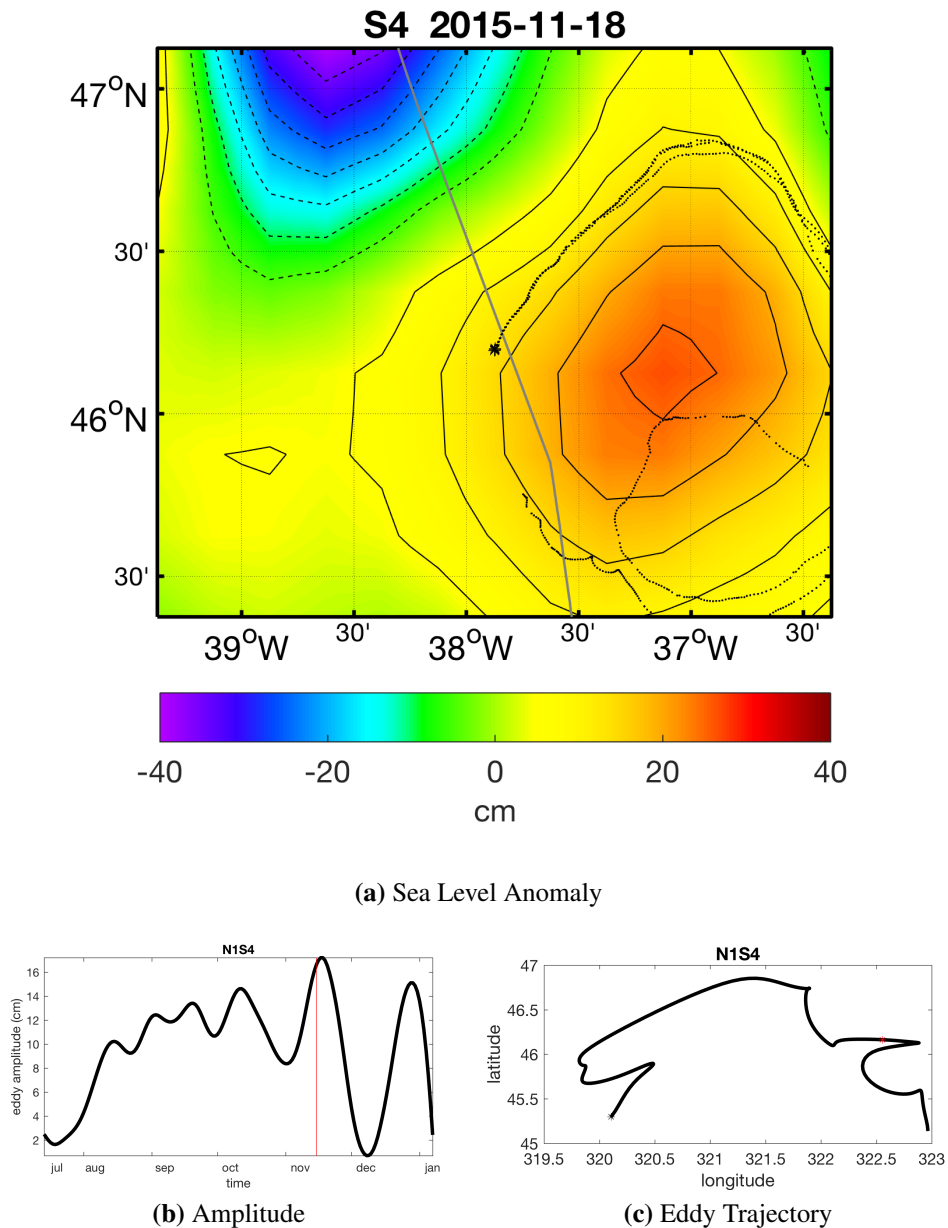


Figure 16: Same as Fig 7

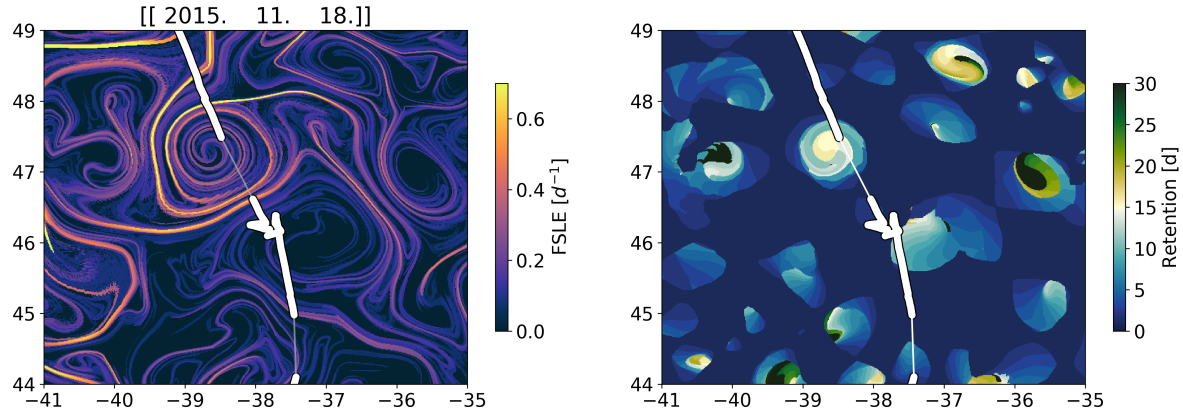


Figure 17: FSLE and RP calculated for Station 4.

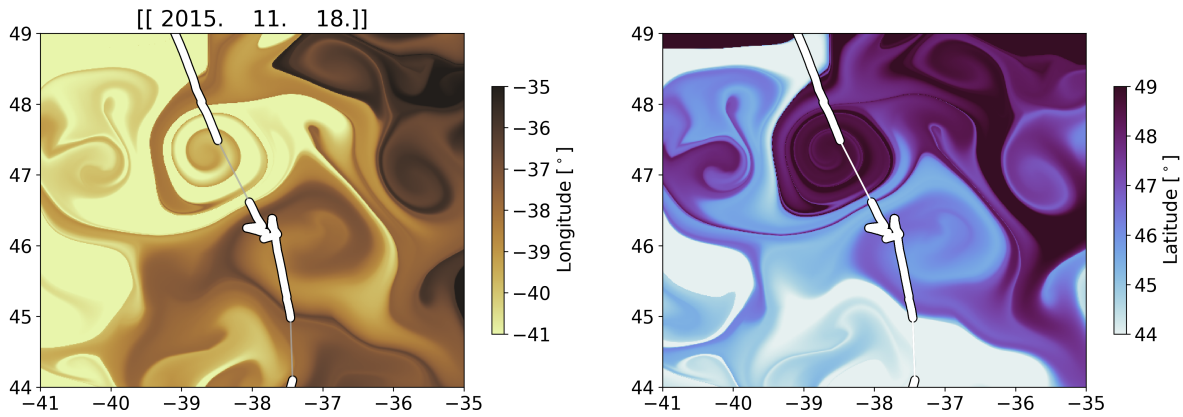


Figure 18: Water origin (longitude and latitude) for Station 4.

6.5 S5 NAAMES-1

Station 5 represents the space between two eddies. This is a dynamic region characterized by robust geostrophic currents. The drifter immediately moved to the north/northeast and made very pronounced inertial loops. After a few days, the drifter was entrained into the adjacent anticyclone.

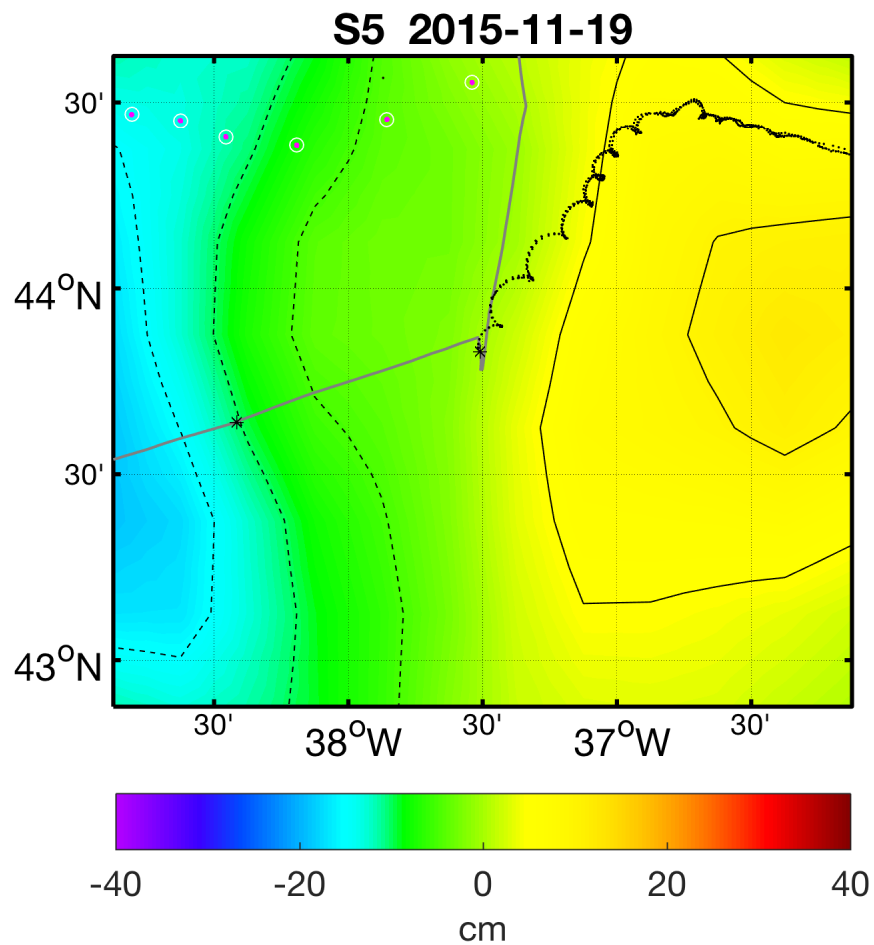


Figure 19: Same as Fig. 10

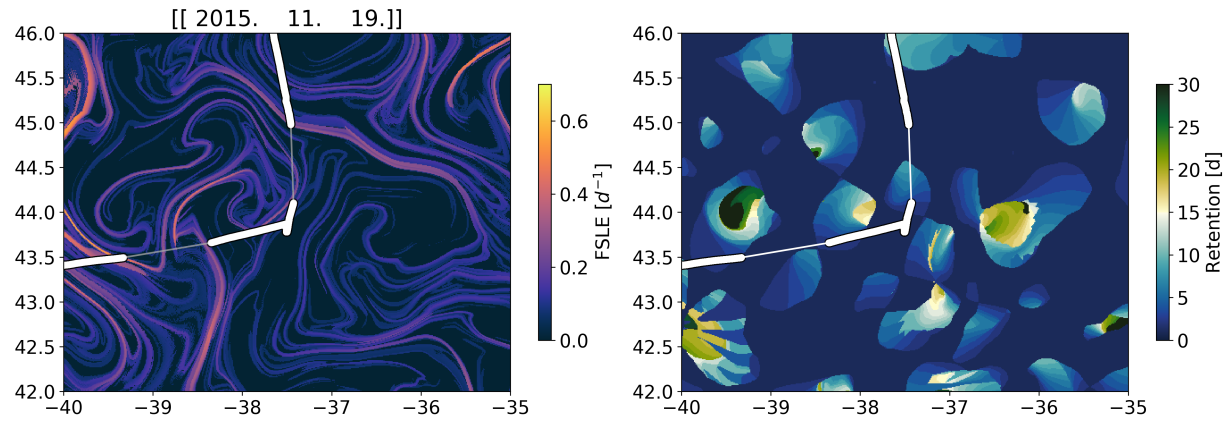


Figure 20: FSLE and RP calculated for Station 5.

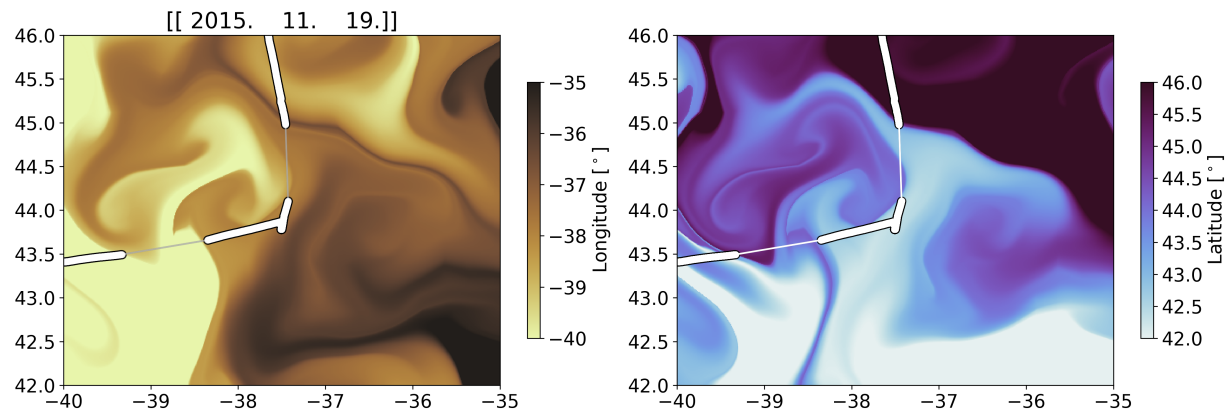


Figure 21: Water origin (longitude and latitude) for Station 5.

6.6 S5b NAAMES-1

Station 5b was an in-between station. It was not located in an eddy.

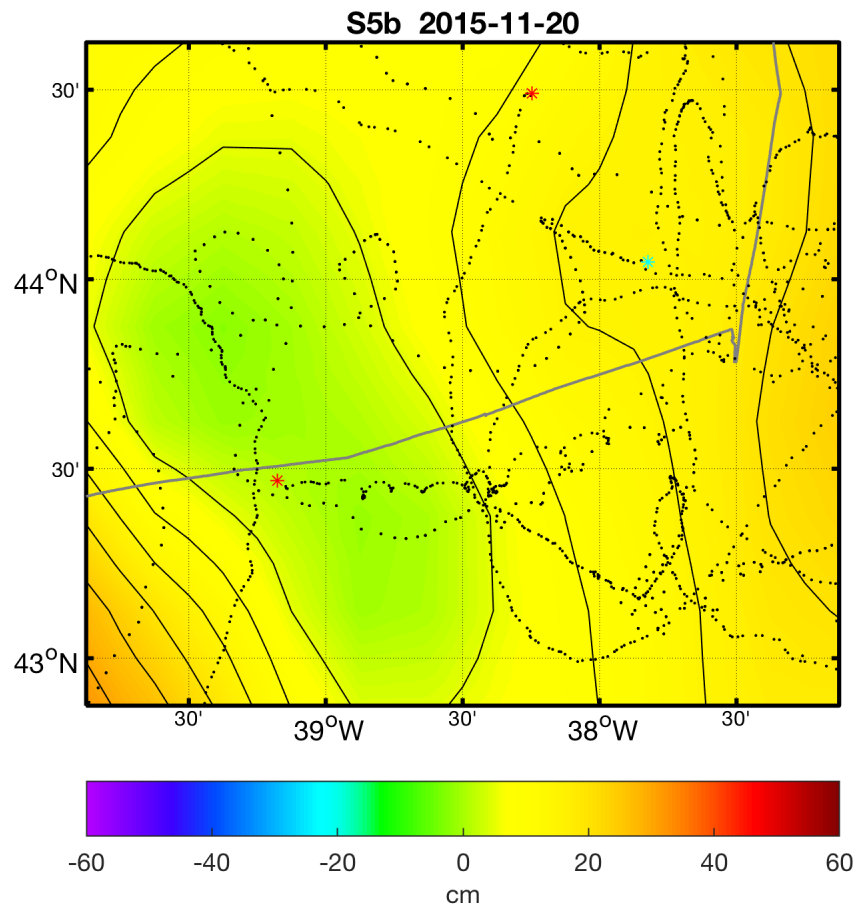


Figure 22: Same as Fig. 10

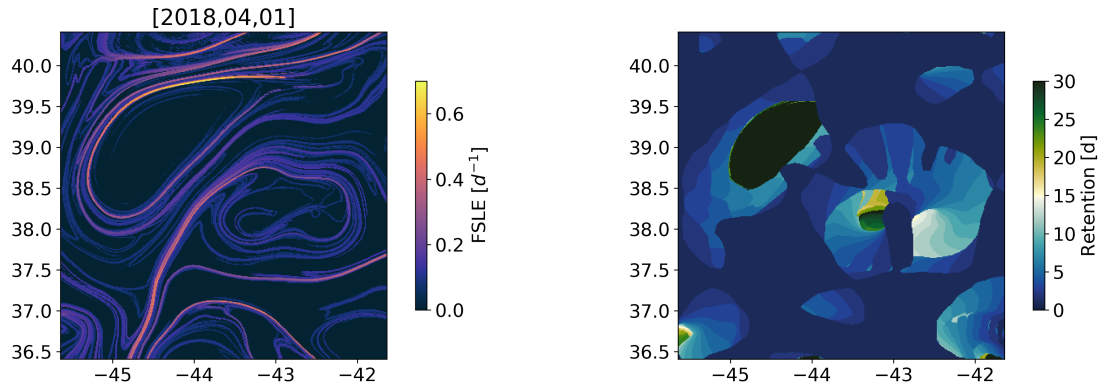


Figure 23: FSLE and RP calculated for Station 5b.

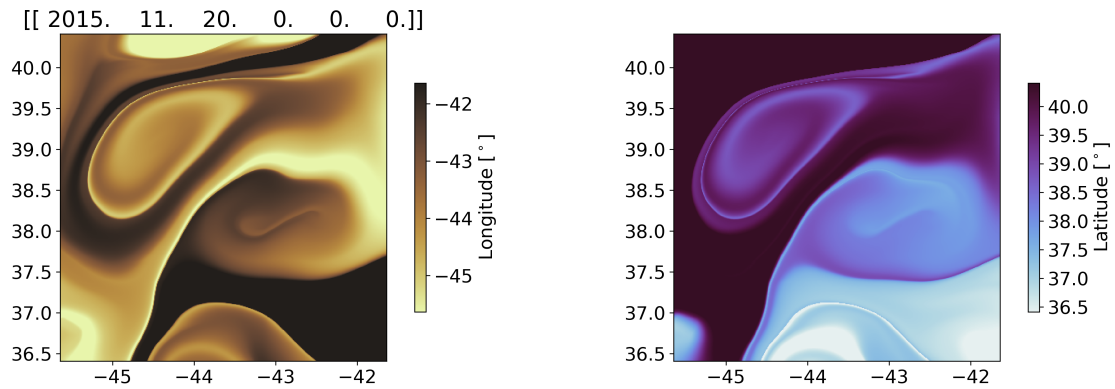


Figure 24: Water origin (longitude and latitude) for Station 5.

6.7 S6 NAAMES-1

Another stop along the periphery of a relatively small anticyclone, Station 6 was a location of the deployment of a number of drifters. Most of the drifters were advected southward by the clockwise-rotating eddy. This eddy was short lived and had a maximum amplitude of 19 cm (Fig. 25).

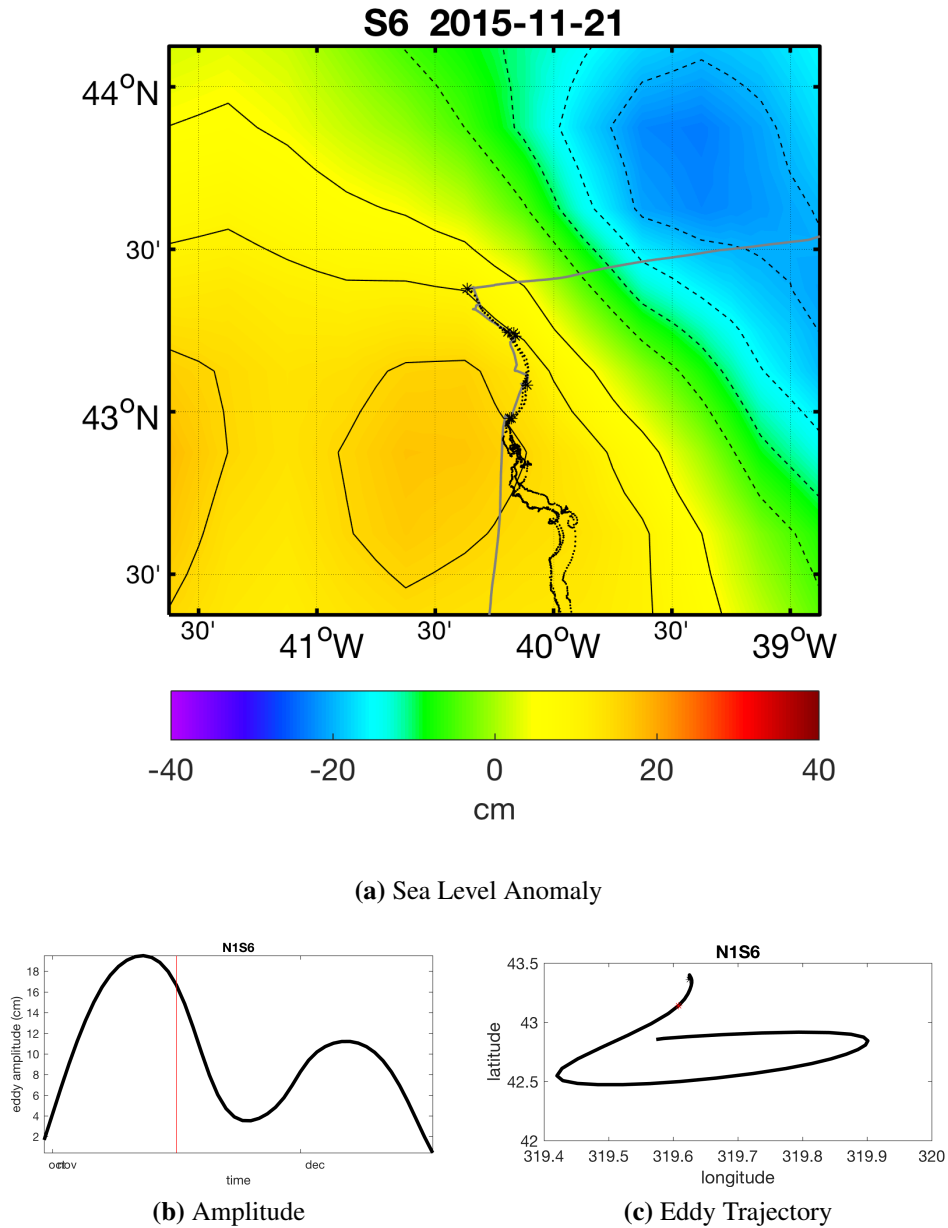


Figure 25: Same as Fig 7

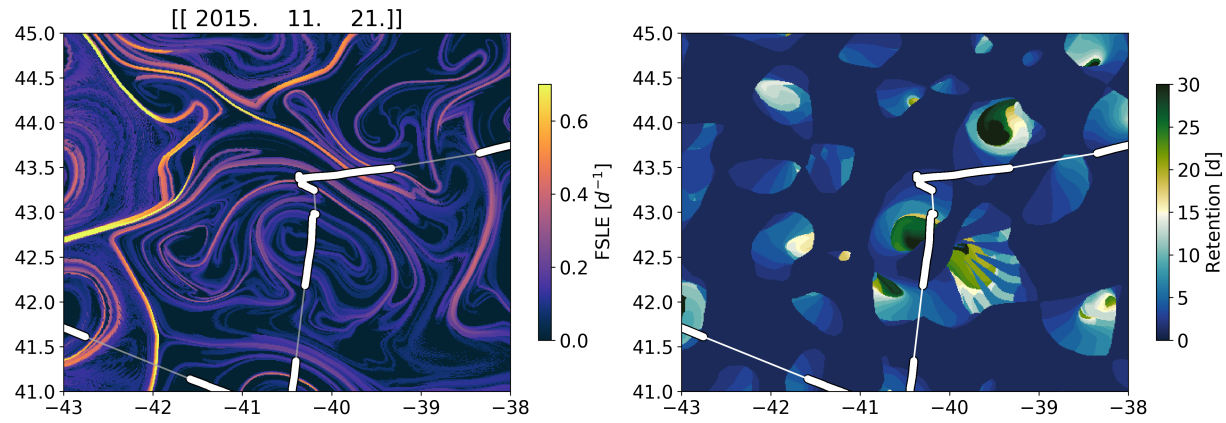


Figure 26: FSLE and RP calculated for Station 6.

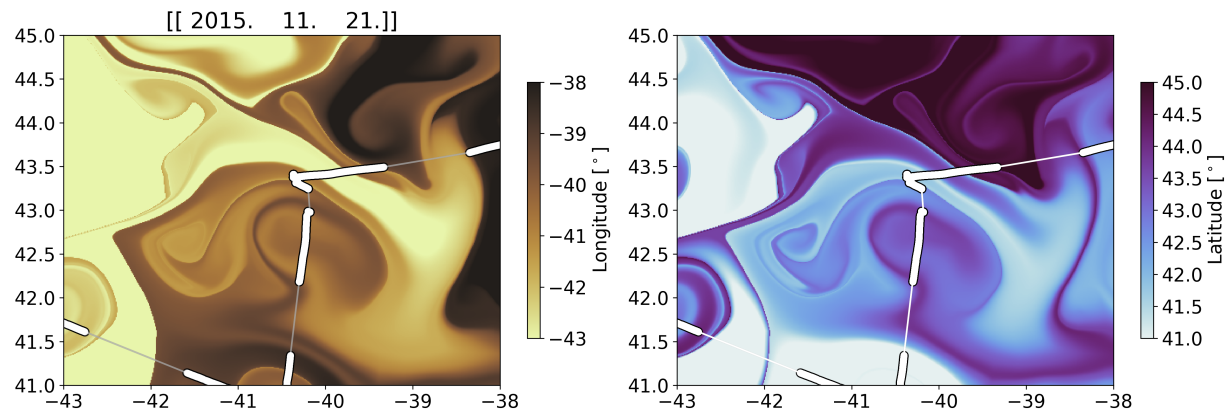


Figure 27: Water origin (longitude and latitude) for Station 6.

6.8 S7 NAAMES-1

Station 7 was in a coherent and retentive cyclone located south of the Gulf Stream. The drifters were effectively trapped by this eddy for nearly a month following deployment. This station represents the conditions in a cyclonic eddy in the southern most reaches of the NAAMES region.

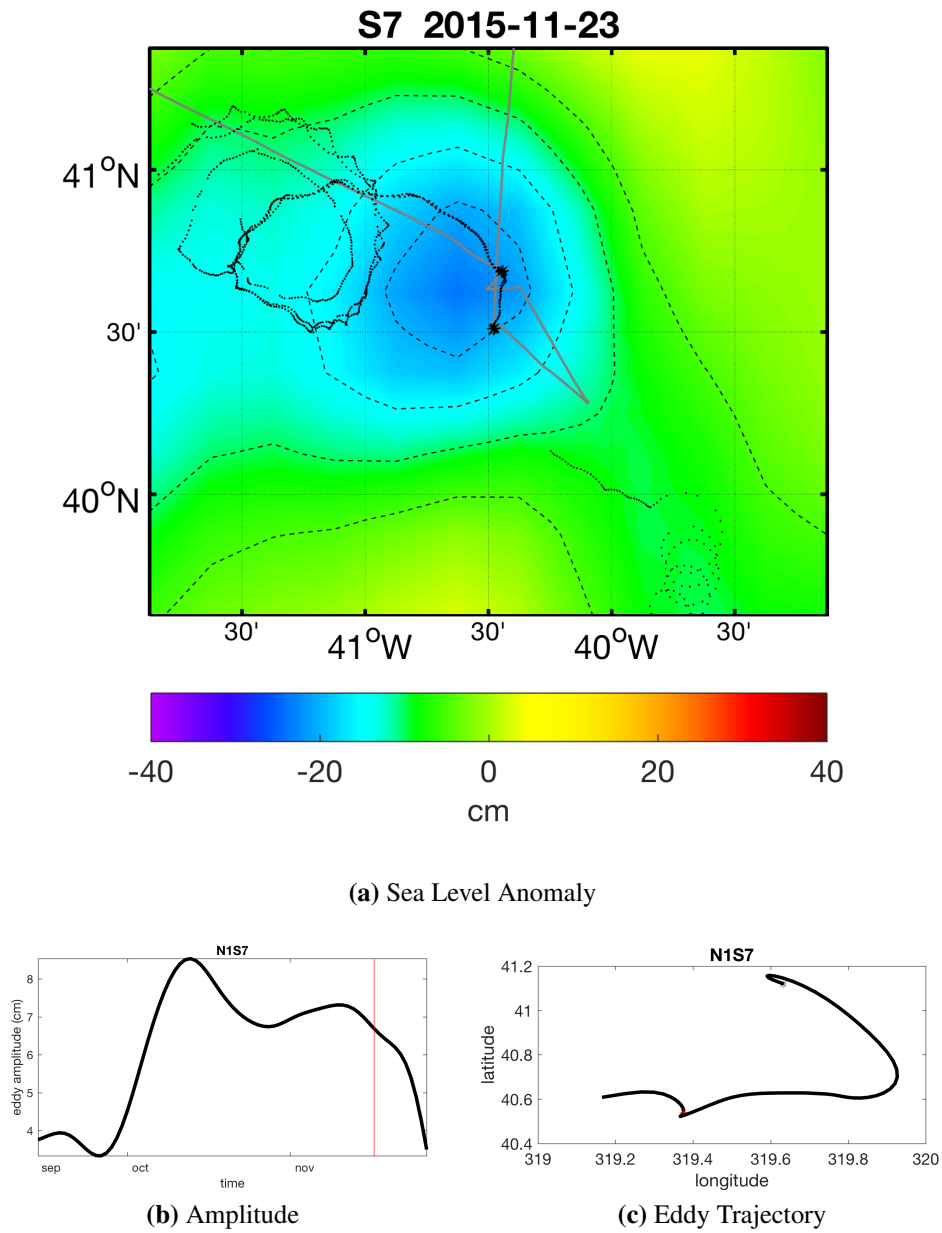


Figure 28: Same as Fig 7

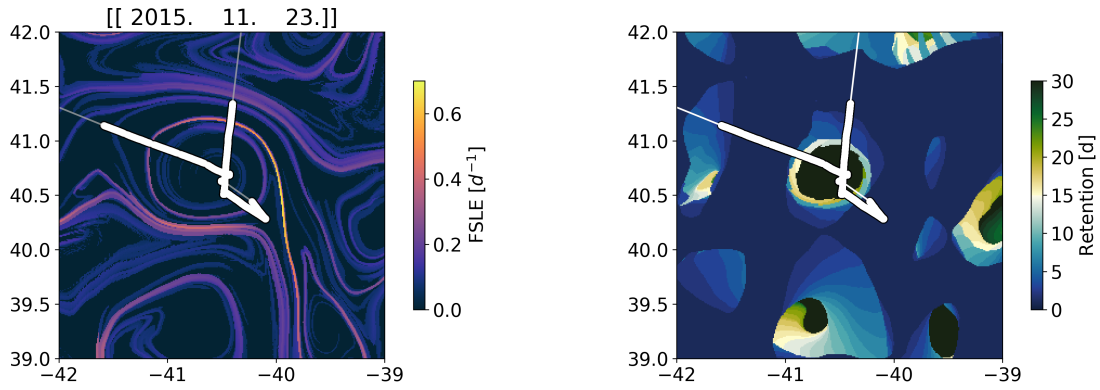


Figure 29: FSLE and RP calculated for Station 7.

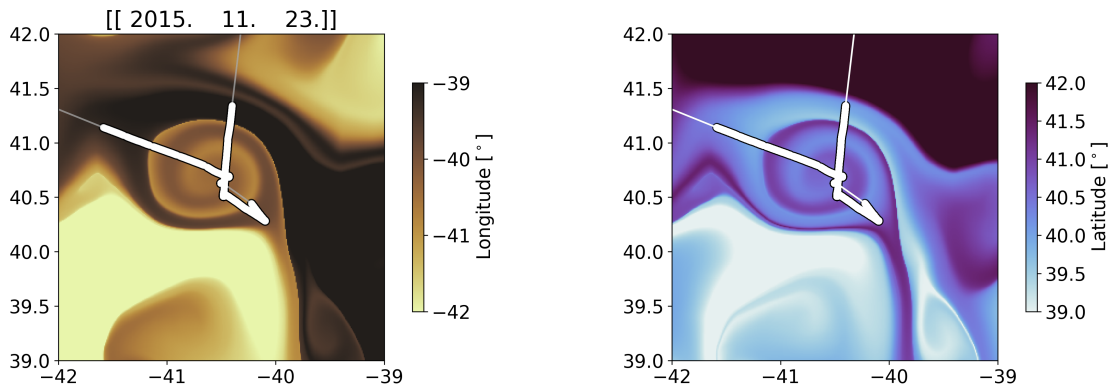


Figure 30: Water origin (longitude and latitude) for Station 7.

7 NAAMES 2016

7.1 S0 NAAMES-2

Station “zero” was once again used as a dry run. This station was outside of any eddies.

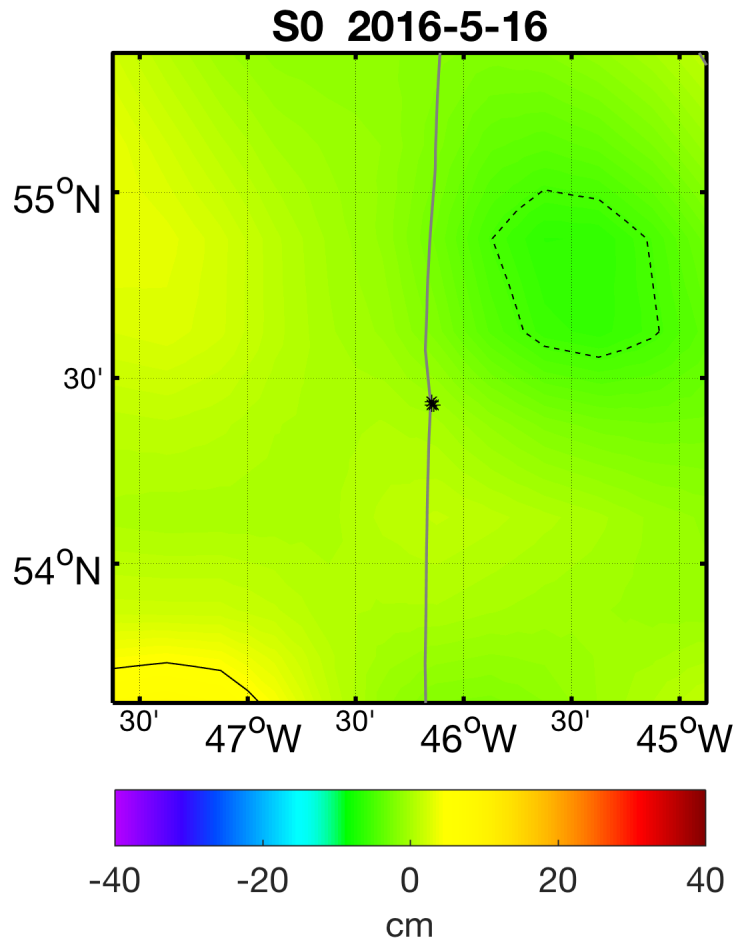


Figure 31: Same as Fig. 10

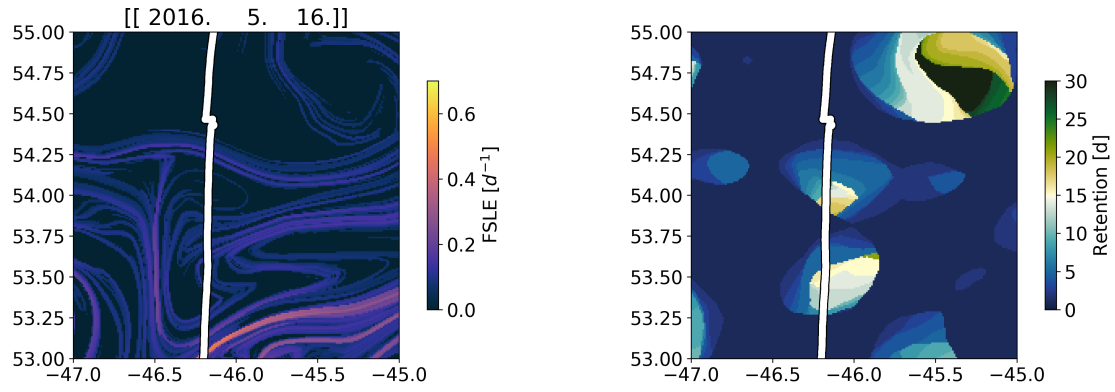


Figure 32: FSLE and RP calculated for Station 0.

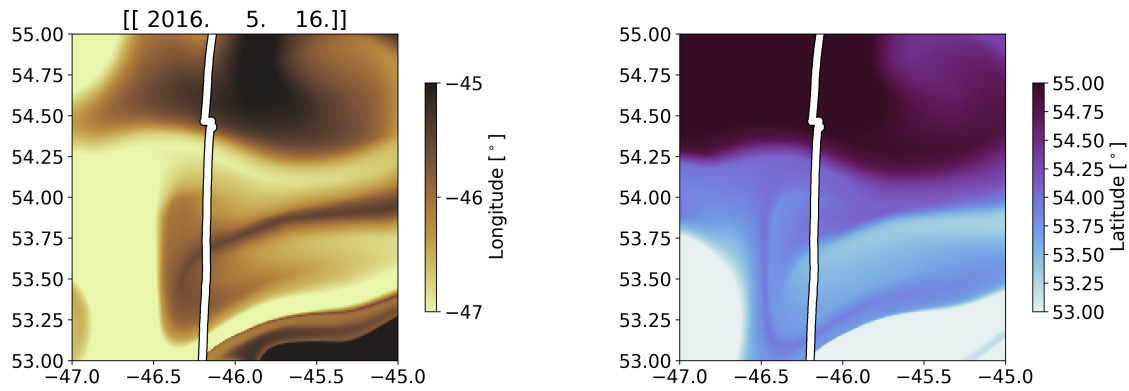


Figure 33: Water origin (longitude and latitude) for Station 0.

7.2 S1 NAAMES-2

Station 1 was our northern-most station on NAAMES-2, even further north than S1 on NAAMES-1. This station was located in a region that could be called an “eddy desert.” The trajectories of the drifters indicate that there was cyclonic rotation in the region, suggesting an eddy was present. Indeed, When SLA field is displayed with colorbar scaling 1/4 that of the other images, a cyclonic eddy is very clear (Fig. 37b)

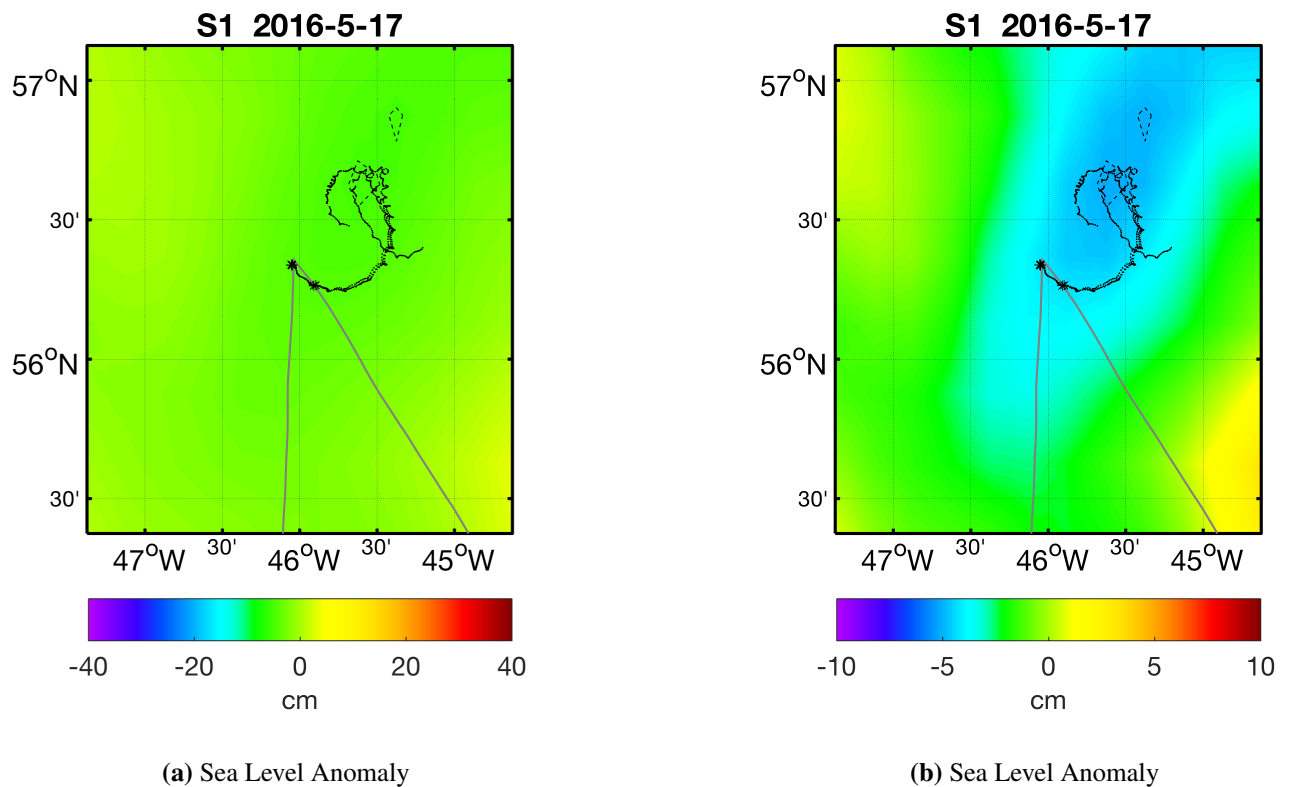


Figure 34: (a) Same as Fig. 10, (b) same as panel a, but colorbar scaling adjusted to show small cyclonic eddy.

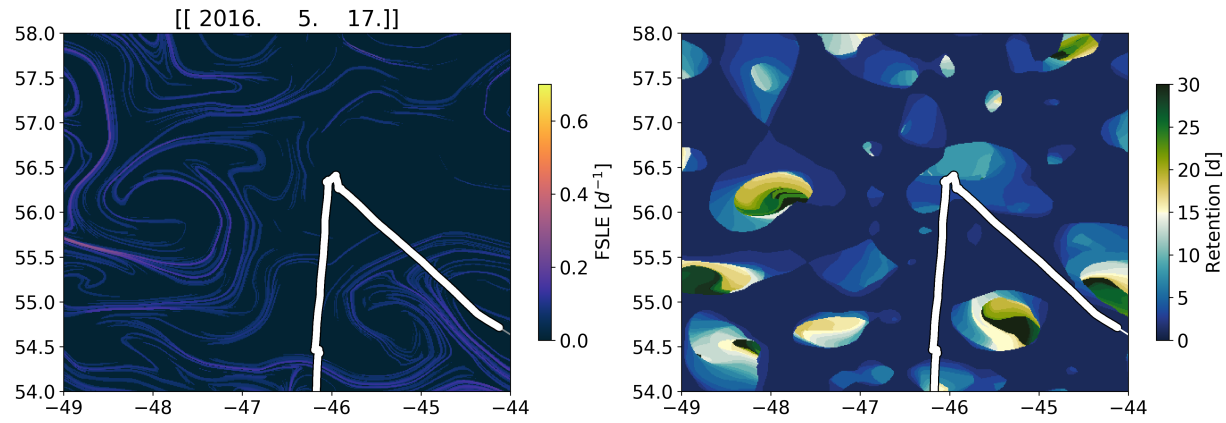


Figure 35: FSLE and RP calculated for Station 1.

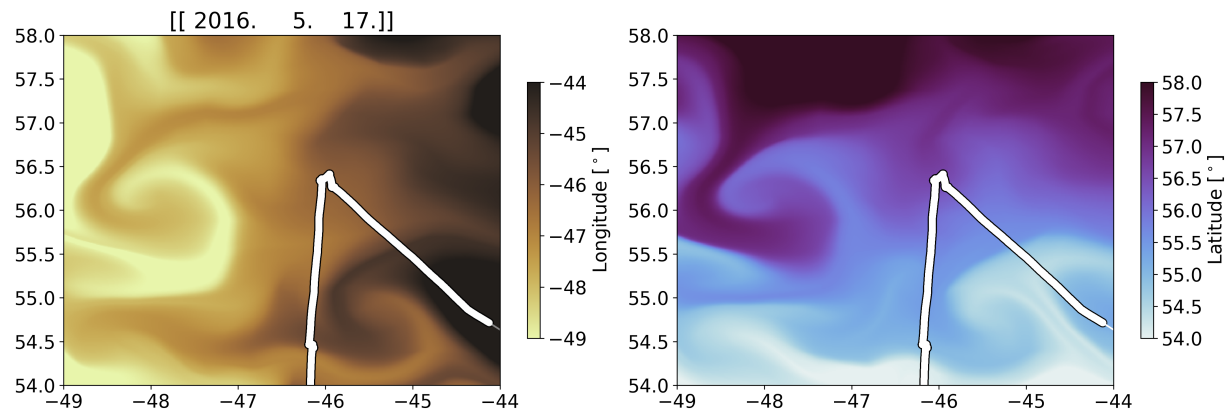


Figure 36: Water origin (longitude and latitude) for Station 1.

7.3 S2 NAAMES-2

This stations was located at the last-known surfacing of a Bio-Argo float (It would be good to track down a float number and who deployed it, and if it is a NAAMES float?). The location was near a non-retentive anticyclonic eddy and the rotational currents of this eddy are readily visible at the station in the tracks of the drifters (Fig. 37).

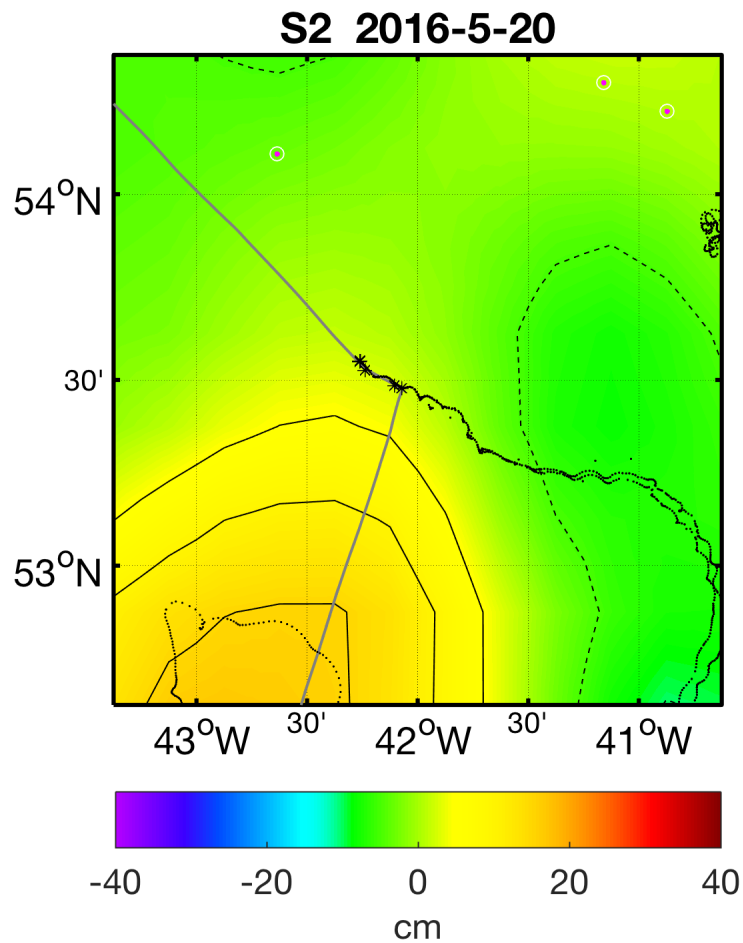


Figure 37: Same as Fig. 10

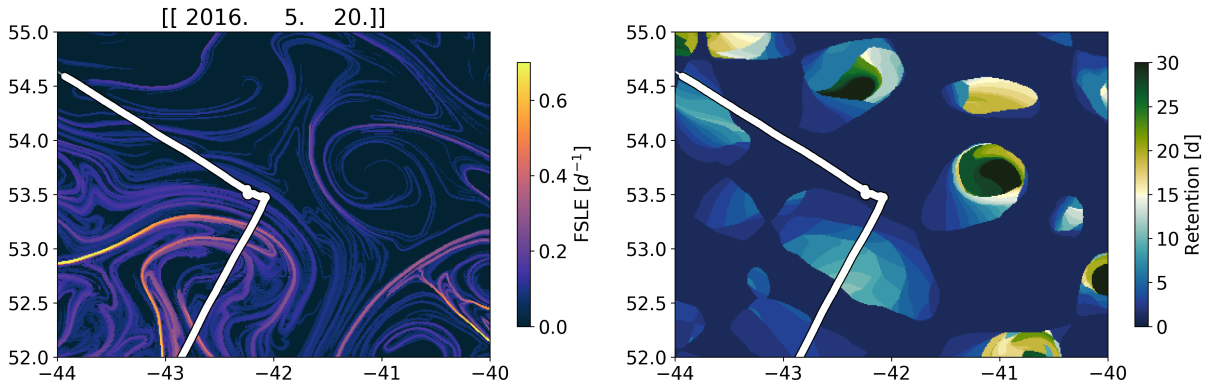


Figure 38: FSLE and RP calculated for Station 2.

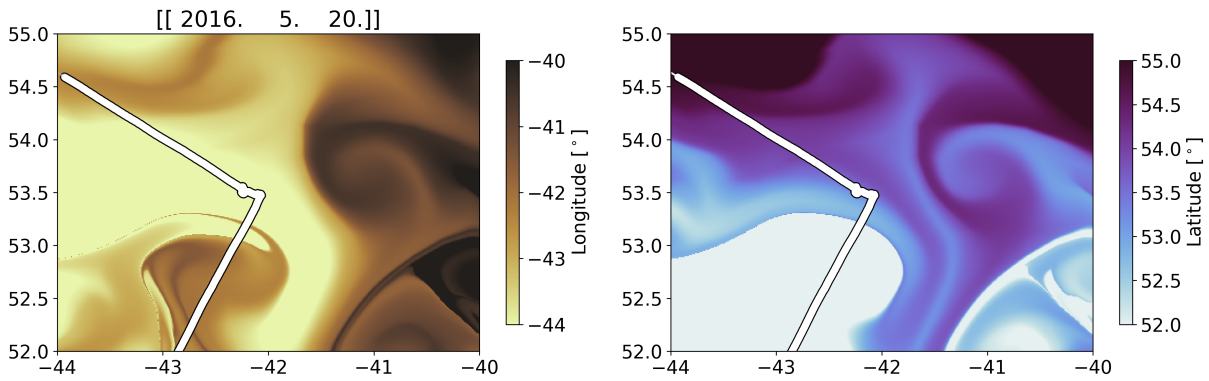


Figure 39: Water origin (longitude and latitude) for Station 2.

7.4 S3 NAAMES-2

This location was chosen to be at the center of an anticyclonic eddy. This is the same anticyclone that was sampled at S1 on NAAMES-1 (See Fig. 7). This is a perfect example of the danger inherent in using optimally interpolated SLA products to guide field work. Although the station appeared to be in the core of the eddy according to the SLA signature (Fig. 37a), the station was actually just outside of the eddy core and along the periphery, which is indicated by the trajectories of the drifters. In addition, a few days after we departed the station, clear-sky conditions allowed for the collection of high-resolution CHL images that show the station was indeed outside of the core of the anticyclone (Fig. 37b).

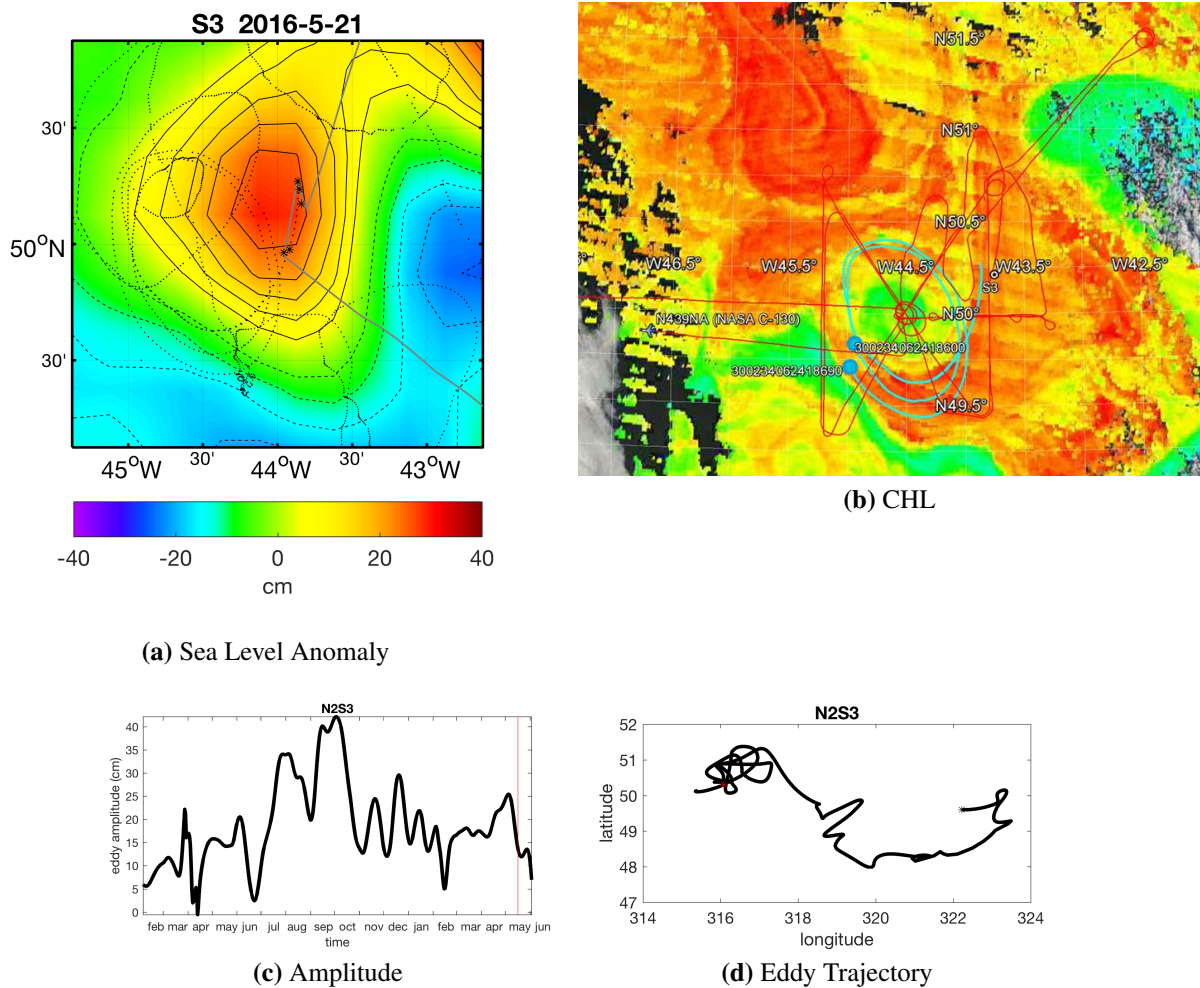


Figure 40: Same as Fig 7

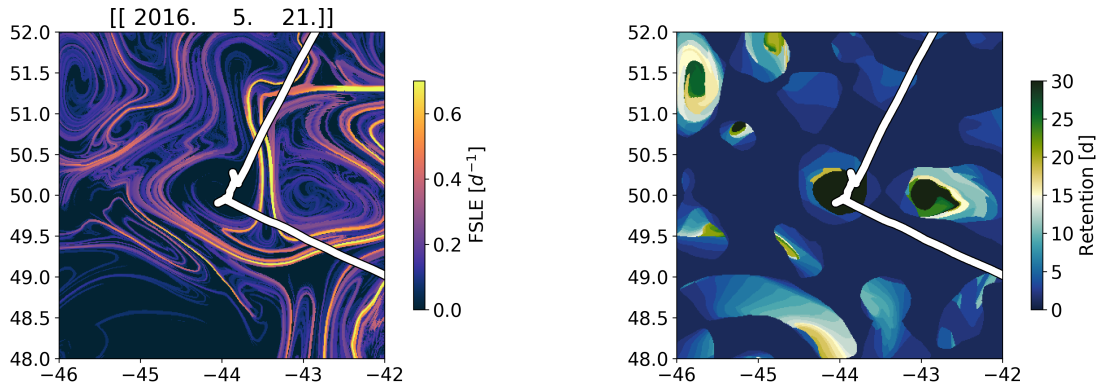


Figure 41: FSLE and RP calculated for Station 3.

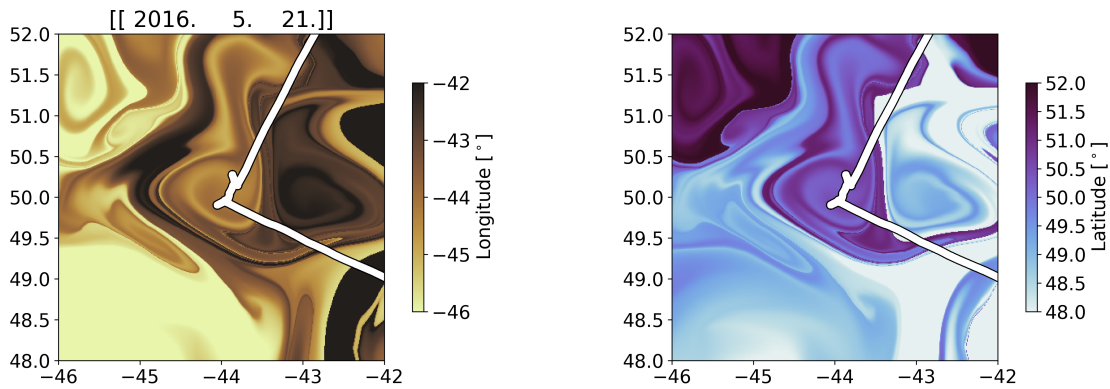


Figure 42: Water origin (longitude and latitude) for Station 3.

7.5 S4 NAAMES-2

Station 4 was our special baby. We arrived in this anticyclones, and much to the shock of many of us, there was effectively zero CHL in the water. The first few casts indicated that the surface was well mixed to a depth of ≈ 230 m (Fig. 85b). Within the first 24 hour, the water column began to stratify and the surface mixing layer was constrained to upper ≈ 20 m (Fig. 85b). This resulted in many interesting changes in the ecosystem both in the mixing layer and below it.

The trajectory of the drifter was due southeast, likely as a result of the rotational currents of the anticyclone and the wind. We continued to follow the drifter and the float for 4 days. The trajectory of the *R/V Atlantis* such that this station was able to pick up the radial gradient of the physical and biological properties of the eddy from the center to the periphery. This is evident in the shoaling of the base of the mixed layer during the latter period of occupation (Fig. 85b).

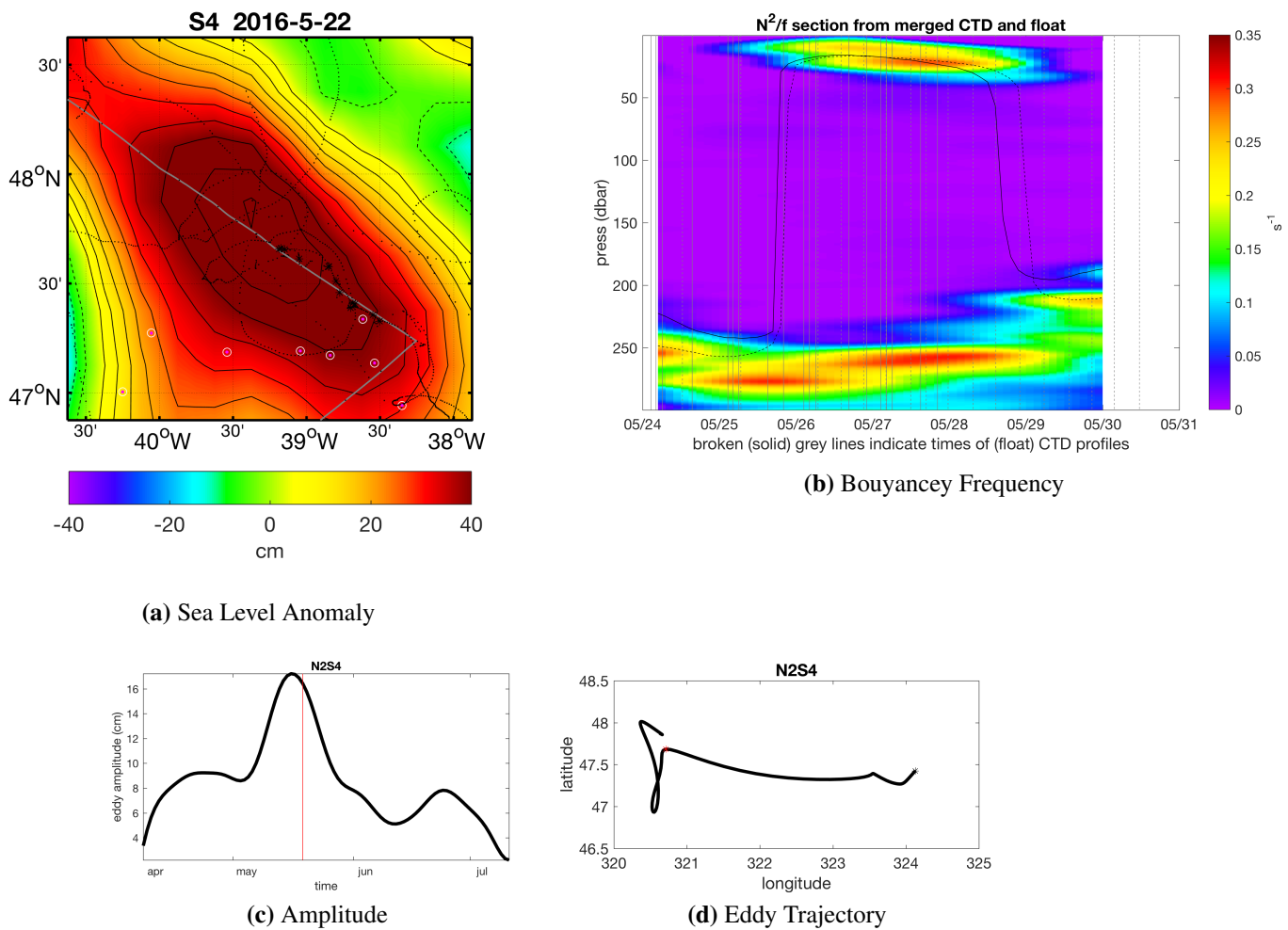


Figure 43: (a) Mapped sea level anomaly at Station 4. Solid (broken) black contours indicate SLA at an interval of 5 cm. Grey line is the track of the *R/V Atlantis*. Small black points indicate hourly drifter location for all drifters within the region starting on the first day of occupation of the station and continuing for 15 days. Black * indicate the location of CTD cast. (b) and (c) same as previous figures.

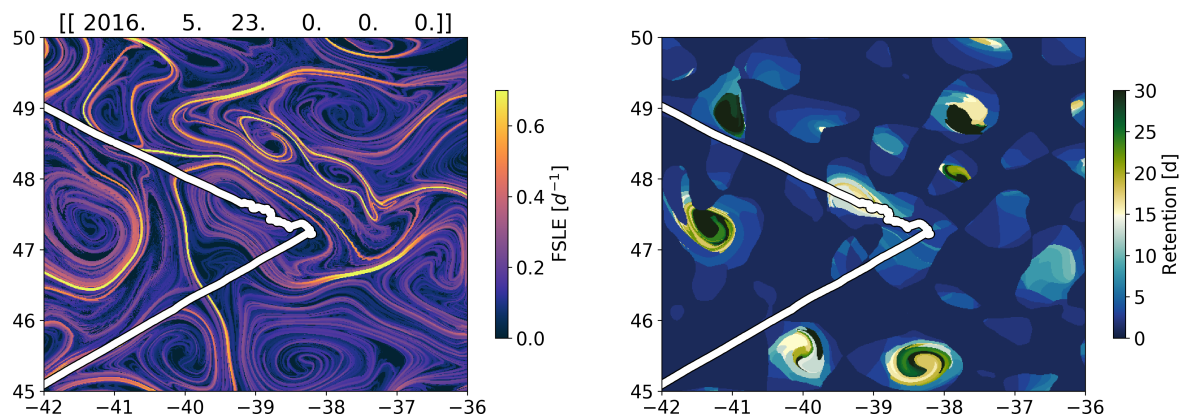


Figure 44: FSLE and RP calculated for Station 4.

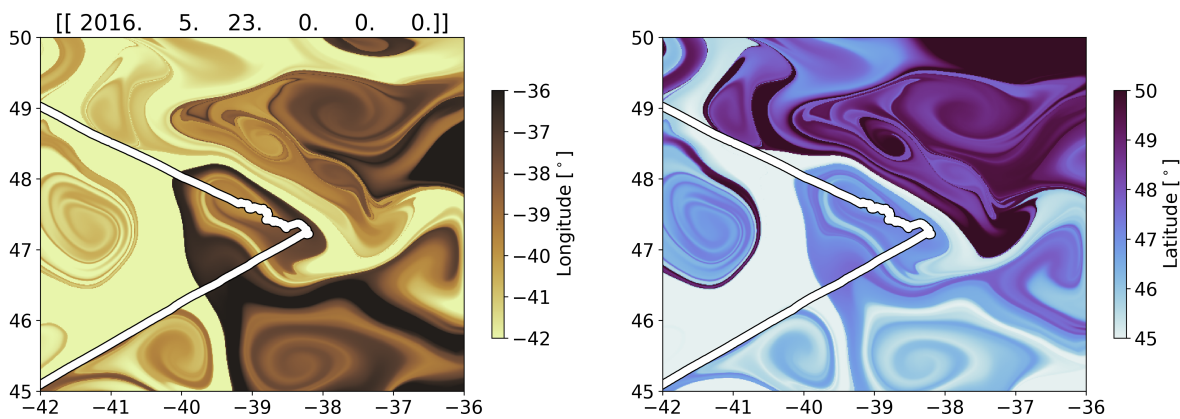


Figure 45: Water origin (longitude and latitude) for Station 4.

7.6 S5 NAAMES-2

Station 5 was the final station for NAAMES-2. We chose the station based on the location of a Bio-Argo float. This station was also on the edge of a non-retentive cyclonic eddy (Fig. 46). We were able to conduct standard science operation throughout the first day and then the following 40 hour were spent riding out a storm. This is why the ship track and drifters head northeast following our arrival on station.

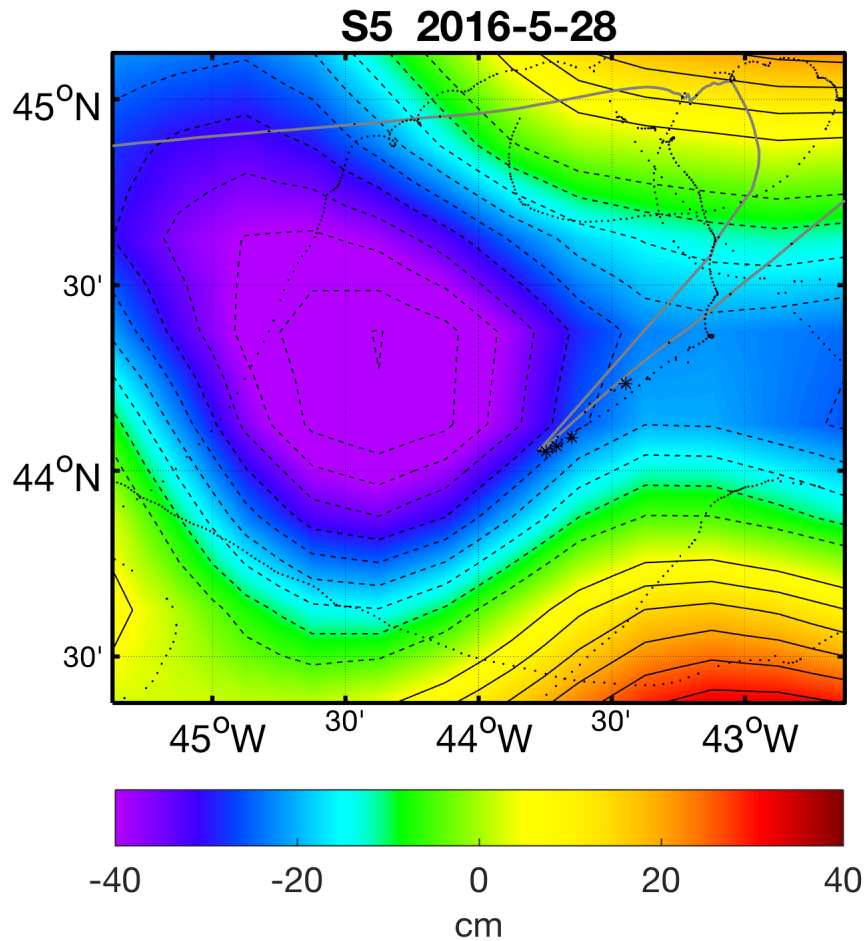


Figure 46: Same as Fig. 10

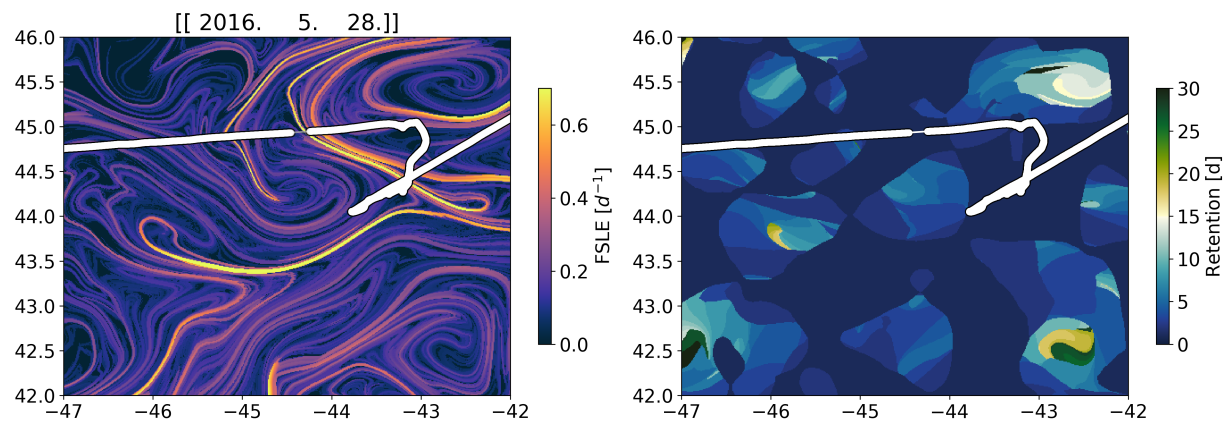


Figure 47: FSLE and RP calculated for Station 5.

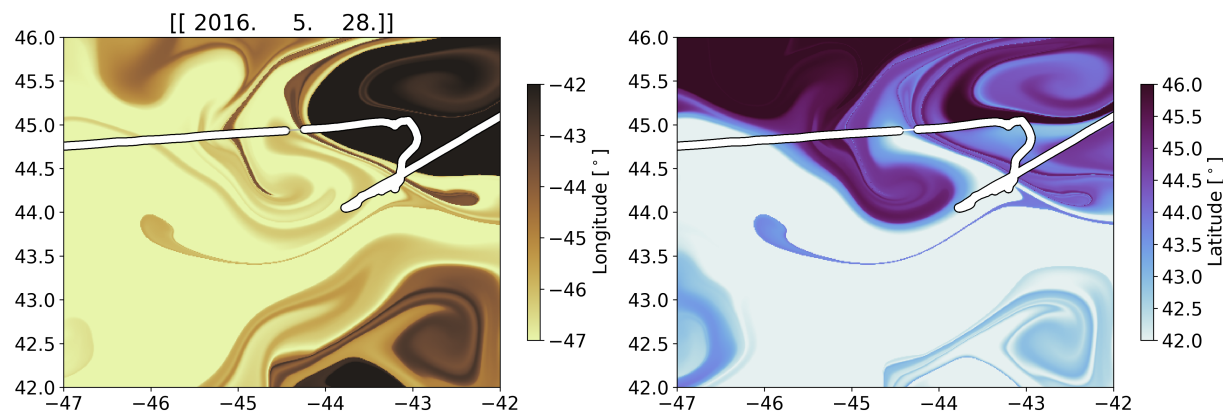


Figure 48: Water origin (longitude and latitude) for Station 5.

8 NAAMES 2017

8.1 S1a NAAMES-3

Station 1a was not located within an eddy. The waters sampled at this station have a very different origin compared to Station 1 as they are separated by a strong gradient in water origin (Figure 51).

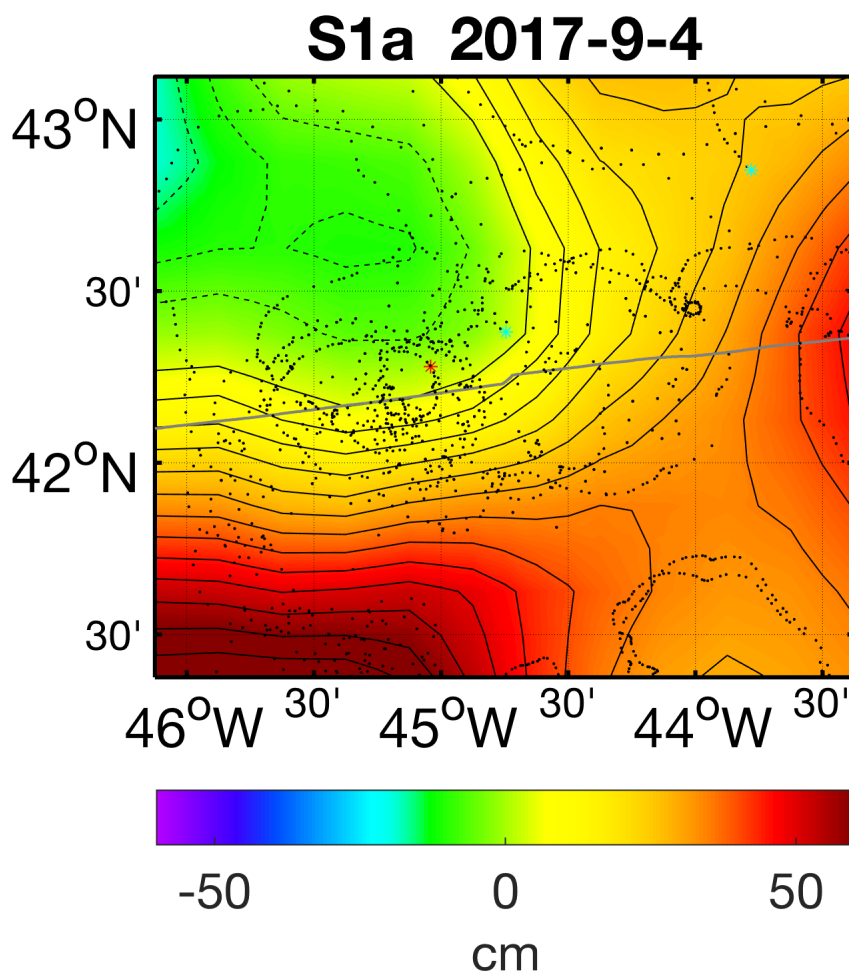


Figure 49: Same as Fig. 10

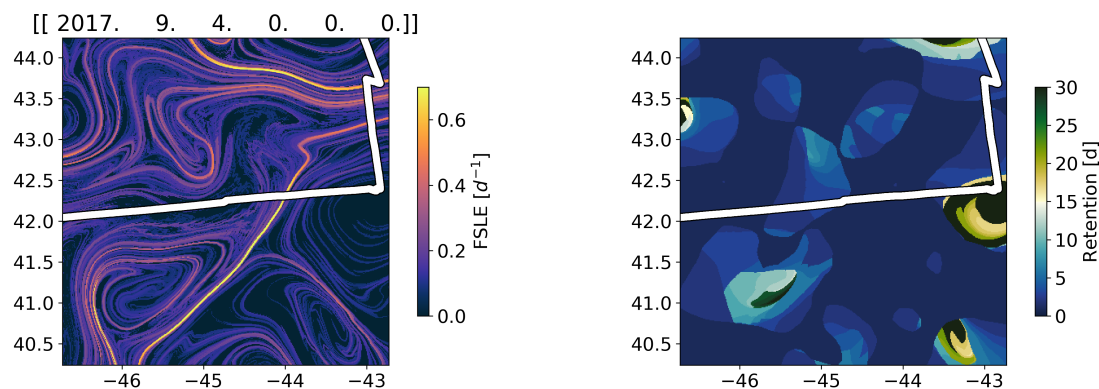


Figure 50: FSLE and RP calculated for Station 1.a.

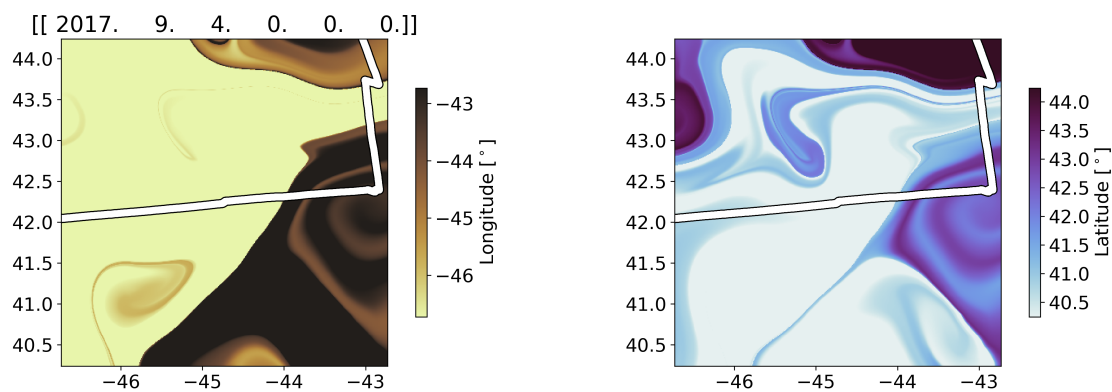


Figure 51: Water origin (longitude and latitude) for Station 1a.

8.2 S1 NAAMES-3

Station 1 was located within a retentive anticyclonic eddy. The strong signal in SLA suggests strong geostrophic velocities that may have been able to trap water parcels and cause high retention within the eddy core (Figure 53) and separate the eddy from the waters coming from the south-east (Figure 54). However, the deployed drifters did not stay within the eddy core, suggesting that the currents in the top 15m may have caused this eddy to "leak" water parcels near the surface.

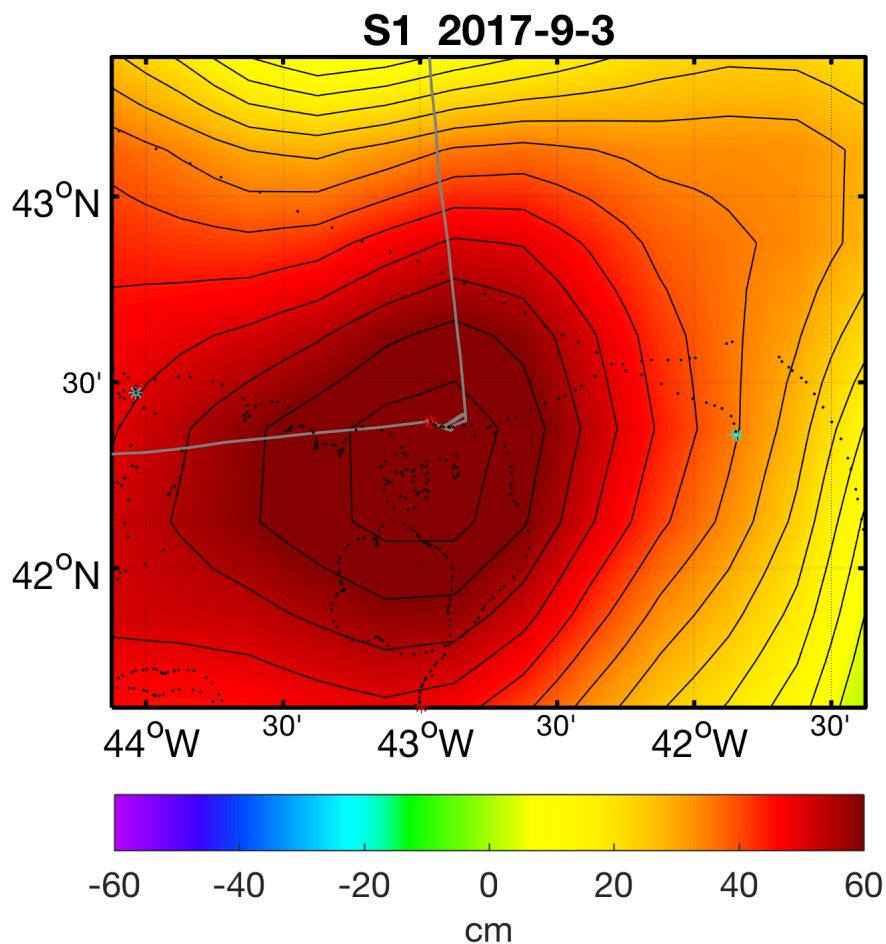


Figure 52: Same as Fig. 10

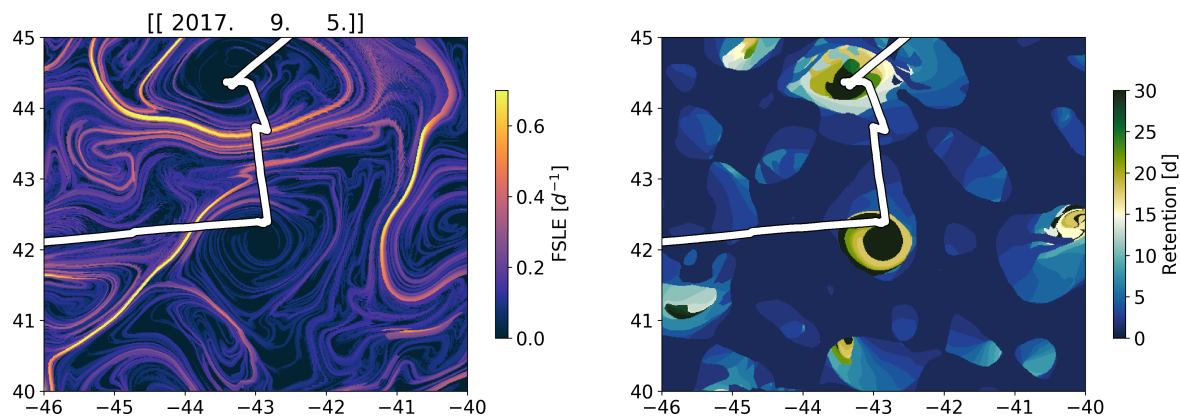


Figure 53: FSLE and RP calculated for Station 1.

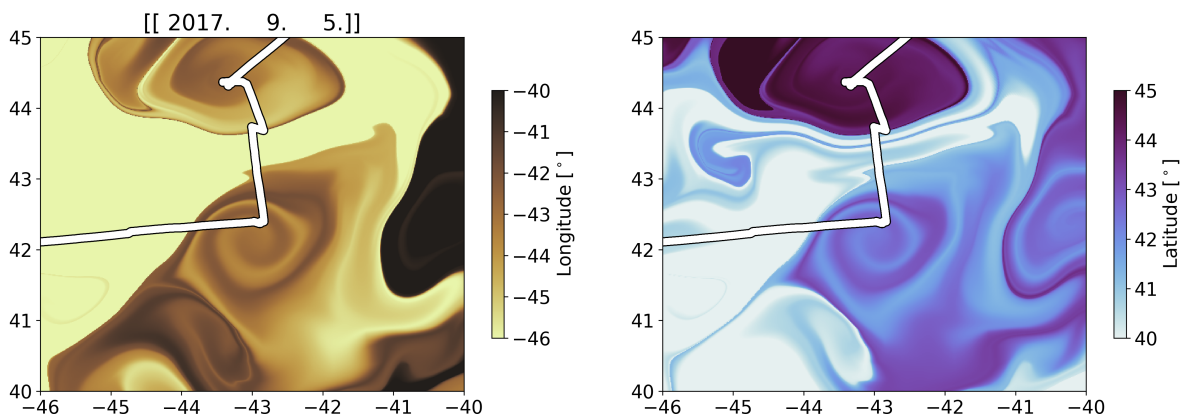


Figure 54: Water origin (longitude and latitude) for Station 1.

8.3 S1.5 NAAMES-3

Station 1.5 was an in-between station. It was located between the two mesoscale eddies sampled as S1 and S2, an anticyclone and a cyclone respectively.

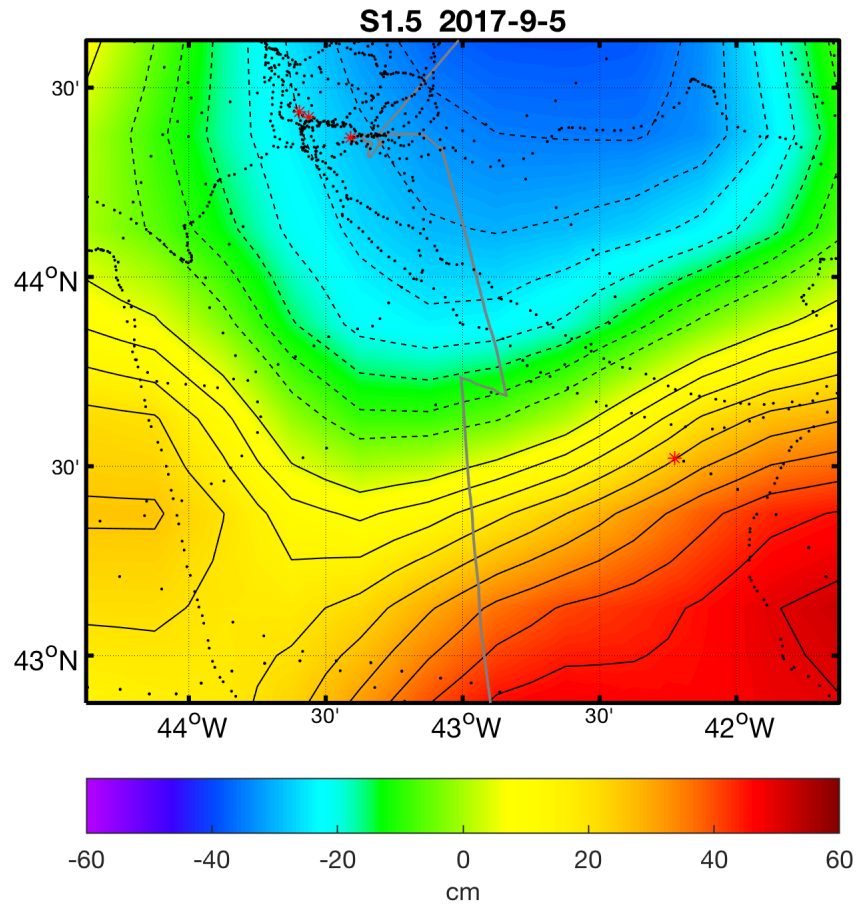


Figure 55: Same as Fig. 10

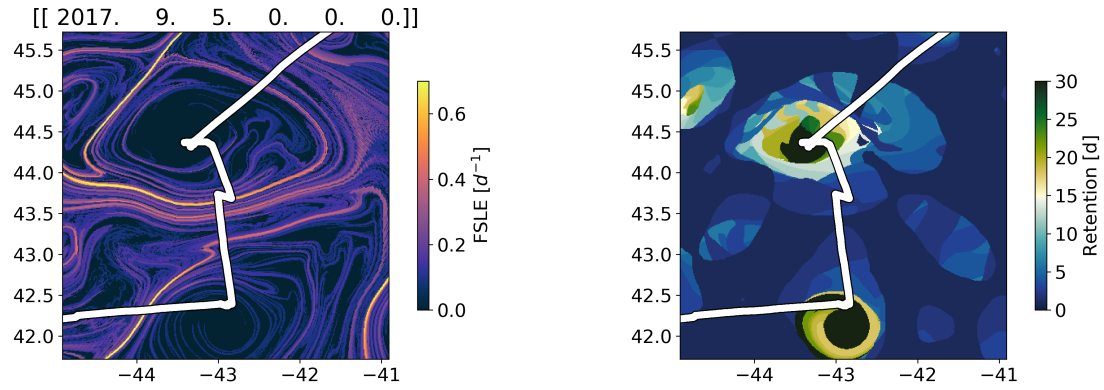


Figure 56: FSLE and RP calculated for Station 1.5.

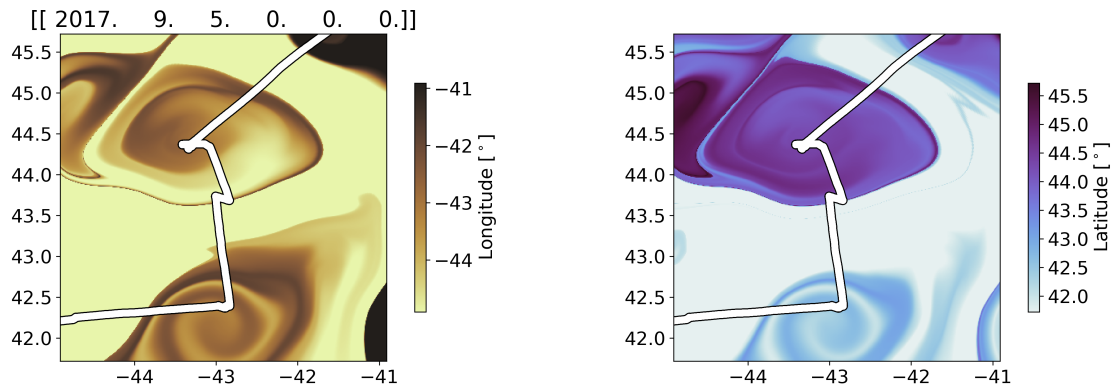


Figure 57: Water origin (longitude and latitude) for Station 5.

8.4 S2 NAAMES-3

Station 2 was set at the center of a cyclonic eddy. This eddy appear from altimetry to be moderately retentive and is separated from the surrounding waters by strong transport fronts (highlighted by the high values of FSLEs in Figure 59). The deployed drifters were entrained within the eddy core for several rotations before they exited the eddy.

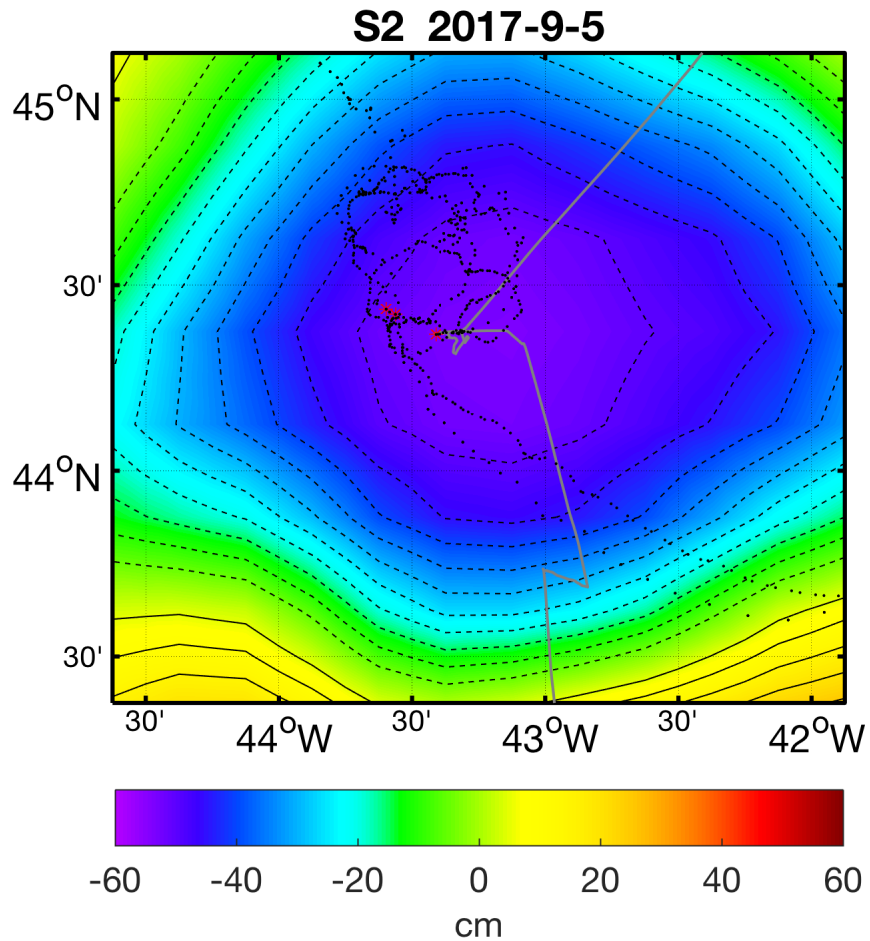


Figure 58: Same as Fig. 10

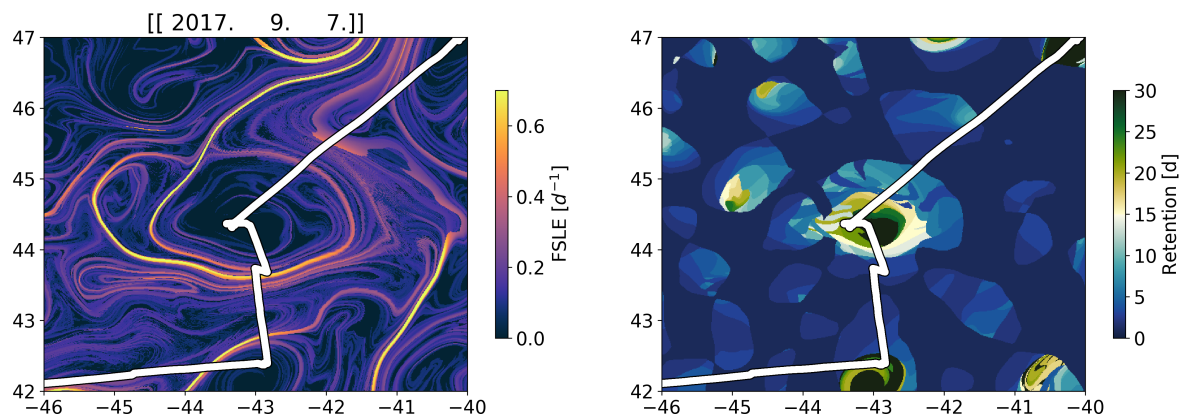


Figure 59: FSLE and RP calculated for Station 2.

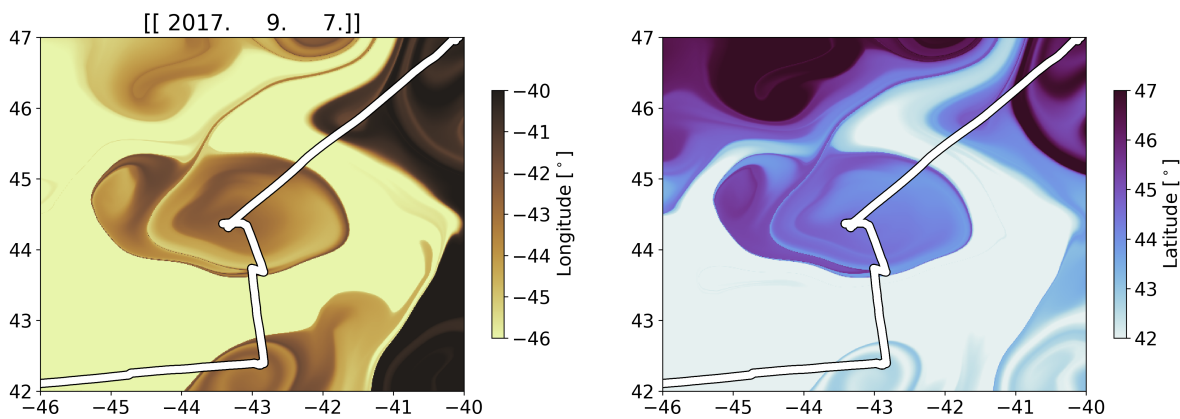


Figure 60: Water origin (longitude and latitude) for Station 2.

8.5 S3 NAAMES-3

Station 3 was located at the center of a mode-water eddy [McGillicuddy et al. (2007)]. Mode-water eddies are a feature of the northwestern subtropical Atlantic: they rotate as anticyclones (*i.e.* clockwise) and are indistinguishable from anticyclones from their altimetric signature (see Figure ??). However, their vertical structure is very different (as it was observed during the CTD casts): the main thermocline is deepened (as in anticyclones) whereas the seasonal thermocline is shoaled (as in cyclones). As a consequence, just as cyclones, mode-water eddies are expected to bring nutrients into the euphotic zone during their formation and intensification phases. This specific mode-water eddy appeared particularly retentive in the layer dominated by geostrophic velocities and was separated from the surrounding waters by strong transport fronts (Figures ?? and ??).

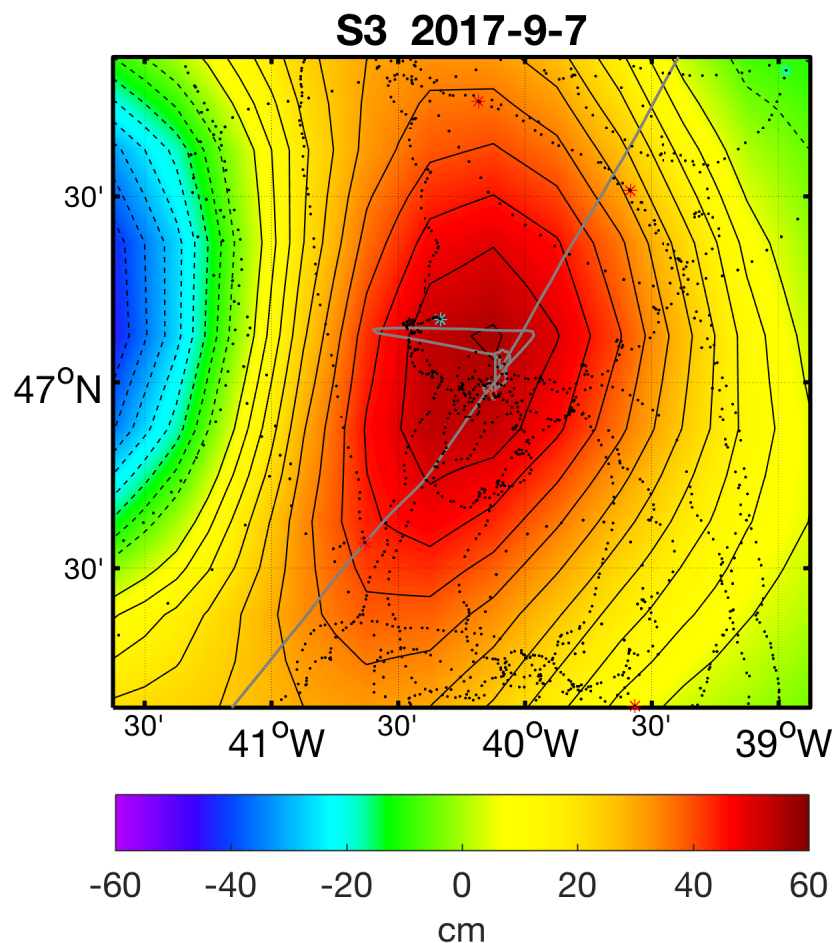


Figure 61: Same as Fig. 52

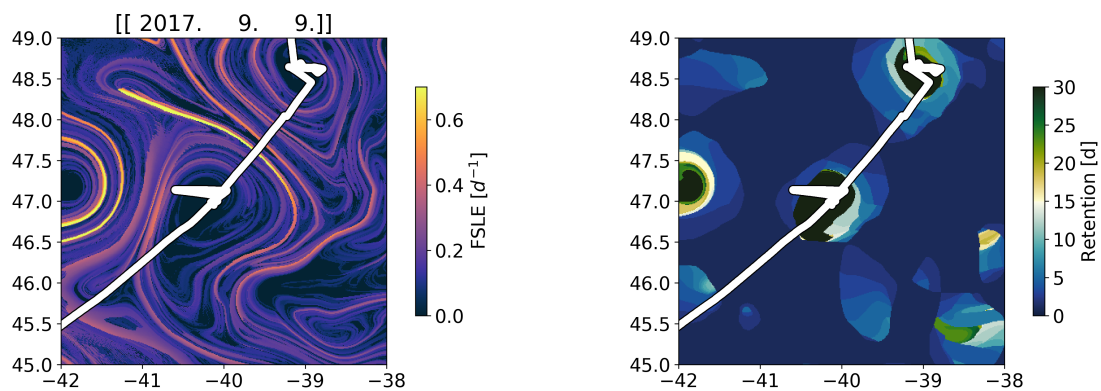


Figure 62: FSLE and RP calculated for Station 3.

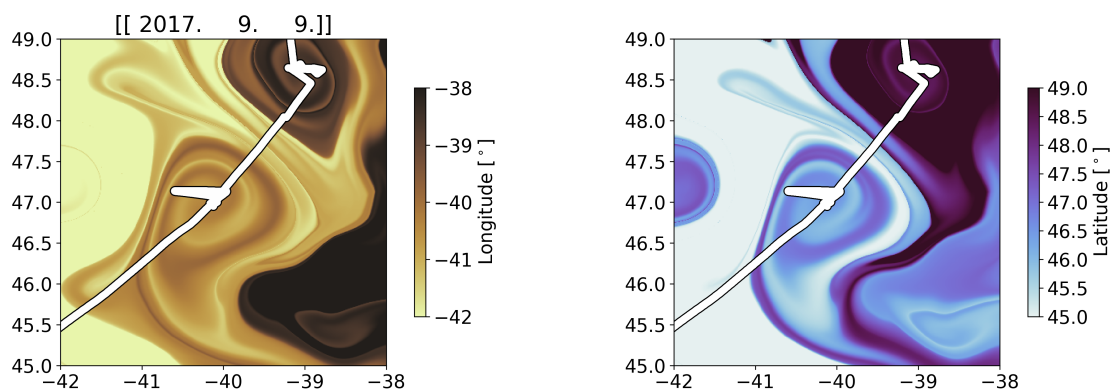


Figure 63: Water origin (longitude and latitude) for Station 3.

8.6 S3.5 NAAMES-3

This "in-between" station was located between the mode water eddy sampled at Station 3 and the small retentive cyclone sampled at station 4.

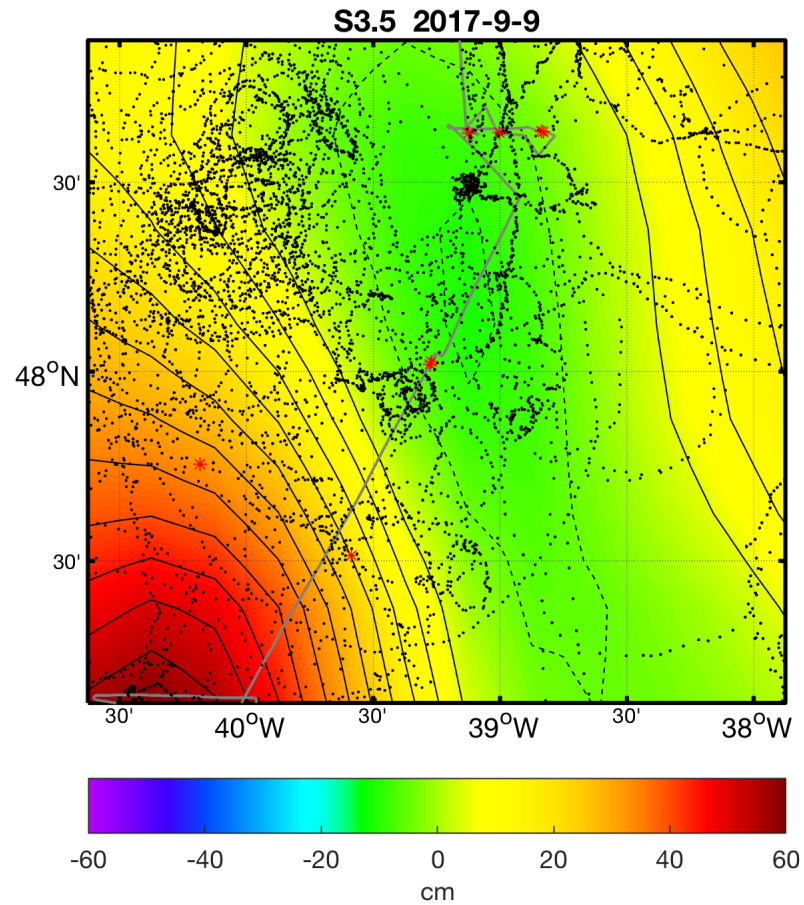


Figure 64: Same as Fig. 52

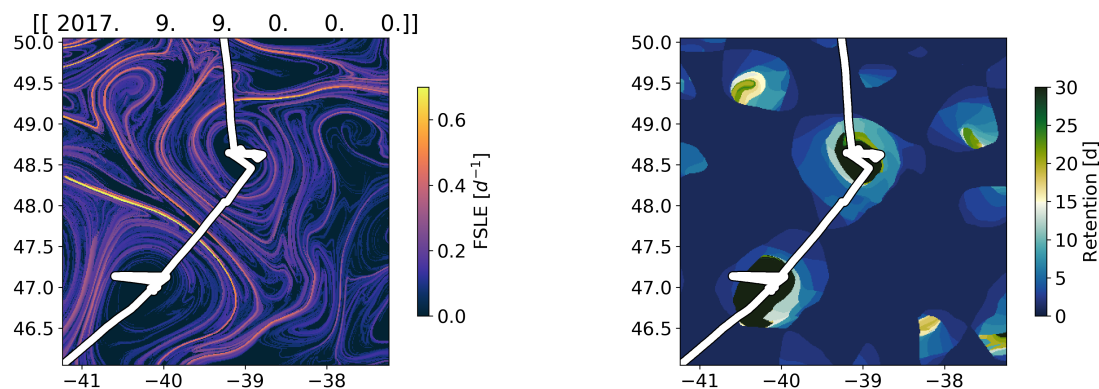


Figure 65: FSLE and RP calculated for Station 3.5.

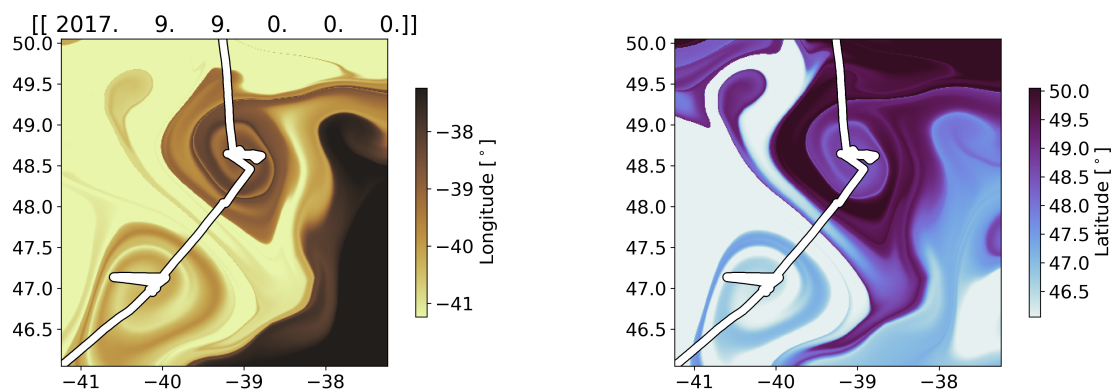


Figure 66: Water origin (longitude and latitude) for Station 3..5

8.7 S4 NAAMES-3

We aimed at locating Station 4 at the center of a small, but strongly retentive cyclone. Locating the center of this very small cyclone was extremely difficult and the station may have been located in the proximity of the eddy center, but likely few kms away. The deployed drifters did not appear to be trapped by the eddy when they were deployed. However, the trajectories of some of them suggest, from a preliminary analysis, that may have ended been trapped in an eddy after a short time (likely the eddy sampled in Station 4).

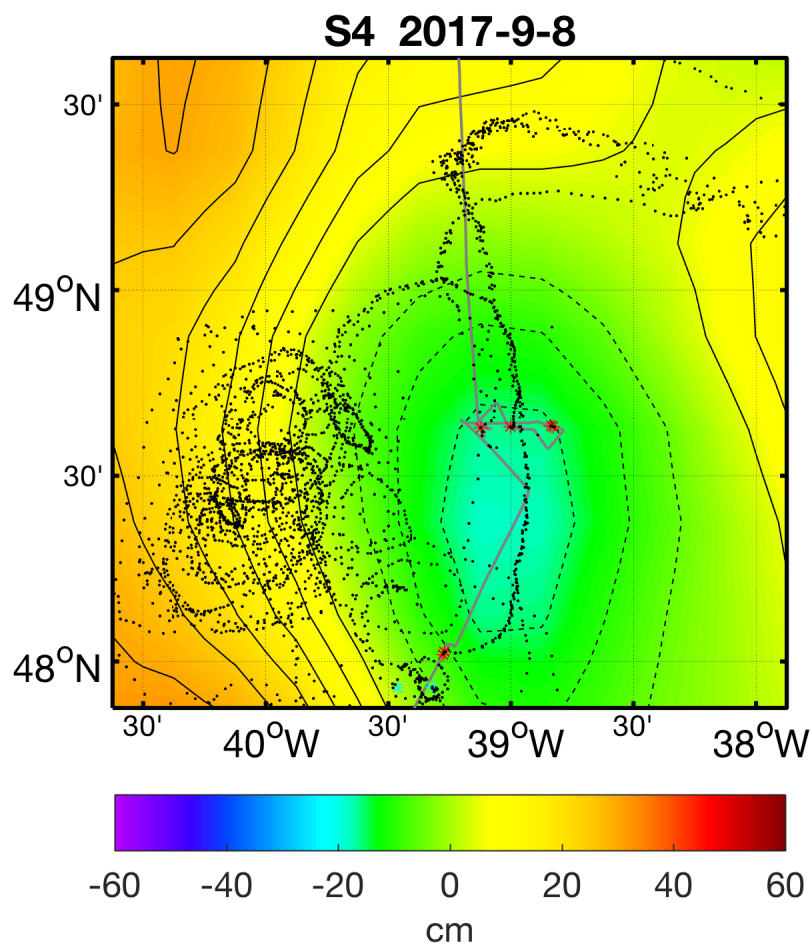


Figure 67: Same as Fig. ??

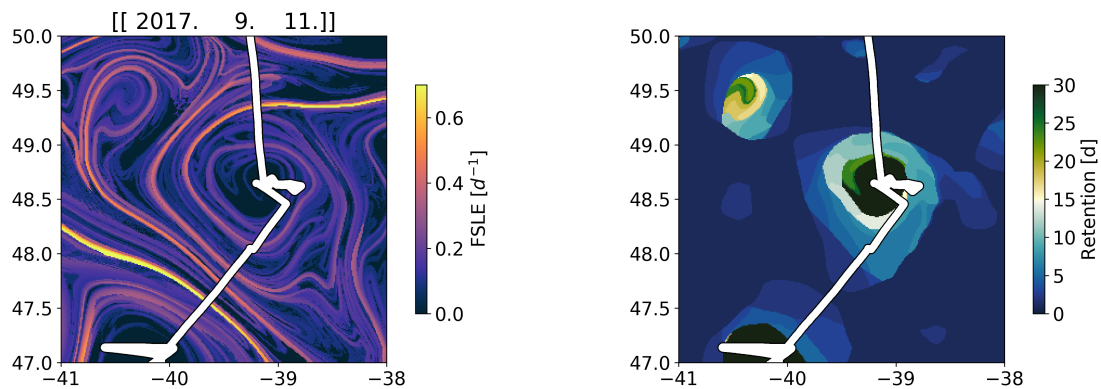


Figure 68: FSLE and RP calculated for Station 4.

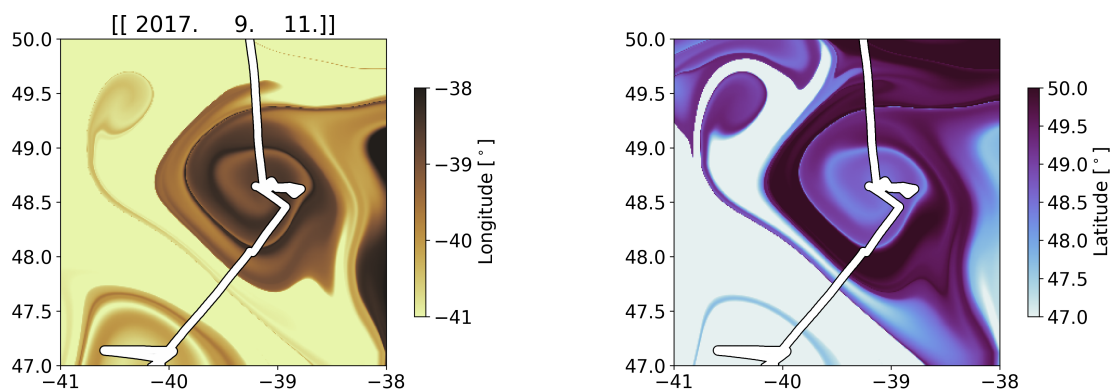


Figure 69: Water origin (longitude and latitude) for Station 4.

8.8 S4.5 NAAMES-3

This "in-between" station was not located in the close proximity of any eddy. The Lagrangian re-analyses of water parcels' trajectories suggest that the CTD cast was performed in the proximity of a small horizontal latitudinal gradient (Figure 71).

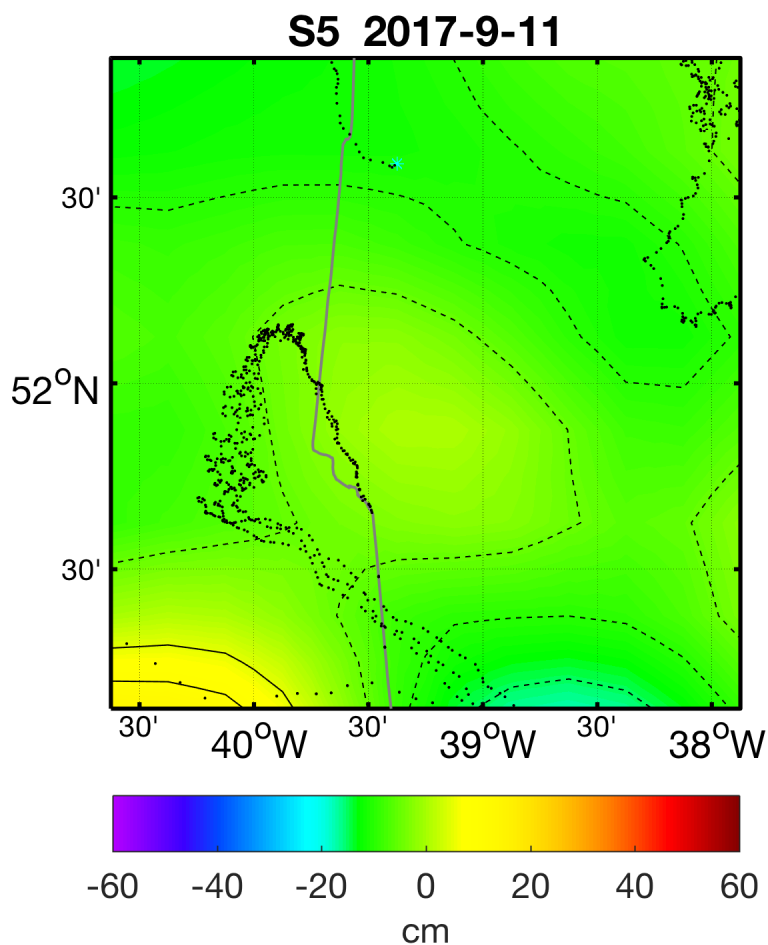


Figure 70: Same as Fig. 52

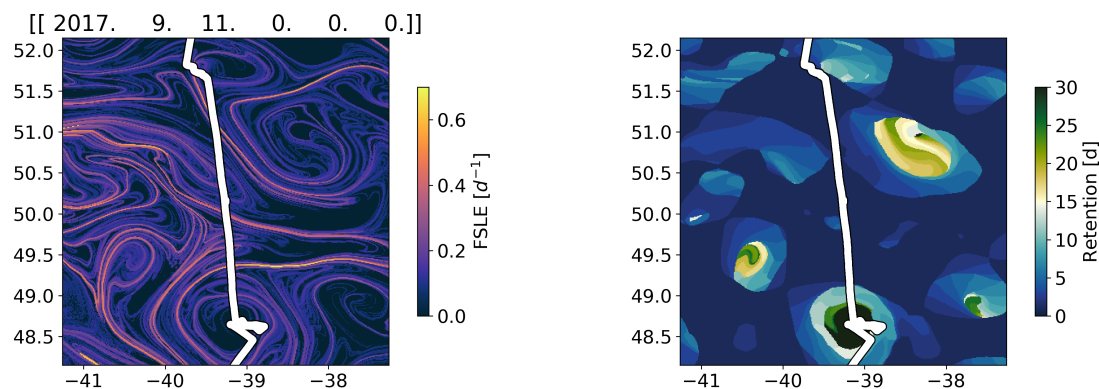


Figure 71: FSLE and RP calculated for Station 4.5.

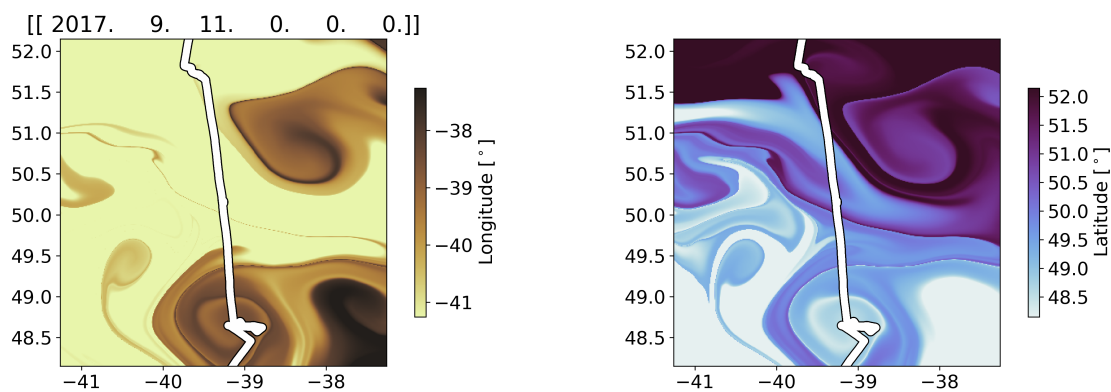


Figure 72: Water origin (longitude and latitude) for Station 4..5

8.9 S5 NAAMES-3

Station 5 was chosen as a "non-eddy station" and it appears to be in relatively uniform waters (in the proximity of a weak recirculation structure).

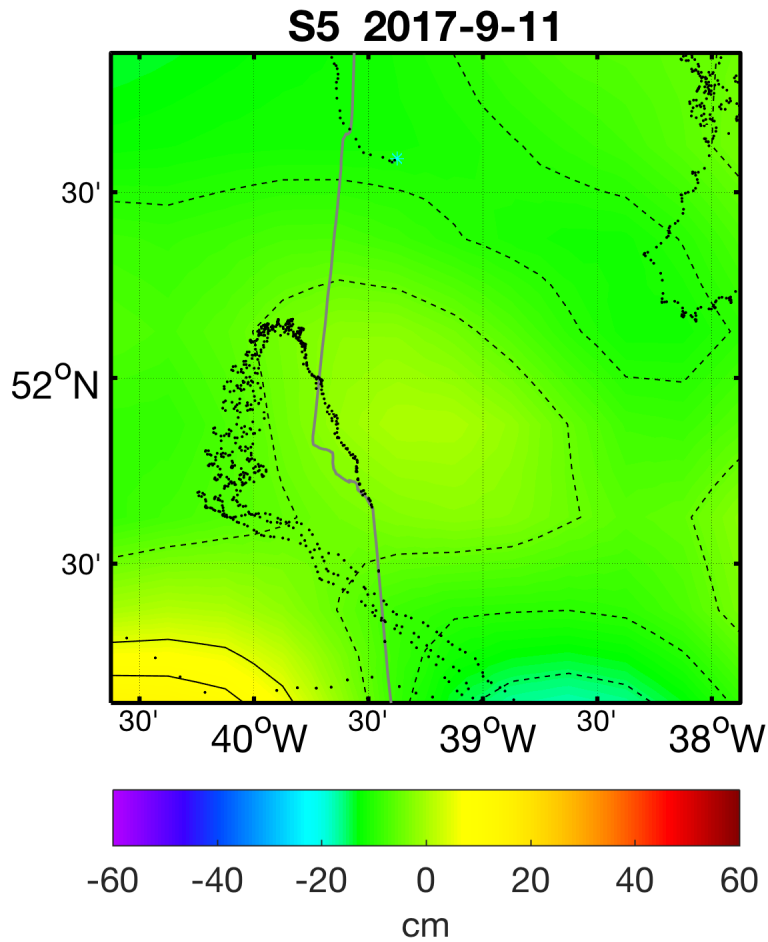


Figure 73: Same as Fig. 10

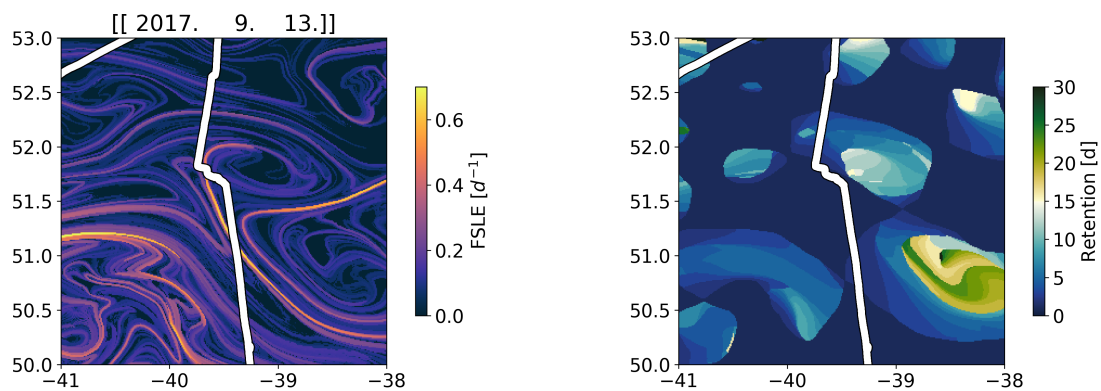


Figure 74: FSLE and RP calculated for Station 5.

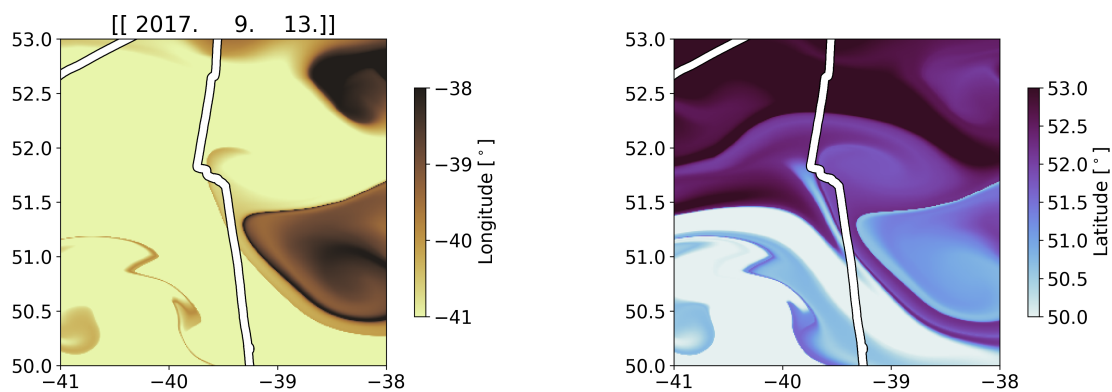


Figure 75: Water origin (longitude and latitude) for Station 5.

8.10 S5.5 NAAMES-3

This was an "in-between" station.

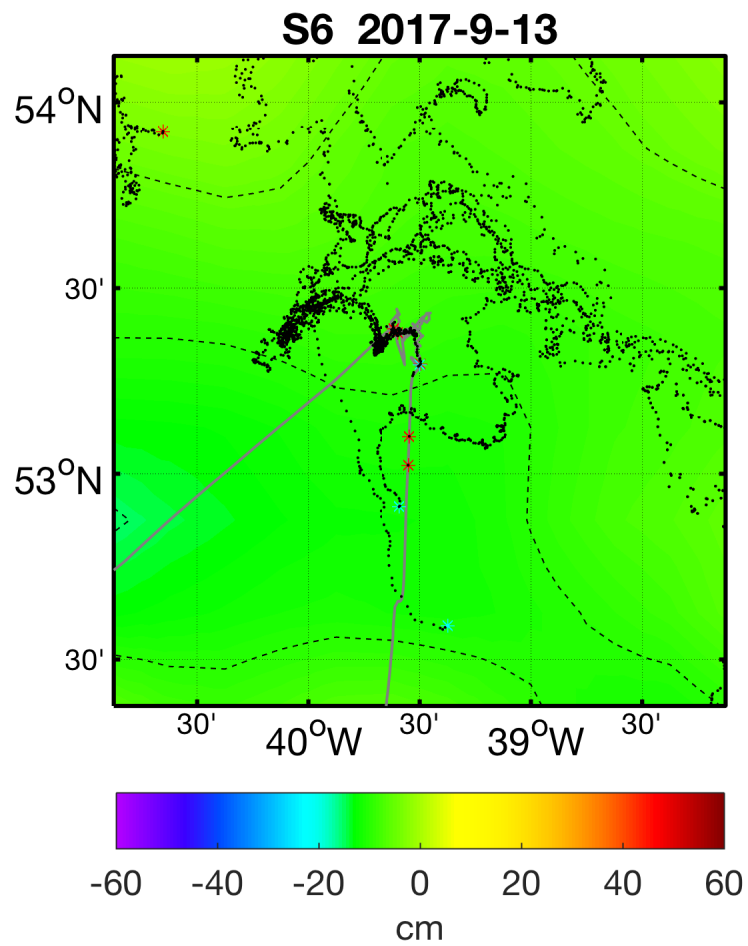


Figure 76: Same as Fig. 52

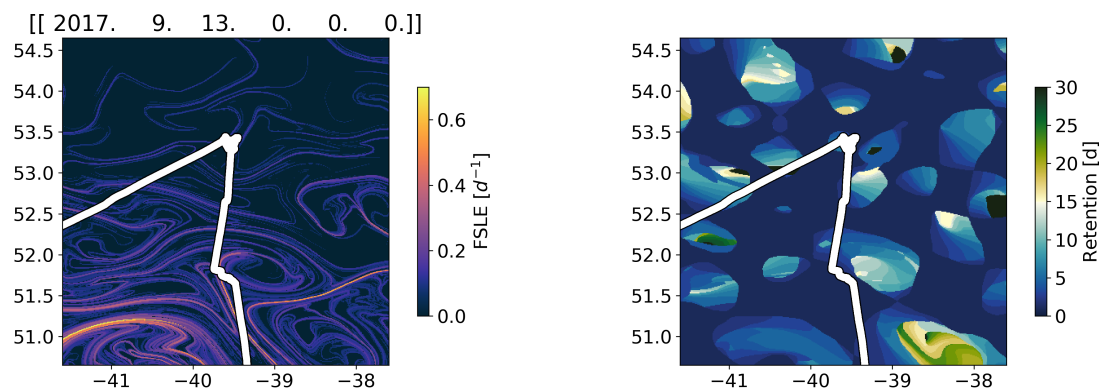


Figure 77: FSLE and RP calculated for Station 5.5.

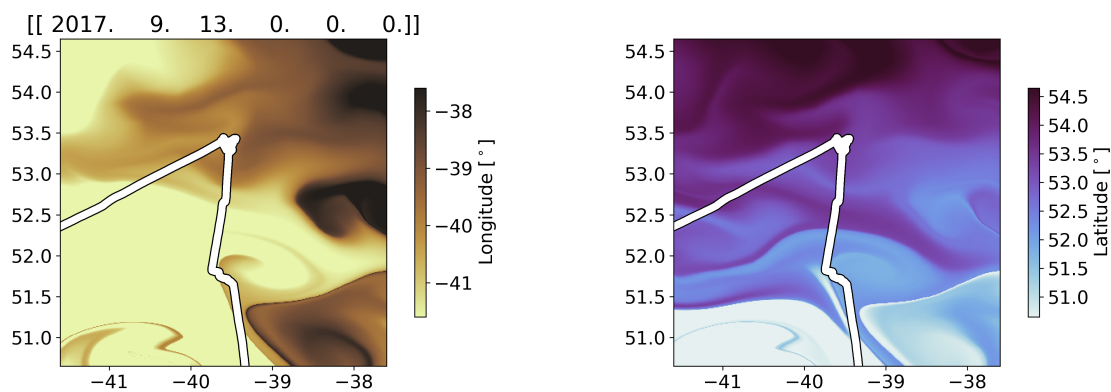


Figure 78: Water origin (longitude and latitude) for Station 5.5

8.11 S6 NAAMES-3

Station 6 was the northernmost station sampled during this cruise. It was chosen because of its proximity to a float and displayed no signature in SLA. The drifters deployed at this station were advected east by the large scale wind-driven circulation of this region.

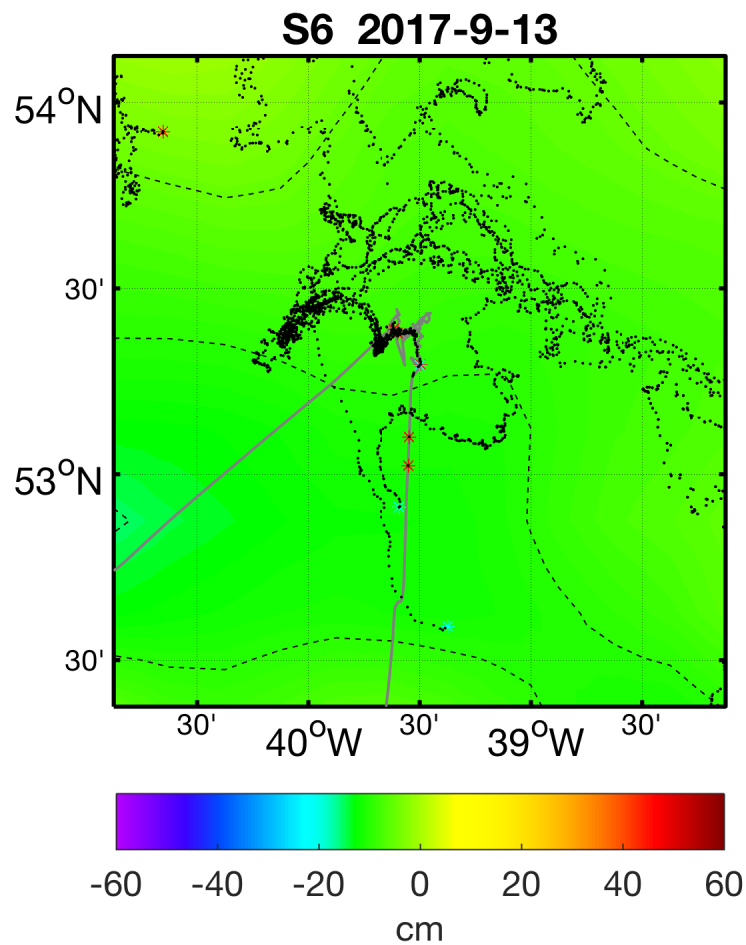


Figure 79: Same as Fig. 10

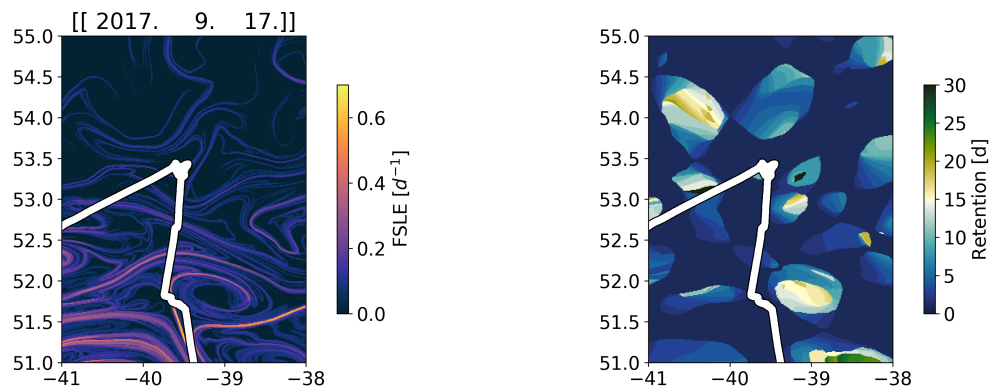


Figure 80: FSLE and RP calculated for Station 6.

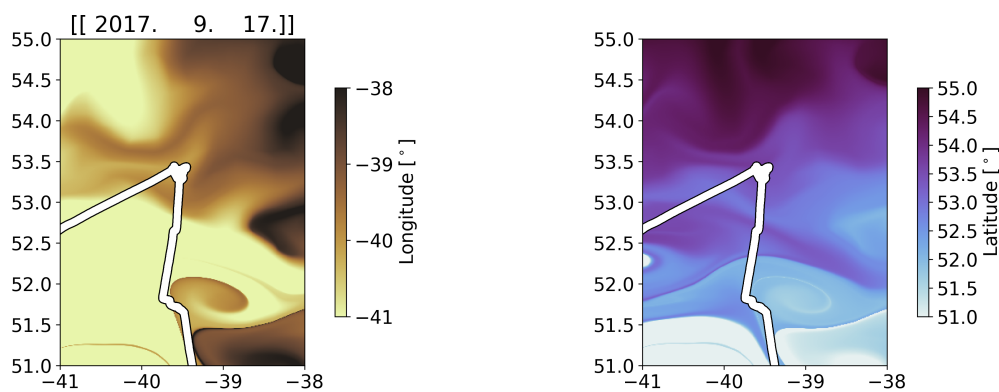


Figure 81: Water origin (longitude and latitude) for Station 6.

9 NAAMES 4

9.1 S1 NAAMES-4

As most stations during the NAAMES 4 expedition, this station was determined to be in the vicinity of a float. The station is not located in an eddy, but it is relatively close to a frontal structure (that was crossed before reaching the station) separating waters coming from the north (where the station was actually located) and waters from the south (corresponding to the region crossed just before reaching station).

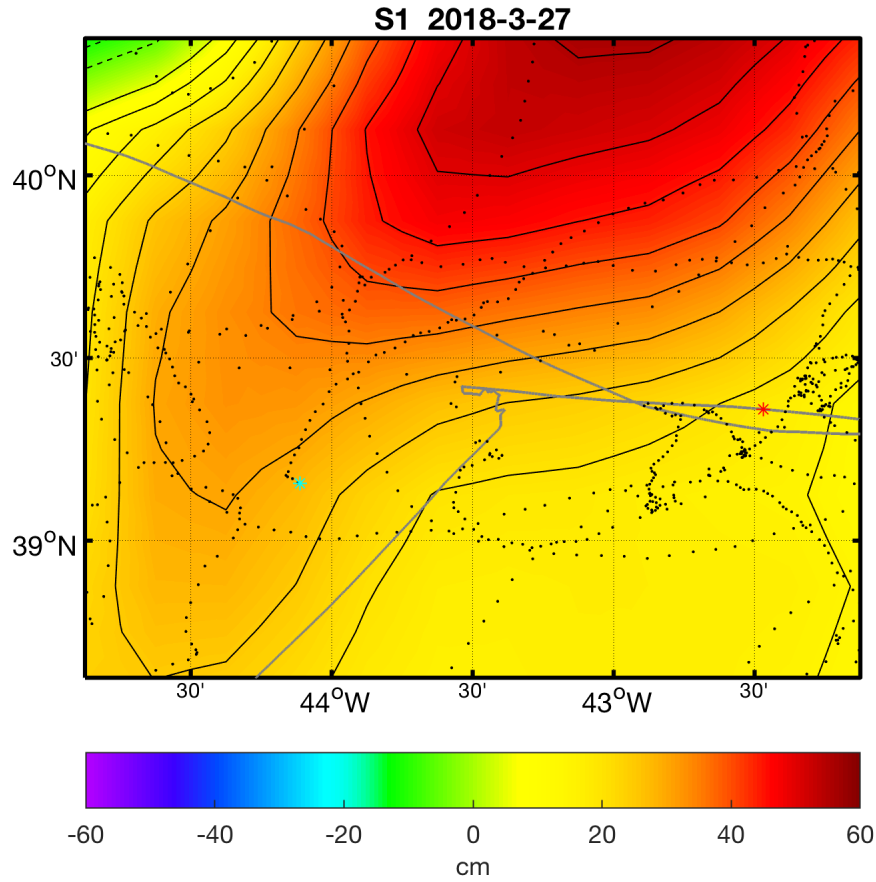


Figure 82: Same as Fig. 52

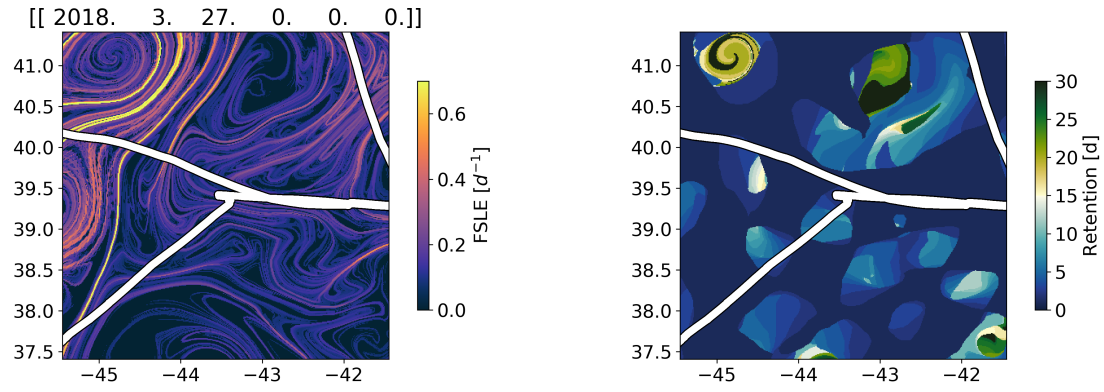


Figure 83: FSLE and RP calculated for Station 1.

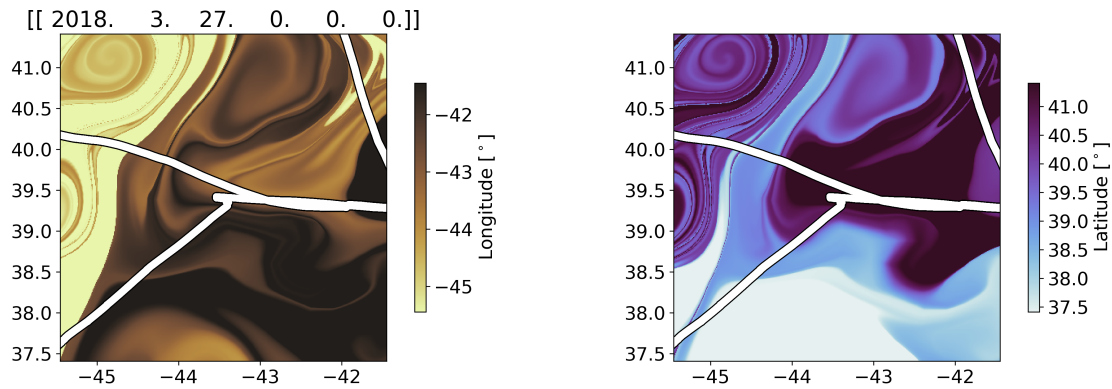


Figure 84: Water origin (longitude and latitude) for Station 1.

9.2 S2 NAAMES-4

This station was chosen to be in the proximity of a float and happened to be located between two weakly retentive mesoscale eddies (Figure 86). A Lagrangian drifter was deployed at this location and the ship returned at the drifters' location for station 2-Return-Drifter.

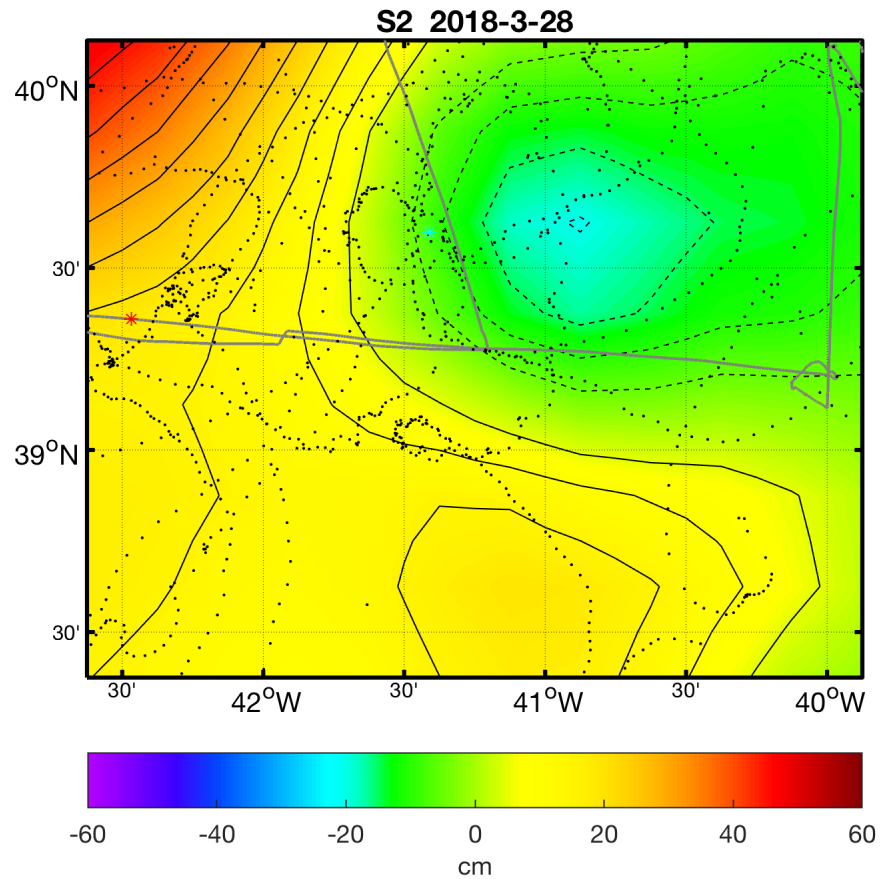


Figure 85: Same as Fig. 52

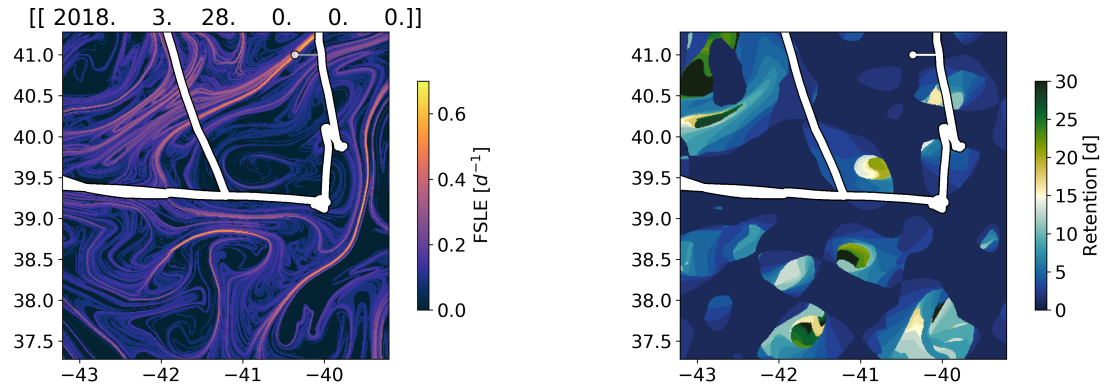


Figure 86: FSLE and RP calculated for Station 2.

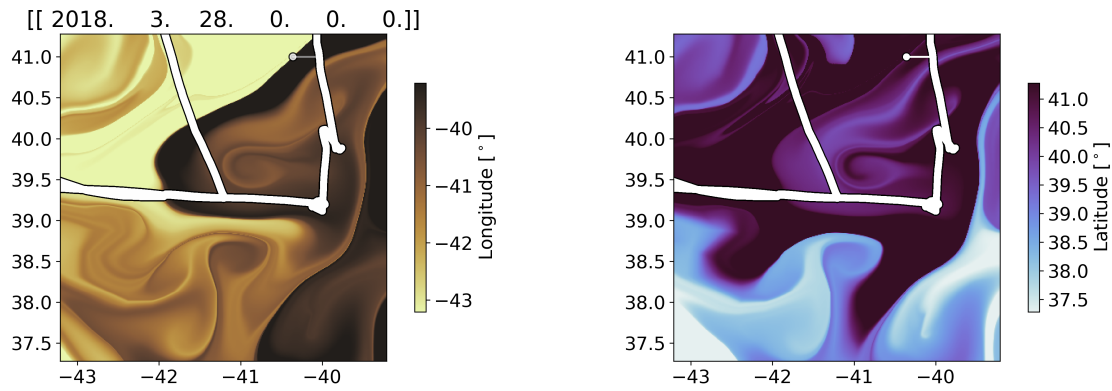


Figure 87: Water origin (longitude and latitude) for Station 2.

9.3 S2.5 NAAMES-4

This *in-between* station was located in a minor circulation feature (a filament?) characterized by water parcels that were stationary in the last two weeks but were surrounded by waters coming from the south-west (Figure 90).

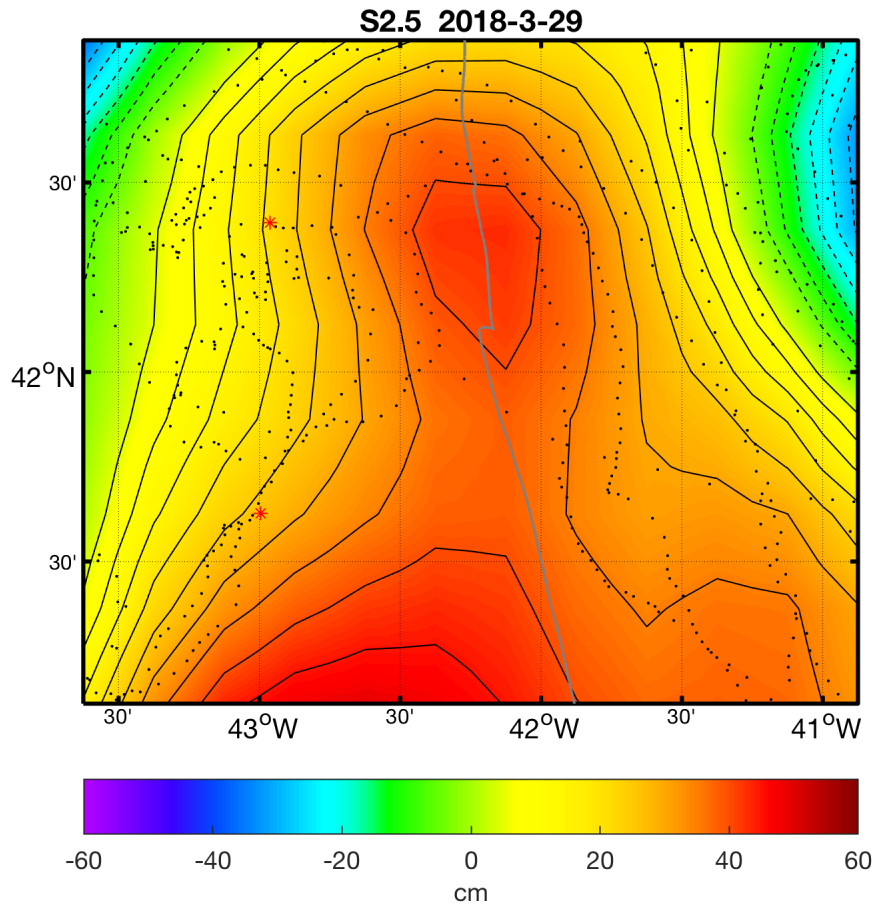


Figure 88: Same as Fig. 52

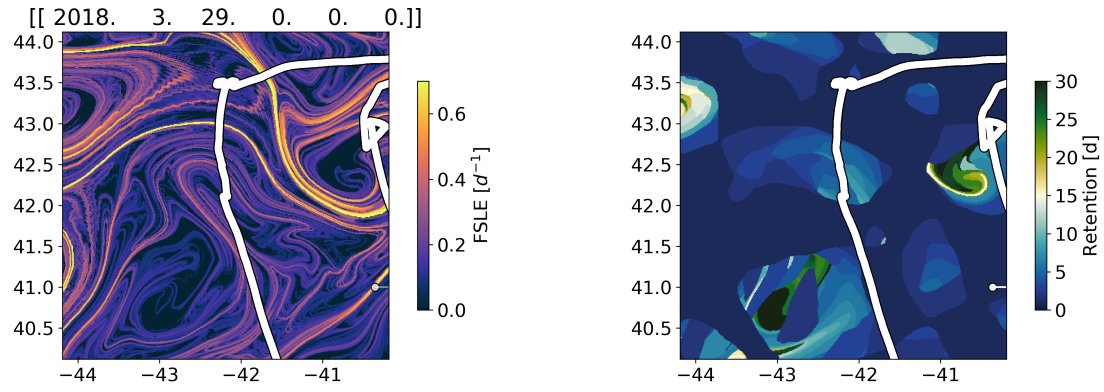


Figure 89: FSLE and RP calculated for Station 2.5.

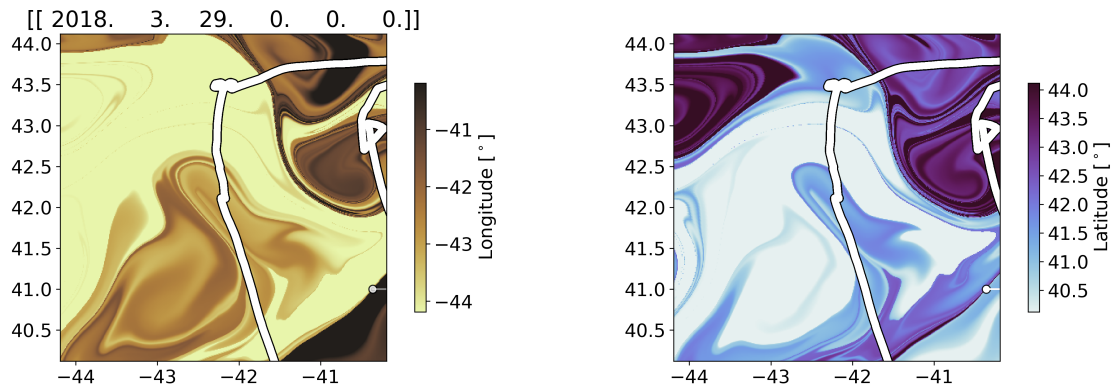


Figure 90: Water origin (longitude and latitude) for Station 2.5.

9.4 S3 NAAMES-4

Station 3 was chosen because of its proximity to a float.

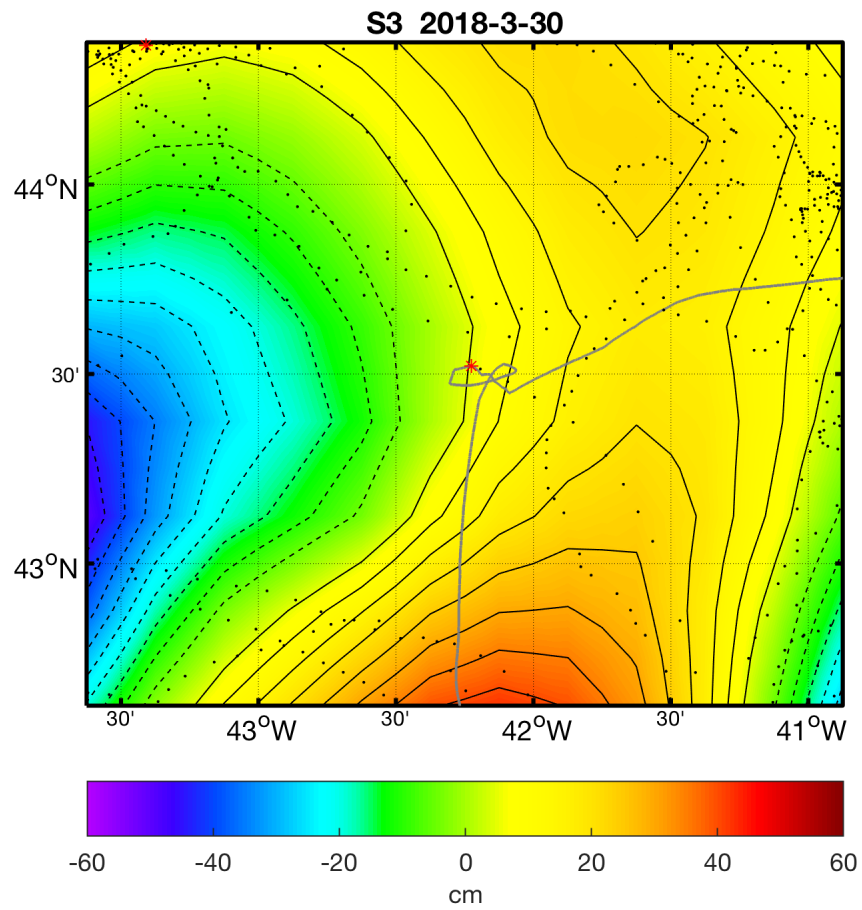


Figure 91: Same as Fig. 52

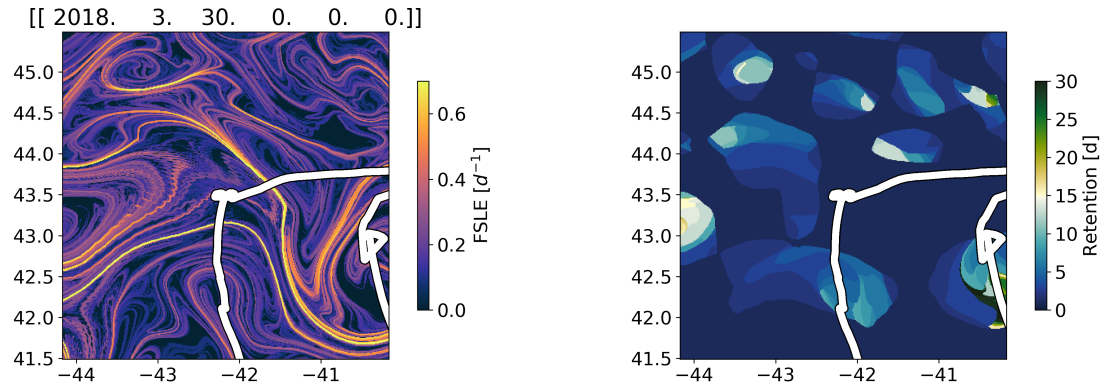


Figure 92: FSLE and RP calculated for Station 3.

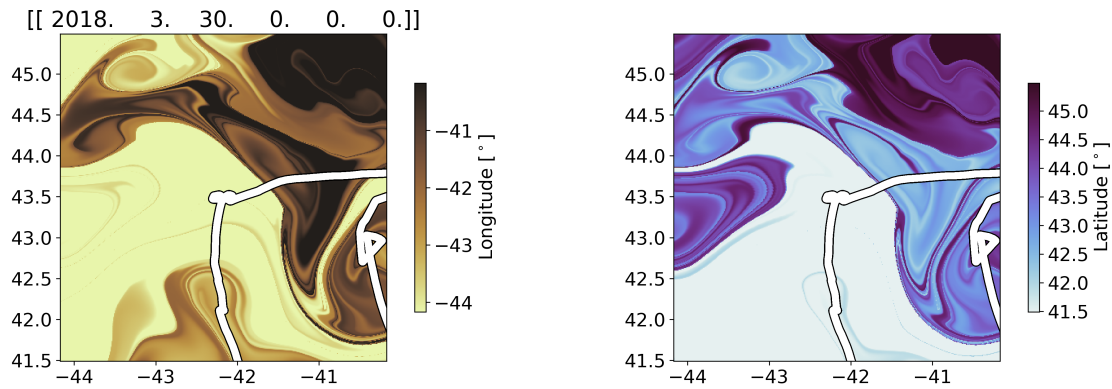


Figure 93: Water origin (longitude and latitude) for Station 3.

9.5 S4 NAAMES-4

This station was chosen because of its proximity to a float. It was the northernmost station sampled during this cruise. Lagrangian re-analyses indicate that the sampled water is likely to have been advected from further north locations (Figure 96).

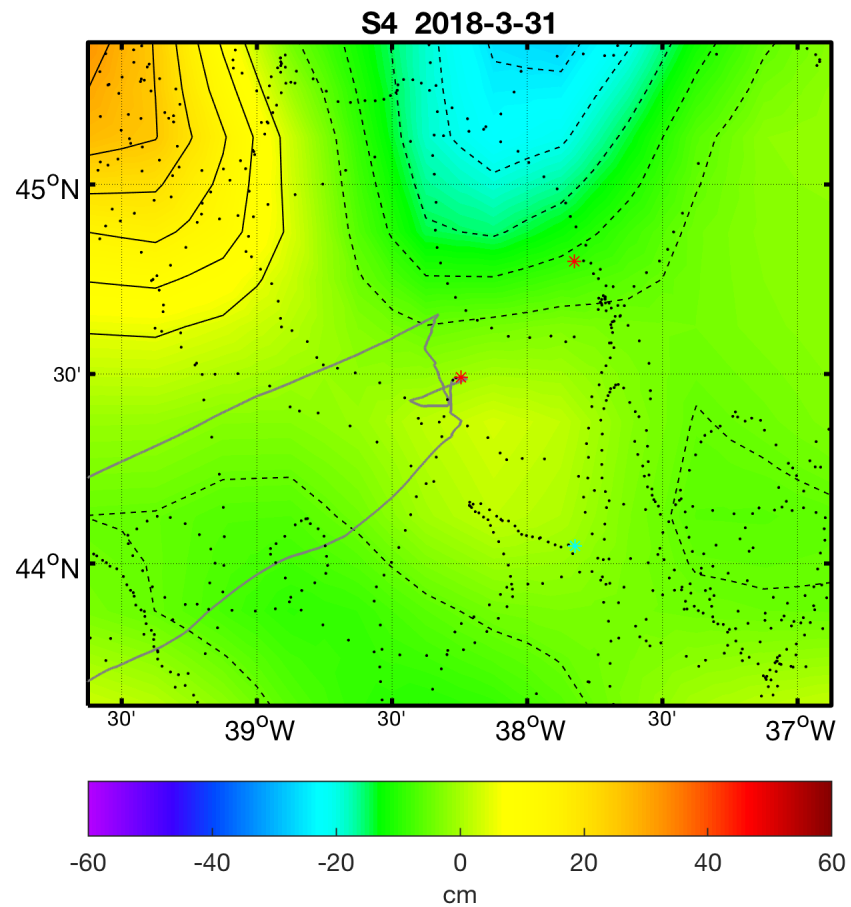


Figure 94: Same as Fig. 52

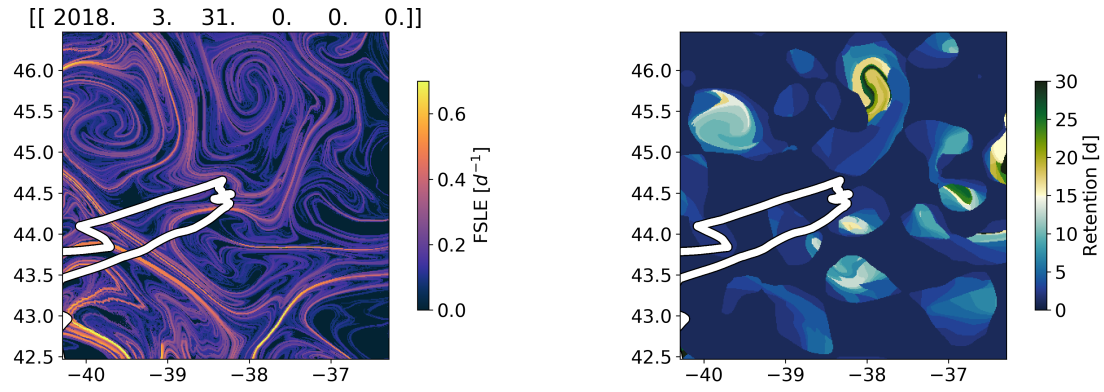


Figure 95: FSLE and RP calculated for Station 4.

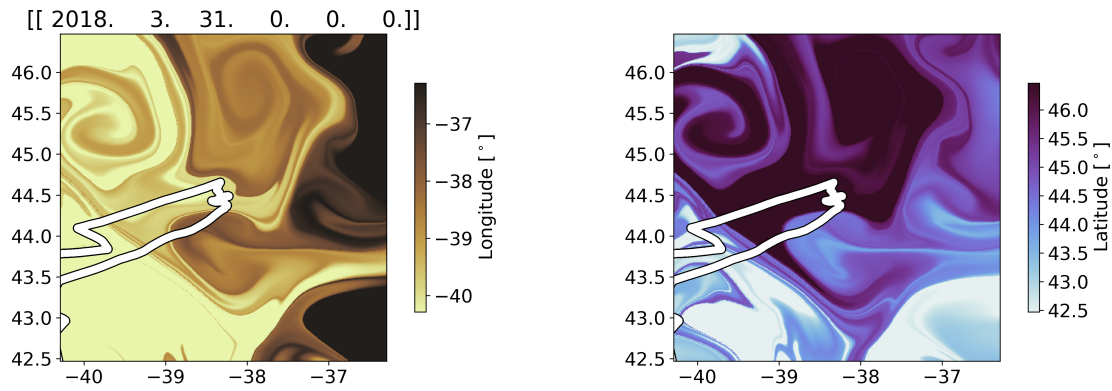


Figure 96: Water origin (longitude and latitude) for Station 4.

9.6 SE4 NAAMES-4

This short station was part of an intensive eddy sampling conducted using the flow-through system and ADCPs. Station E4 was supposed to be located at the center of a cyclonic eddy. The station was more likely located at the eddy periphery of this weakly retentive eddy (Figure 95).

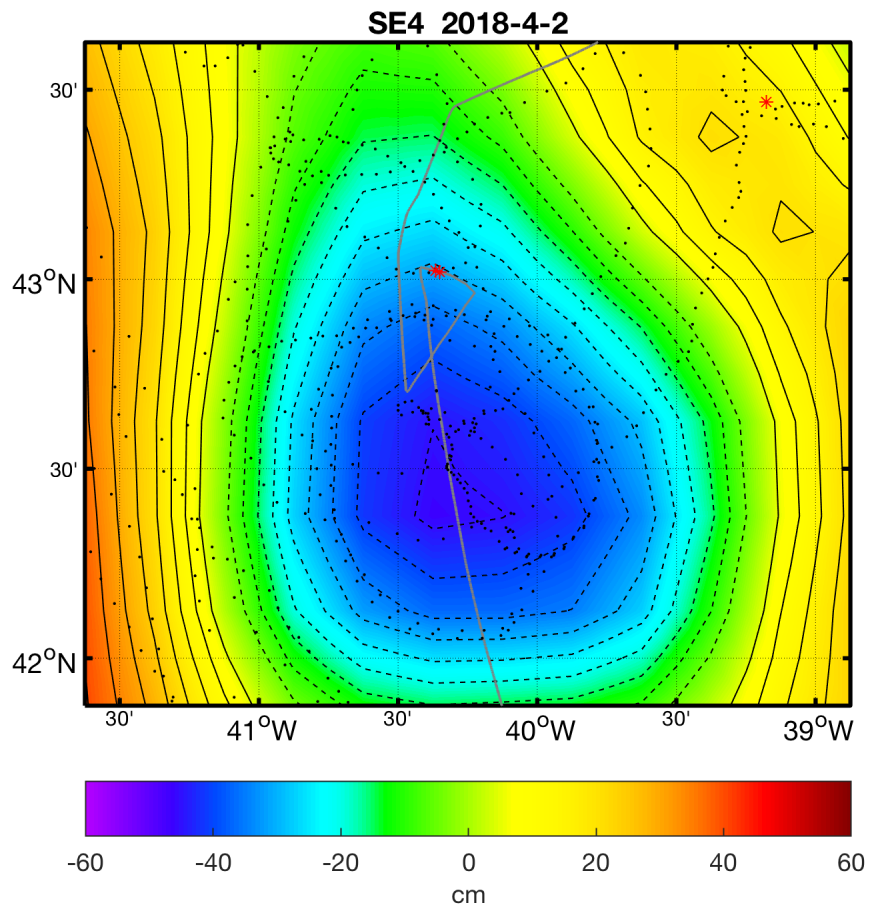


Figure 97: Same as Fig. 52

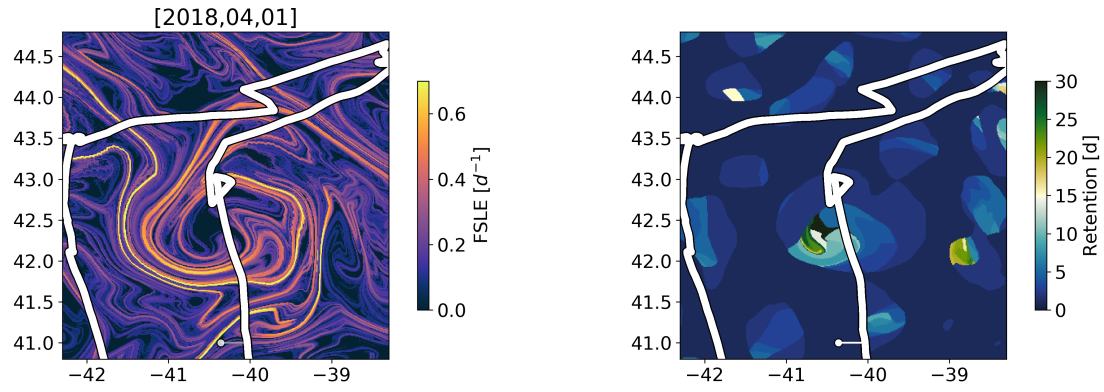


Figure 98: FSLE and RP calculated for Station Eddy 4.

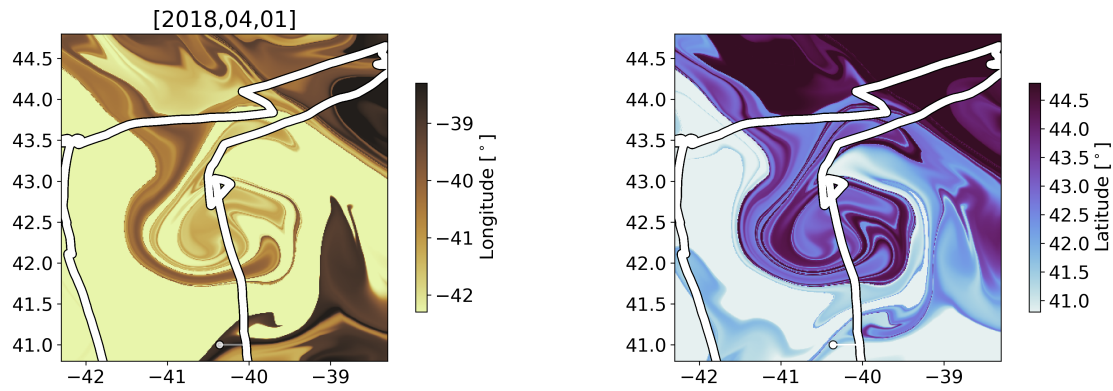


Figure 99: Water origin (longitude and latitude) for Station Eddy 4.

9.7 S2RD NAAMES-4

Station 2 Return-Drifter was located at the updated position of the drifter deployed during the occupation of Station 2.

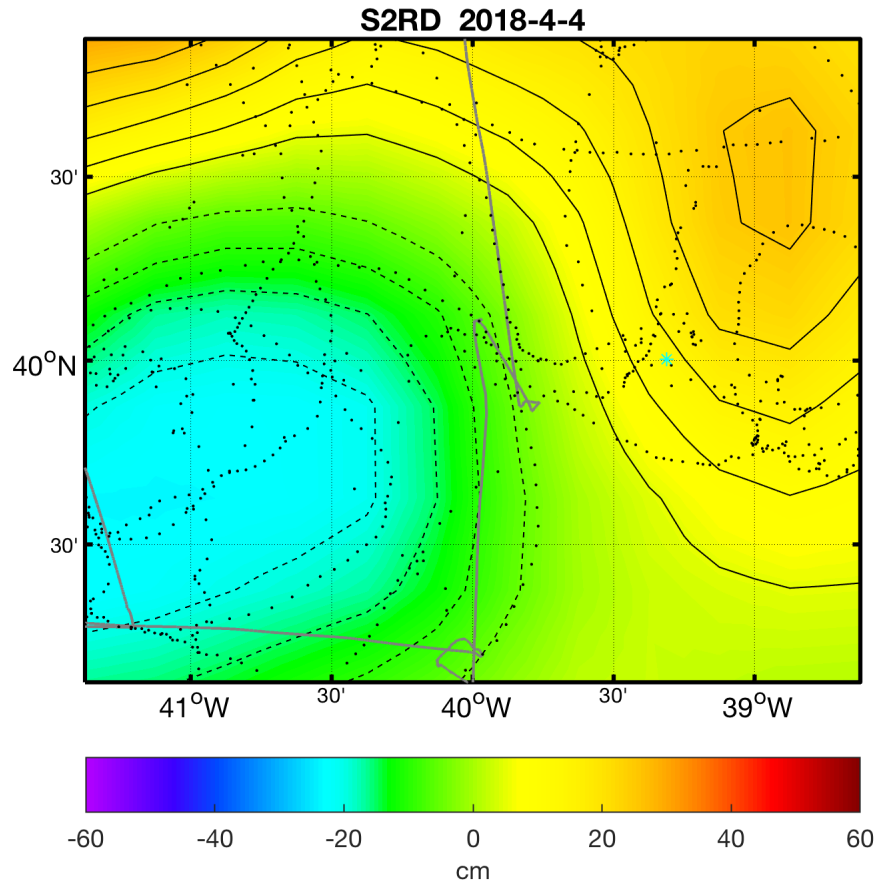


Figure 100: Same as Fig. 52

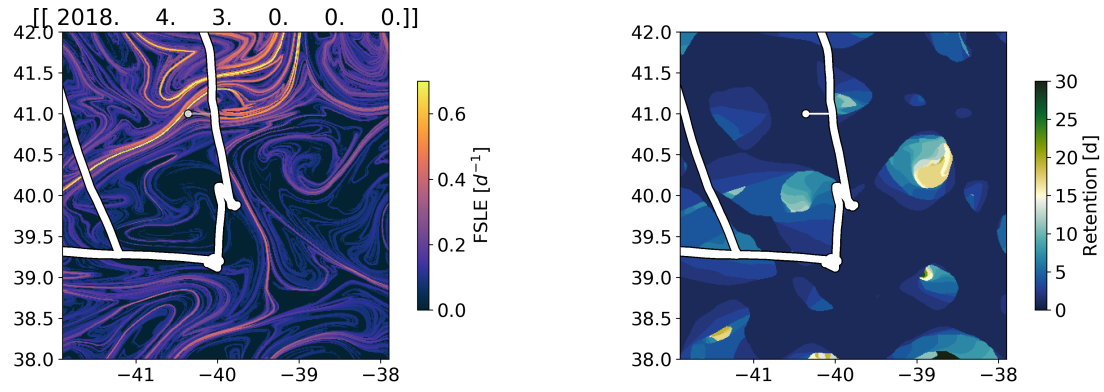


Figure 101: FSLE and RP calculated for Station 2- Return-Drifter.

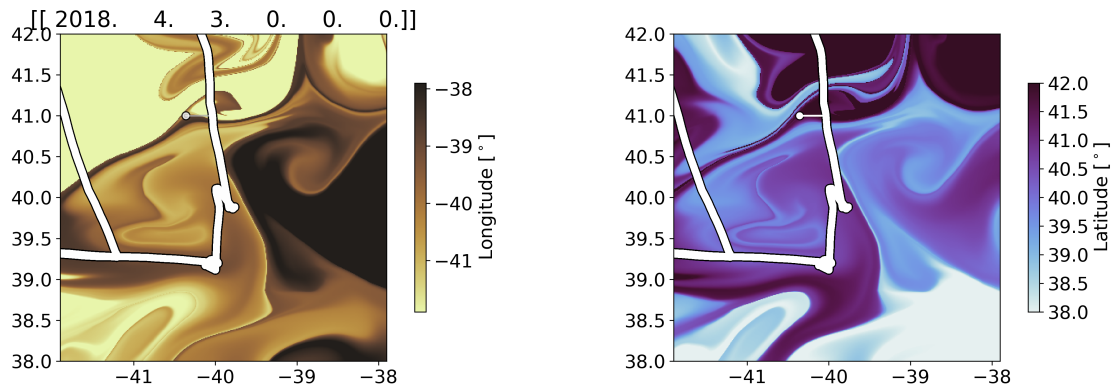


Figure 102: Water origin (longitude and latitude) for Station 2-Return-Drifter.

9.8 S2RF NAAMES-4

Station 2 Return-Float was located at the updated position of the float used to identify Station 2.

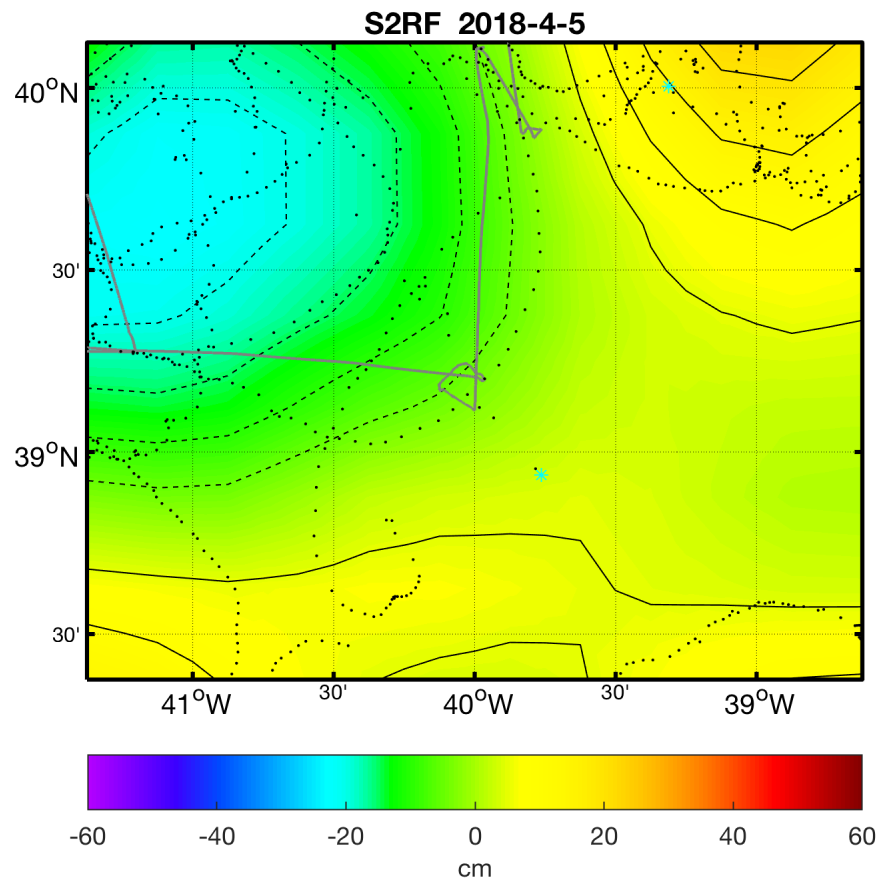


Figure 103: Same as Fig. 52

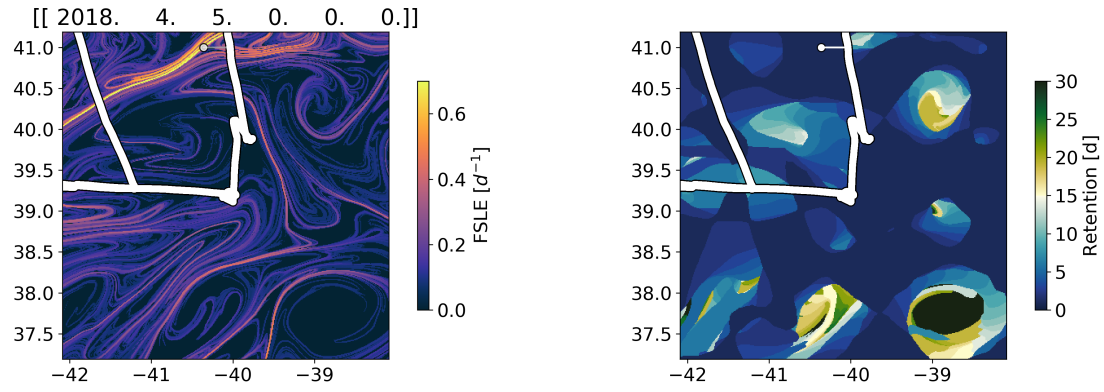


Figure 104: FSLE and RP calculated for Station 2- Return-Float.

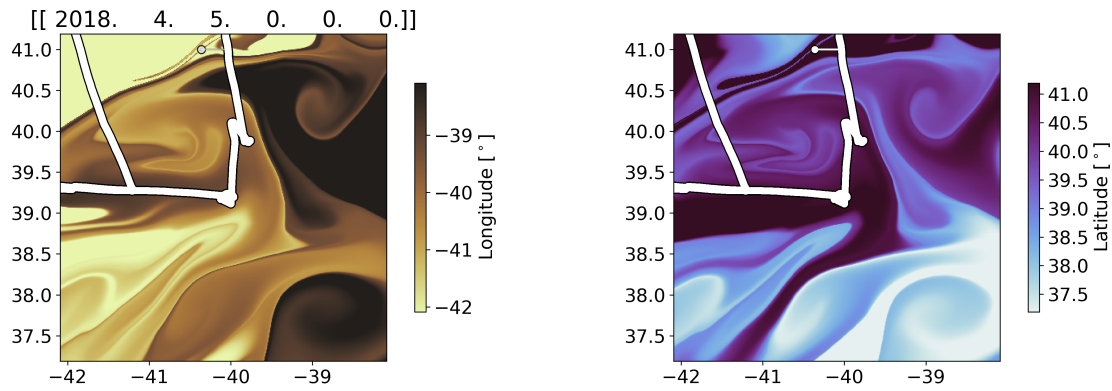


Figure 105: Water origin (longitude and latitude) for Station 2-Return-Float.

10 Planned Additions and Updates

Here is a brief list of some of the items that we plan on adding to the document:

1. Summary Table of all eddy parameters for NAAMES
2. Ancillary data tables to help bring more information into the document as a function of the different stations.

References

- Cotté, C., d'Ovidio, F., Dragon, A.-C., Guinet, C., and Lévy, M. (2015). Flexible preference of southern elephant seals for distinct mesoscale features within the antarctic circumpolar current. *Progress in Oceanography*, 131:46–58.
- De Monte, S., Cotté, C., d'Ovidio, F., Lévy, M., Le Corre, M., and Weimerskirch, H. (2012). Frigatebird behaviour at the ocean–atmosphere interface: integrating animal behaviour with multi-satellite data. *Journal of The Royal Society Interface*, 9:3351–3358.
- De Monte, S., Soccodato, A., Alvain, S., and d'Ovidio, F. (2013). Can we detect oceanic biodiversity hotspots from space&quest. *The ISME journal*, 7(10):2054–2056.
- Della Penna, A., De Monte, S., Kestenare, E., Guinet, C., and d'Ovidio, F. (2015). Quasi-planktonic behavior of foraging top marine predators. *Scientific reports*, 5.
- Della Penna, A., Koubbi, P., Cotté, C., Bon, C., Bost, C.-A., and d'Ovidio, F. (2017). Lagrangian analysis of multi-satellite data in support of open ocean marine protected area design. *Deep Sea Research Part II: Topical Studies in Oceanography*, 140:212–221.
- d'Ovidio, F., De Monte, S., Della Penna, A., Cotte', C., and Guinet, C. (2013). Ecological implications of eddy retention in the open ocean: a lagrangian approach. *Journal of Physics A*.
- d'Ovidio, F., Della Penna, A., Trull, T. W., Nencioli, F., Pujol, I., Rio, M. H., Park, Y.-H., Cotté, C., Zhou, M., and Blain, S. (2015). The biogeochemical structuring role of horizontal stirring: Lagrangian perspectives on iron delivery downstream of the kerguelen plateau. *Biogeosciences*, 12(1):779–814.
- d'Ovidio, F., Monte, S. D., Alvain, S., Dandonneau, Y., and Lévy, M. (2010). Fluid dynamical niches of phytoplankton types. *Proceedings of the National Academy of Sciences*, 107:18366–18370.
- Kai, E. T., Rossi, V., Sudre, J., Weimerskirch, H., Lopez, C., Hernandez-Garcia, E., Marsac, F., and Garçon, V. (2009). Top marine predators track lagrangian coherent structures. *Proceedings of the National Academy of Sciences*, 106:8245–8250.
- Lehahn, Y., d'Ovidio, F., Lévy, M., and Heifetz, E. (2007). Stirring of the northeast atlantic spring bloom: A lagrangian analysis based on multisatellite data. *Journal of Geophysical Research*, 112:15.
- McGillicuddy, D., Anderson, L., Bates, N., Bibby, T., Buesseler, K., Carlson, C., Davis, C., Ewart, C., Falkowski, P., Goldthwait, S., et al. (2007). Eddy/wind interactions stimulate extraordinary mid-ocean plankton blooms. *Science*, 316(5827):1021.

- Okubo, A. (1970). Horizontal dispersion of floatable particles in the vicinity of velocity singularities such as convergences. *Deep Sea Research and Oceanographic Abstracts*, 17:445–454.
- Prants, S., Budyansky, M., and Uleysky, M. Y. (2014). Identifying lagrangian fronts with favourable fishery conditions. *Deep Sea Research Part I: Oceanographic Research Papers*, 90:27–35.
- Sanial, V., van Beek, P., Lansard, B., d’Ovidio, F., Kestenare, E., Souhaut, M., Zhou, M., and Blain, S. (2014). Study of the phytoplankton plume dynamics off the crozet islands (southern ocean): A geochemical-physical coupled approach. *Journal of Geophysical Research: Oceans*, 119(4):2227–2237.
- Weiss, J. (1991). The dynamics of enstrophy transfer in two-dimensional hydrodynamics. *Physica D: Nonlinear Phenomena*, 48:273–294.